Alma Mater Studiorum – Università di Bologna

DOTTORATO DI RICERCA IN

SCIENZE BIOMEDICHE

Ciclo XVIII

Settore Concorsuale di afferenza: 05/D1

Settore Scientifico disciplinare: BIO/09

CDKL5 DISORDER: A NOVEL THERAPEUTIC STRATEGY TO IMPROVE BRAIN DEVELOPMENT IN A NEWLY GENERATED CDKL5 KO MOUSE MODEL

Presentata da: **Dott.ssa Marianna De Franceschi**

Coordinatore Dottorato

Chiar.mo Prof. Lucio Ildebrando Cocco

Relatore

Prof.ssa Elisabetta Ciani

Esame finale anno 2016

SUMMARY

1 AIM OF THE STUDY

Cyclin-dependent kinase like-5 (CDKL5) disorder is a rare neurodevelopmental disease caused by mutations in the CDKL5 gene, located in the X-chromosome. The consequent unsuccessful CDKL5 protein expression in the nervous system leads to a severe phenotype characterized by intellectual disability, early-onset intractable epilepsy and motor impairment, which, together with a complex corollary symptomatology, resembles Rett syndrome.

Currently, there is no cure or effective treatment for CDKL5 disorder, and the mainstay of care for this disorder is support for the families. Therefore, identification of specific therapies will represent an important achievement in the field of public health.

In theory, for a monogenic disease such as the CDKL5 disorder, delivery of a wild type copy of the CDKL5 gene to cells lacking functional CDKL5 represents a therapeutic approach worth considering. **There are encouraging proof-of-concept studies which demonstrate the potential for gene therapy, but also highlight significant caveats** for treatment of brain diseases. A new alternative approach to gene therapy, named "protein transduction" or "protein therapy", has emerged, enabling the trans-vascular delivery of an exogenous protein to the brain following a simple systemic injection. It has been discovered that certain proteins and peptides exhibit the unique property of efficient translocation across cell membranes. This unique translocation is usually due to the presence of a Protein Transduction Domain (PTD) in these molecules. The HIV-1 Transactivator of Transcription (TAT) protein is the best characterized viral PTD containing protein. Earlier experiments with the TAT-PTD protein domain demonstrated successful transduction of high molecular weight proteins into the mouse brain [Xia, Mao, and Davidson 2001; Schwarze et al. 1999; Nagahara et al. 1998]. Importantly, no toxic effects or immunogenicity problems of the TAT-PTD have been reported so far.

Based on these premises **the overall goal of the study was to develop a protein replacement therapy for CDKL5 disorder aimed to compensate for the lack of function of the CDKL5 protein, exploiting a mouse model of the pathology.** Importantly, this protein therapy has the advantage of a potentially rapid translation from the animal model to patients.

2 INTRODUCTION

2.1 CDKL5 disorder: overview

CDKL5 (cyclin-dependent kinase-like 5) disorder is a severe X-linked neurodevelopmental disease characterized by severe intellectual disability, generalized developmental delay and early-onset intractable seizures. It is caused by mutations in the CDKL5 gene, leading to altered functionality of CDKL5 protein kinase, whose expression is high in the developing brain in physiological conditions.

The CDKL5-related epileptic encephalopathy affects mostly girls and due to the numerous clinical features that overlap with the more characterized Rett syndrome (RTT), it has been initially termed as "early seizure variant" or "Hanefeld variant" of RTT. Rett syndrome etiopathogenesis mainly involves mutations in another X-linked gene, encoding for methyl-CpG-binding protein 2 (MeCP2), a methylation-dependent transcriptional repressor [Lewis et al. 1992] and splicing regulator [Young et al. 2005]. Nonetheless a significant fraction (around 30%) of children initially diagnosed with RTT does not carry mutation in MeCP2 gene, and recent findings highlighted the fact that mutations in other genes, such as CDKL5 (on X chromosome) and FOXG1 (on human chromosome 14) genes, are responsible for new disorders that in many aspects overlap RTT but are also characterized by specific traits [Evans et al. 2005; Fehr et al. 2013; Guerrini and Parrini 2012].

Similarities between MeCP2-CDKL5-FOXG1 encephalopathies are related to the severe neurodevelopmental impairment and the consequently reduced behavioral repertoire of affected patients, while the characteristics of associated epilepsy are quite different [Guerrini and Parrini 2012]. Efforts have been made to unravel the molecular bases that might underlie phenotypic similarities related to mutations, duplications or deletions of these genes. Notably, CDKL5 and MeCP2 are widely coexpressed in the brain and are similarly activated during neuronal maturation and synaptogenesis [Mari et al. 2005; Rusconi et al. 2008]. Furthermore, a direct interaction between MeCP2 and CDKL5 has been demonstrated. CDKL5 can bind and phosphorylate MeCP2 *in vitro*, and MeCP2 can in turn regulate CDKL5 gene expression, at least in certain brain areas [Bertani et al. 2006; Carouge et al. 2010; Mari et al. 2005]. In addition, both proteins bind to different regions of DNA methyltransferase 1 (DNMT1), further suggesting their possible participation to common pathways [Kameshita et al. 2008].

Nevertheless, in the last few years increasing knowledge of clinical and molecular aspects of

MeCP2- and CDKL5- as well as FOXG1-related encephalopathies have rise the idea that they should be considered independent clinical entities [Fehr et al. 2013; Melani et al. 2011; Wang et al. 2012].

2.1.1 Rett syndrome

Rett syndrome (RTT) is a childhood neurological disease characterized by features that are observed in many other disorders ranging from autism to Parkinson's disease and dystonia. The disorder affects ~1 in 10,000 females and is most often caused by mutations in the gene encoding methyl-CpG-binding protein 2 (MeCP2), a transcriptional regulatory protein. Loss-of-function mutations in MeCP2, which is on X chromosome, account for the vast majority (~95%) of typical RTT cases. Most mutations arise spontaneously (de novo) in the paternal germ line; thus, individuals with RTT are typically females who, owing to X-chromosome inactivation, are somatic mosaics for normal and mutant MeCP2. Boys with mutations that cause RTT in females typically die before or soon after birth with a severe encephalopathy. Mutations in other genes such as cyclin-dependent kinase like 5 (CDKL5) and forkhead box G1 (FOXG1) can cause phenotypes overlapping with those seen in RTT; however, several features, such as congenital onset and infantile spasms in CDKL5-mutant patients, and congenital onset and hypoplasia of the corpus callosum in FOXG1-mutant patients, distinguish these disorders from typical RTT.

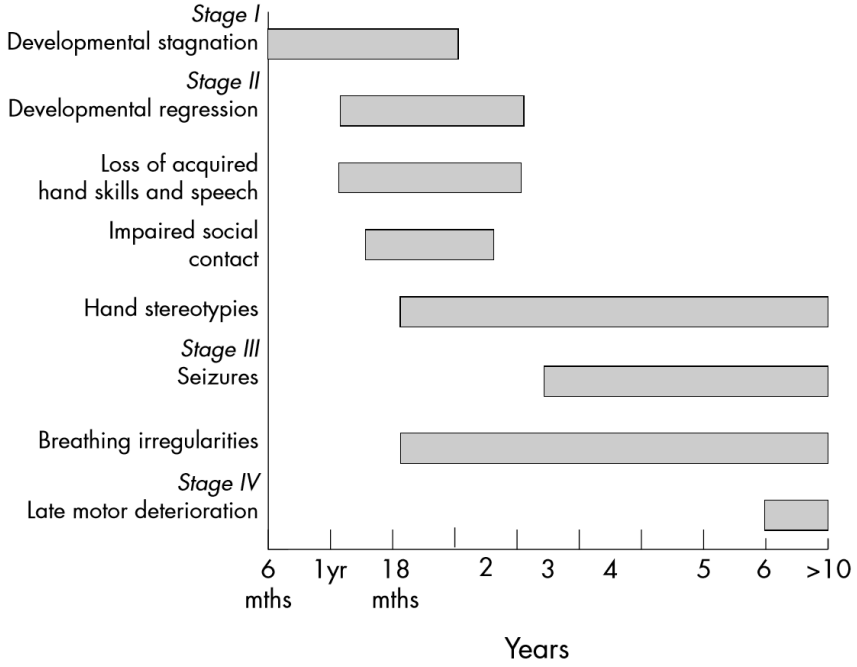

Figure 1. Staging system for classical RTT derived from Hagberg and Witt-Engerstroem. *(Image taken from [Weaving et al. 2005]).*

RTT is characterized by its unique time course and phenotypic complexity. Fig. 1 shows a proposed staging system basing on progress of symptoms. Affected individuals present with postnatal neurological regression, usually starting between 1.5 and 3 years of age (but sometimes as early as 6 months of age), with loss of acquired hand skills and spoken language and, in some cases, social withdrawal or extreme irritability that can resemble autism. After regression, there is a stabilization of skills, rather than a relentless progression, a feature that differentiates RTT from neurodegenerative conditions such as Batten disease or Huntington's disease. During this pseudo-stationary or plateau stage, characteristic features of RTT such as repetitive hand movements (stereotypies shown in Fig. 2), which can be present before or during regression, become more prominent. Later in life, many affected individuals enter a stage of motor decline in which ambulation can be lost, and Parkinsonian features such as rigidity and hypomimia become prominent. During the regression stage, some individuals with RTT develop autistic features that include social withdrawal, avoidance of eye contact and indifference to visual or auditory stimuli. After regression, some of these autistic features decrease, and most affected individuals develop intense eye gaze that they use for communication. Features such as stereotypies and lack of language skills persist throughout the life of affected individuals, although hand stereotypies can change from rapid movements to midline hand clasping with age.

Figure 2. Stereotypic hand movements in a 4-years old girl with RTT. *(Image taken from [Borg et al. 2005]).*

Additional behavioral problems include anxiety in response to novel situations, increased behavioral rigidity and increased pain tolerance. Individuals with RTT are considered to have severe intellectual disability; however, because affected individuals have severe impairments in their ability to communicate, it is difficult to make accurate assessments of their intellectual ability. Movement

abnormalities are a major issue in RTT, with the most obvious being the repetitive hand stereotypies, which seem to interfere with volitional hand use. Gait is almost always disrupted, with evidence of ataxia and apraxia. Dystonia is common, seen first in the ankles and eventually progressing to many joints. Axial hypotonia is present early in the disease course but, as children become young adults, increased tone with features of rigidity becomes more prominent. Additional movement abnormalities include tremor, myoclonus, chorea, facial grimacing and severe teeth grinding. Most individuals with RTT have scoliosis, and some require surgical intervention. Nutrition and gastrointestinal function are also major clinical issues in RTT, and there is marked growth failure in most affected individuals. It has long been recognized that head growth is impaired, resulting in acquired microcephaly, and height and weight are usually markedly diminished. However, a subset of individuals with RTT are overweight or obese, a feature that is often associated with higher functioning and possibly improved oromotor skills. Many individuals with RTT have various gastrointestinal problems, including significant chewing and swallowing difficulties, gastroesophageal reflux, gastrointestinal dysmotility and severe constipation, which severely decrease the quality of life for patients and their families. Dysregulation of breathing and autonomic homeostasis are very common in RTT. Respiratory abnormalities, which include periods of forceful breathing (hyperventilation), severe pauses in breathing (including breath holds) that can cause cyanosis and even loss of consciousness, and abnormal cardiorespiratory coupling, are more severe during wakefulness than during sleep and can be exaggerated during periods of excitement or stress. Autonomic abnormalities include periods of vasomotor disturbance (usually associated with cold hands and feet), abnormal sweating, decreased heart rate variability, evidence of sympathetic-parasympathetic imbalance and prolongation of corrected QT interval (an indication of abnormal cardiac electrical activity) in a subset of individuals. One quarter of deaths in RTT are sudden and unexpected, and might result from complications of cardiorespiratory dysfunction. Brain electrical activity is not typical in individuals with RTT, as shown by the markedly disrupted pattern observed on electroencephalograms (EEGs) and the high probability of seizures. Seizures, ranging from complex partial to generalized tonic-clonic, are most commonly seen after other symptoms appear (usually after age two) and correlate with the severity of the phenotype. In addition to true epileptic events, individuals with RTT also have non-epileptic paroxysmal events, and video EEG is needed to differentiate between them. Despite the severity and phenotypic complexity of RTT, the brains of individuals with RTT do not show gross neuropathological changes, nor evidence of neuronal or glial atrophy, degeneration, gliosis, or demyelination, indicating that RTT is not a neurodegenerative disorder. Smaller total brain volume and smaller neurons (but with a higher cell density) have been observed in several brain regions, including the cerebral cortex, hypothalamus and the hippocampal

formation. The size and complexity of dendritic trees are reduced in cortical pyramidal cells, and levels of microtubule-associated protein-2 (MAP-2), a protein involved in microtubule stabilization, are lower throughout the neocortex of RTT autopsy material. In addition, the density of dendritic spines is lower in pyramidal neurons of the frontal cortex and in the CA1 region of the hippocampus.

To date, no therapies are available to treat the most debilitating symptoms of RTT. However, the compelling need for effective treatments for RTT, coupled with the availability of good mouse models, is fuelling interest in translational studies aimed at identifying potential new therapeutics. Interestingly, it has been shown that many of the features of RTT are reversible in mice, and that these features are probably due to dysfunction of neurons and supporting cells, rather than neural degeneration. These findings provide hope that some and perhaps most symptoms can be reversed in affected individuals if effective therapies that can overcome the consequences of loss of function or dysfunction of MeCP2 will be discovered [Katz et al. 2012].

Even though Rett syndrome and CDKL5 disorder are almost worldwide considered different clinical entities, similarities between these encephalopathies are due to common molecular mechanisms and thus it is reasonable to think that pharmacological therapies targeted to altered pathways in Rett syndrome may be suitable also for CDKL5 disorder and vice versa.

2.1.2 CDKL5 disorder clinical presentation and natural history

The CDKL5 kinase was initially identified through a positional cloning study aimed at isolating disease genes mapping on the X-chromosome. Sequence analysis revealed homologies to several serine-threonine kinase genes and identified one protein signature specific for this subgroup of kinases, therefore, leading the authors to name the gene STK9 (Serine Threonine Kinase 9) [Montini et al. 1998].

The first described mutations in CDKL5 were reported in 2003, when Vera Kalscheuer and colleagues identified balanced translocations in two unrelated girls exhibiting infantile spasms and profound developmental delay. In both patients the CDKL5 gene was disrupted by a breakpoint on the X chromosome [Kalscheuer et al. 2003].

Due to some overlapping clinical similarities between the two reported patients and the early seizure variant of Rett syndrome, in the following years, other researchers studied the CDKL5 gene in patients who had been diagnosed with classical or variant Rett and were mutation negative to MeCP2 testing. These studies led to identification of intragenic CDKL5 mutations/deletions in girls with early onset severe seizures [Tao et al. 2004; Weaving et al. 2004].

In the last several years, the large number of patients reported, with detailed description of

epilepsy and EEG features, has permitted the delineation of a phenotypic spectrum spanning from milder forms – which include the possibility of autonomous walking and less severe epilepsy that is amenable to control – to severe forms featuring intractable seizures, more severe microcephaly and absence of motor milestones. In this spectrum several of the distinctive clinical features of Rett syndrome are lacking. For instance, girls with CDKL5 mutations do not exhibit a clear period of regression, neither do they present the intense eye gaze and impaired neurovegetative function typically seen in girls with RTT [Guerrini and Parrini 2012].

RTT Diagnostic Criteria 2010

Consider diagnosis when postnatal deceleration of head growth observed.

Required for typical or classic RTT

1	A period of regression followed by recovery or stabilization*
2	All main criteria and all exclusion criteria
3	Supportive criteria are not required, although often present in typical RTT

Required for atypical or variant RTT

1	A period of regression followed by recovery or stabilization*
2	At least 2 out of the 4 main criteria
3	5 out of 11 supportive criteria

Main Criteria

1	Partial or complete loss of acquired purposeful hand skills.
2	Partial or complete loss of acquired spoken language**
3	Gait abnormalities: Impaired (dyspraxic) or absence of ability.
4	Stereotypic hand movements such as hand wringing/squeezing, clapping/tapping, mouthing and washing/rubbing automatisms

Exclusion Criteria for typical RTT

1	Brain injury secondary to trauma (peri- or postnatally), neurometabolic disease, or severe infection that causes neurological problems***
2	Grossly abnormal psychomotor development in first 6 months of life#

Supportive Criteria for atypical RTT##

1	Breathing disturbances when awake
2	Bruxism when awake
3	Impaired sleep pattern
4	Abnormal muscle tone
5	Peripheral vasomotor disturbances
6	Scoliosis/kyphosis
7	Growth retardation
8	Small cold hands and feet
9	Inappropriate laughing/screaming spells
10	Diminished response to pain
11	Intense eye communication - "eye pointing"

Table 1. Revised diagnostic criteria for Rett syndrome. *(Table taken from [Neul et al. 2010])*

Strikingly, only less than one-quarter of individuals with CDKL5 mutations meet the criteria for the early-onset seizure variant of RTT (see Table 1), as CDKL5 disorder was initially defined. Furthermore, besides clinical differences, recent data from characterization of CDKL5 mouse models support the increasing awareness that CDKL5-related encephalopathy is an independent disorder with an independent pathogenic mechanism. To outline the difference with respect to Rett syndrome, in the last few years the definition of CDKL5 gene–related epileptic encephalopathy has been proposed by different clinicians and researchers, and CDKL5 disorder is by this time considered an independent clinical entity [Amendola et al. 2014; Fehr et al. 2013; Melani et al. 2011; Wang et al. 2012].

Furthermore, in the last years the screening of CDKL5 mutations has been extended to cohorts of both genders with undefined diagnosis of epileptic encephalopathy, infantile spasms or West syndrome. Interestingly, Intusoma and colleagues [Intusoma et al. 2011] suggested that screening among patients having intractable seizures with an onset before 6 months of age gives even a higher score than screening among MeCP2-negative RTT patients.

For, the central feature of CDKL5-related phenotype is an early onset epileptic encephalopathy, which is associated with severe developmental delay, deceleration of head growth, impaired communication and, often, hand stereotypies. Several dozen girls and a few boys with CDKL5 gene mutations, or genomic deletions, have been reported, all having early onset intractable seizures. Males are at the more severe end of the phenotypic spectrum with virtually no motor acquisitions. Patients with CDKL5-gene abnormalities are reported to be normal in the first days of life to subsequently exhibit early signs of poor developmental skills, including poor sucking, and poor eye contact, even before seizure onset. Subsequently, absent purposeful hand use, severe developmental delay, and absent language skills become apparent. About only one third of patients will eventually be able to walk [Guerrini and Parrini 2012]. Sleep and respiratory disturbances represent a major issue for many patients. Isolated studies on small number of patients with CDKL5 mutations demonstrated the presence of cardiorespiratory dysrhythmias such as tachypnoea, deep breathing, apnoeas and breath holding [Pini et al. 2012]. Polysomnography revealed central apnoeas when awake, low rapid eye movement sleep, frequent awakenings, and low sleep efficiency [Hagebeuk, van den Bossche, and de Weerd 2013]. Other common features of CDKL5 patients include autonomic features, gastroesophageal reflux, hypotonia and scoliosis.

Figure 3. Characteristic facial, hand and feet features in males and females with CDKL5 disorder. *(Image taken from [Fehr et al. 2013]).*

The described clinical symptoms are differently distributed, while early-onset epilepsy is a common feature of all CDKL5 patients. Epilepsy is typically manifested as an epileptic encephalopathy with infantile spasms starting between the first days and fourth month of life. Patients show a peculiar seizure pattern with generalized tonic–clonic events, gradually translating into repetitive distal myoclonic jerks. A generalized ictal pattern in neonates or very young infants has been described, but is considered to be exceptional, owing to the lack of both the functional cortical organization that is necessary to propagate and sustain the electrical discharge and the failure of interhemispheric transmission resulting from commissural immaturity. Whether this peculiar ictal pattern represents a unique seizure type or just an unusual expression of infantile spasms in the immature, and possibly malformed, brain of children with CDKL5-gene abnormalities is open to speculation. Follow-up studies of children older than 3 years indicate that about half of them can experience seizure remission, whereas the remaining continue to have intractable spasms, often associated with multifocal and myoclonic seizures. Early EEG findings vary from normal background to moderate slowing, with superimposed focal or multifocal interictal discharges and, in some cases a suppression burst pattern.

There are no neuropathologic studies that have examined the brain of patients with CDKL5 mutations. Imaging data are also scanty and nonquantitative. Bahi-Buisson et al. in 2008 reported "cortical atrophy" in 13 of 20 girls, associated with areas of increased T2 signal in the white matter, especially in the temporal lobes in some [Guerrini and Parrini 2012].

The clinical understanding of CDKL5 disorder still remains limited, with most information being derived from small patient groups seen at individual centers. Its genetic link to neurodevelopmental disorders highlights the need to characterize CDKL5 biological function, understand the mechanisms underlying CDKL5-related disorder, and identify effective therapies targeted toward slowing or reversing disease progression.

2.1.3 CDKL5 mutations and genotype-phenotype relationship

With the exception of one instance of familial occurrence, likely due to gonadal mosaicism, all reported cases of CDKL5 disorder are sporadic. Although the risk of gonadal mosaicism and consequent familial recurrence is low, genetic counseling should be offered to couples with a child with CDKL5-related epileptic encephalopathy [Guerrini and Parrini 2012].

Since 2003, when Kalscheuer et al. identified the first mutations in CDKL5 in two unrelated girls who, in addition to mental retardation, had hypsarrhythmia and infantile spasms [Kalscheuer et al. 2003], patients with different phenotypic outcome of the disorder, harboring a wide range of pathogenic mutations, have been described in literature. About a hundred different CDKL5 patients, harboring a wide range of pathogenic mutations, have been described so far, including missense and nonsense mutations, small and large deletions, frameshifts and aberrant splicing. This mutational heterogeneity may in part explain the phenotypic heterogeneity. Even considering the small number of patients described, some "hot-spots" and genotype-phenotype correlations have been proposed.

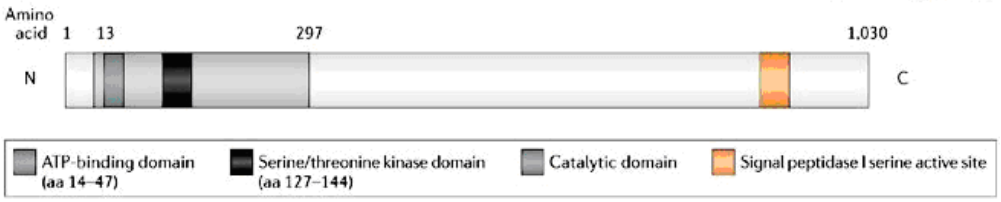

Figure 4. Schematic representation of CDKL5 protein. *(Image taken from [Bienvenu and Chelly 2006]).*

The recurrent mutations identified so far affect different domains of the CDKL5 protein, the most important being: the ATP binding region, the Serine–Threonine protein kinase active site, and a large COOH-terminal extension of almost 700 amino acids, poorly characterized, that probably harbors several functions. Fig. 4 shows a schematic representation of CDKL5 protein important domains. Missense mutations almost exclusively are localized in the N-terminal domain, impairing

the kinase activity of CDKL5, and can therefore in most cases be considered loss-of-function mutations. These mutations are associated with a more severe phenotype, underlining the important role of CDKL5 kinase activity during brain function and development. Patients bearing missense mutations in the ATP binding site (such as the p.Ala40Val mutation) typically walk unaided, have normocephaly, better hand use ability, and less frequent refractory epilepsy when compared to girls with other CDKL5 mutations. On the contrary, truncating mutations can be located anywhere in the gene, leading to CDKL5 derivatives of various lengths. The relevance of the rather uncharacterized C-terminal part of CDKL5 is suggested by the fact that many pathogenic alterations involve the C-terminus. Some reports suggest that stop-codon mutations in the C-terminus originate a milder clinical picture than those caused by mutations in the catalytic domain [Bahi-Buisson et al. 2012]. A regulatory role for the tail of CDKL5 has emerged from the characterization of few C-terminal truncating derivatives. In fact, it seems to act as a negative regulator of the catalytic activity of CDKL5 and to modulate the subcellular distribution, localizing the protein to the cytoplasm. Whether truncated CDKL5 mutants act as loss- or gain-of-function proteins still remains to be understood. Indeed, if expressed, they would be mislocalized hyperfunctional derivatives. However, since CDKL5 seems to exert its functions both in the nucleus and the cytoplasm, it remains possible that the absence of CDKL5 from the cytoplasm might also contribute to the pathogenic phenotype [Kilstrup-Nielsen et al. 2012].

Furthermore, a novel CDKL5 107 kDa isoform with an alternative C-terminus that terminates in intron 18 has been identified and some authors support the idea that mutations affecting this 107 kDa isoform are likely pathogenic, while mutations only affecting the large 115 kDa protein are likely not involved in neurological symptoms [Bahi-Buisson et al. 2012].

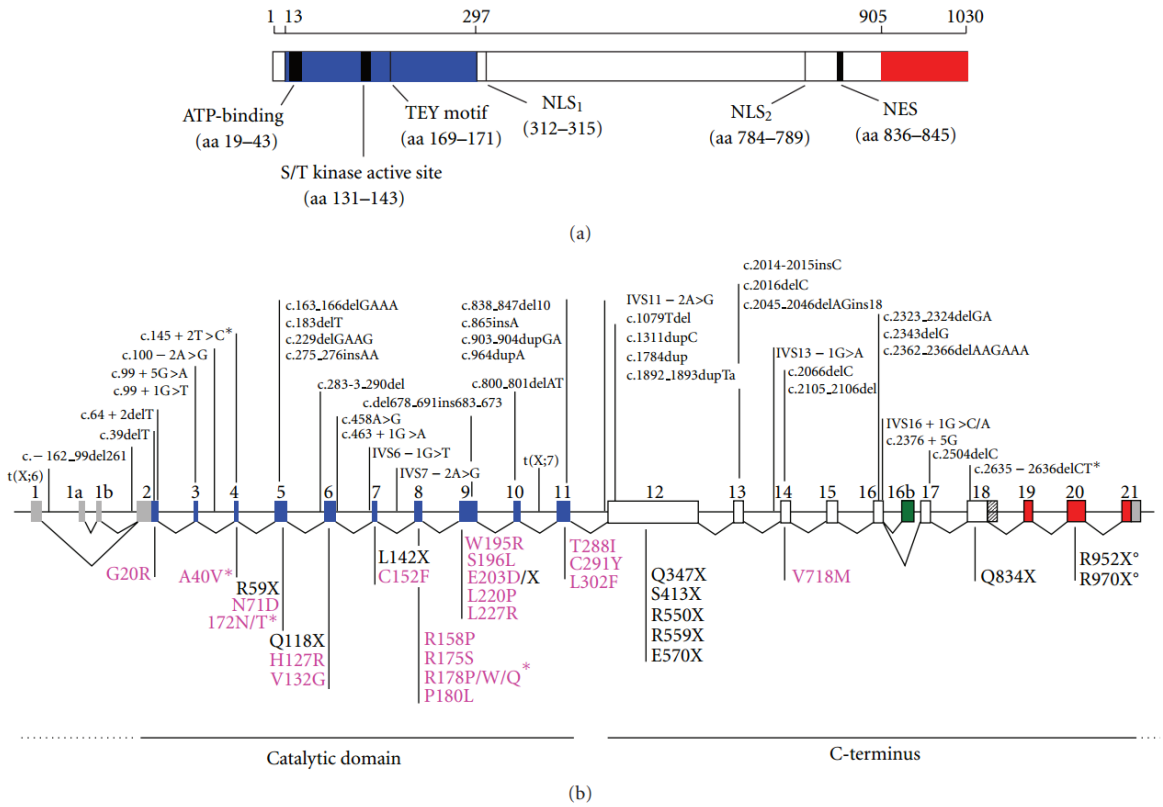

Figure 5. Pathogenic CDKL5 mutations. *(**A**) Schematic representation of CDKL5$_{115}$ protein with functional domains and signatures indicated. NLS: nuclear localization signal; NES: nuclear export signal. (**B**) Various mutations in CDKL5 reported to date are indicated corresponding to their location within the gene. The blue exons make up the catalytic domain, the white exons are the C-terminal region, red and green parts show different versions of the protein. Mutations shown above the CDKL5 gene are deletion and frame shift mutations as well as splice variants indicated with cDNA nomenclature. Missense and nonsense mutations (fuchsia and black, resp.) are represented with amino acid nomenclature below the CDKL5 gene. (Image taken from [Kilstrup-Nielsen et al. 2012]).*

Although it has been observed a relative homogeneity of the clinical phenotype in patients bearing the same mutation, some clinical discrepancies emerged. No clear genotype-phenotype correlation of CDKL5 mutations has been established so far and some authors state that the nature of the mutation does not correlate with the clinical heterogeneity. Accordingly, Weaving et al. reported of two genetically identical CDKL5-mutated twin girls with a significant discordant phenotype. Indeed, one proband showed a clinical phenotype overlapping RTT, whereas her twin sister showed autistic disorder and mild-to-moderate intellectual disability. Since both girls were characterized by

random X-inactivation, probably their phenotypic differences can be attributed to modifier genes that have been differentially influenced by environmental and/or epigenetic factors. Moreover, another report identified an R952X mutation with incomplete penetrance and uncertain pathogenicity. Since this novel mutation occurs in exon 20 that might not be highly expressed in brain, it is reasonable to speculate that modifier genes affecting CDKL5 splicing might be responsible for the observed penetrance.

The behavior of each missense, nonsense, and frameshift mutation might be different and the clinical phenotype associated with each CDKL5 mutation may be the result of the nuclear or cytosolic accumulation of CDKL5, of its ability to bind substrates and of the residual catalytic activity of CDKL5. Future studies, focused on the identification of direct and indirect partners of CDKL5, will help defining its functions and might lead to the identification of modifier genes representing relevant targets for therapeutic approaches [Kilstrup-Nielsen et al. 2012].

2.2 CDKL5 gene and protein

The cyclin-dependent kinase-like 5 gene (CDKL5), located on the X-chromosome, is recognized as one of the genes responsible for a form of epileptic encephalopathy classified as early infantile epileptic encephalopathy 2. It was identified in 1998 through an exon trapping method designed to screen candidate genes in Xp22 region, where several genetic disorders have been mapped [Montini et al. 1998]. The human CDKL5 gene occupies approximately 240 kb and is composed of 24 exons of which the first three exons (exon 1, 1a and 1b) are untranslated, whereas the coding sequence are contained within the exons 2-21. Different isoforms and splicing variants have been identified so far (see Fig. 6 below in the text).

CDKL5 protein contains a conserved serine/threonine kinase domain in its N-terminal, sharing homology to both MAP and cell-cycle–dependent kinases known as the cyclin-dependent kinase-like (CDKL) kinases [Lin, Franco, and Rosner 2005]. The eukaryotic protein kinases represent a large superfamily of homologous proteins, related by the presence of a highly conserved kinase domain of 250-300 amino acids. There are two major subdivisions within the superfamily of eukaryotic protein kinases: the serine-threonine protein kinases and the protein tyrosine kinases. Sequence analysis and further characterization of the predicted CDKL5 protein revealed homologies to several serine-threonine kinases. Consequently Montini and colleagues first named the identified gene STK9 (Serine Threonine Kinase 9) [Montini et al. 1998]. Serine-threonine kinases very frequently have been linked to the pathogenesis of genetic disorders and a substantial number of human genetic disorders have been mapped to the Xp22 region. Montini et al. suggested the Nance-

Horan syndrome (NH), a X-linked recessive disorder characterized by cataract and dental anomalies, as a candidate disorder for STK9 mutations. In the following five years, mutations in this gene were found in epileptic patients and in 2003 Kalscheuer suggested STK9 to be a chromosomal locus associated with X-linked infantile spasms (ISSX) [Kalscheuer et al. 2003]. The X-linked infantile spasm is characterized by early-onset generalized seizures, hypsarrhytmia and mental retardation and majority of cases are due to mutations in the aristaless-related homebox gene (*ARX*), which maps to the Xp21.3-p22.1 interval. Given the strong similarity to some cell division protein kinases, the STK9 gene subsequently got renamed cyclin-dependent kinase like 5, CDKL5.

2.2.1 Protein structure

The CDKL5 protein belongs to the CMGC family of serine-threonine kinases, which include cyclin-dependent kinases (CDKs), mitogen-activated protein kinases (MAP kinases), glycogen synthase kinases (GSKs), and CDK-like (CDKL) kinases. It is characterized by a N-terminal catalytic domain (amino acids 13-297), homologous to that of other CDKL-family members, such as p56KKIAMRE (CDKL1), p42KKIALRE (CDKL2) and NKIAMRE (CDKL3). This N-terminal catalytic domain contains the ATP-binding region (amino acids 13-43), the serine-threonine kinase active site (amino-acids 131-143) and a Thr-Xaa-Tyr motif (TEY) at amino acids 169-171, whose dual phosphorylation is normally involved in activating kinases of the MAP kinase family. In analogy to all the other members of the family of serine-threonine kinases, 12 conserved subdomains can be identified in this 284-amino acid kinase domain. On the contrary, CDKL5 is unique in the CDKL-family as it displays an unusual long tail of more than 600 amino acids without obvious similarity to other protein domains but with a high degree of conservation between different CDKL5 orthologs that differ only in the most extreme C-terminus.

Interestingly, most of the pathogenic missense mutations identified so far involve the catalytic domain, suggesting that the enzymatic activity of CDKL5 is essential for normal neurodevelopment. However the ensemble of CKDL5 phosphorylation targets is hitherto rather uncharacterized. The presence of a critical arginine-residue in the kinase subdomain VIII suggests that CDKL5 might be a proline-directed kinase. Moreover, as some of the other CMGC protein kinases, CDKL5 appears capable of autophosphorylating its TEY motif [Kilstrup-Nielsen et al. 2012]. Since the molecular characterization of CDKL5 started only in 2005, the protein still remains largely uncharacterized.

2.2.2 Protein isoforms

In human CDKL5 the first two reported splice variants differ in the 5'UTRs and produce the same 115 kDa protein. They are referred to as isoform I, containing exon 1, which is transcribed in a wide range of tissues, and isoform II, including exon 1a and 1b, which is limited to testis and fetal brain [Kalscheuer et al. 2003; Williamson et al. 2012]. The resulting CDKL5 transcript generates a protein of 1030 amino acids with molecular weight of 115 kDa ($CDKL5_{115}$) and is mainly expressed in the testis. More recently alternative splicing events have been identified, leading to at least three distinct human protein isoforms. Two of these transcripts, characterized by an altered C-terminal region, are likely to be very relevant for CDKL5 brain functions [Fichou et al. 2011; Williamson et al. 2012]. Firstly, an alternatively spliced isoform has been described in both human and mouse, which has an additional in-frame exon of 123 bp, exon 16b (between exons 16 and 17), producing a predicted protein of 120 kDa in humans and a 110 kDa protein in mice [Fichou et al. 2011; Rademacher et al. 2011]. Interestingly this variant is highly conserved in species through evolution, suggesting a potential functional role, but does not display any homology with other referenced sequences. Fichou et al. also demonstrated that the amount of exon 16b-containing ($CDKL5_{115+ex.16b}$) transcript varies depending on the brain region analyzed and that this transcript is brain specific. The second isoform identified in the same year by Williamson and colleagues is a 107 kDa isoform with an alternative C-terminus that terminates in intron 18 ($CDKL5_{107}$) and is the predominant isoform in human and mouse brains, suggesting that this isoform is likely to be of primary pathogenic importance in the CDKL5 disorder. For, in all human tissues $CDKL5_{107}$ is the most abundant transcript, with tissues expressing 10- to 100-fold or more $CDKL5_{107}$ than $CDKL5_{115}$. In particular, in the whole brain there is 37-fold more of $CDKL5_{107}$ than $CDKL5_{115}$. Testis is the exception, with only 2.5-fold more $CDKL5_{107}$ than $CDKL5_{115}$ reflecting the relative abundance of $CDKL5_{115}$ in this tissue. The C-terminus of CDKL5, which is different in the two isoforms, is important in modulating its subcellular localization, and the accumulation of truncated protein in the nucleus might be of pathogenic significance [Bertani et al. 2006; Rusconi et al. 2008]. Therefore the cellular distribution of the $CDKL5_{107}$ isoform was examined, revealing subcellular localization and catalytic activity that overlap greatly, but not completely, with that of the previously studied human $CDKL5_{115}$ protein. Furthermore, *in vitro* data indicate that proteasomal degradation of the $CDKL5_{115}$ isoform is mediated by a signal between amino acids 904 and 1030, exclusively present in this isoform, whereas $CDKL5_{107}$ is more stable and less prone to degradation through the proteasome pathway. As the C-terminus of the $CDKL5_{107}$ isoform is an intronic sequence, it has not been investigated in most mutation screening studies to date, but after these findings Williamson and colleagues suggested that

screening of the intronic sequence should be included in the genetic analysis of patients with a suggestive clinical phenotype [Williamson et al. 2012].

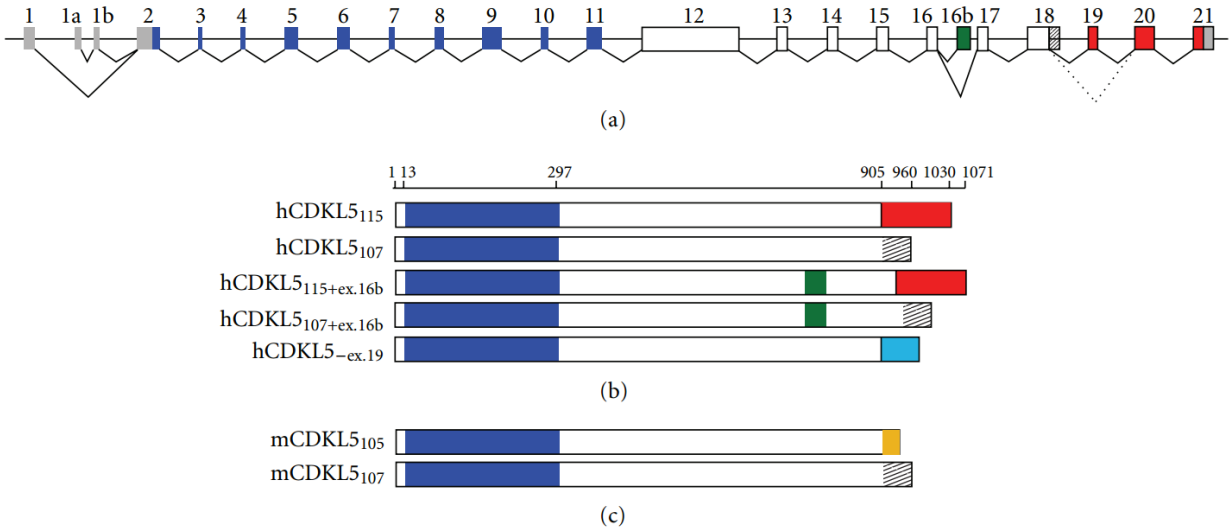

Figure 6. The genomic structure of CDKL5 and its splice variants. *(**A**) Human CDKL5 gene with untranslated sequences in grey and exons encoding the catalytic domain in blue. Exons encoding the common C-terminal region appear in white, whereas isoform-specific sequences are shown in red, green, and as hatched. (**B**) hCDKL5 protein isoforms differing in the C-terminal region. $CDKL5_{115}$ contains the primate specific exons 19-21. In $CDKL5_{107}$, intron 18 is retained. The inclusion of exon 16b would generate $CDKL5_{115+ex.16b}$ and/or $CDKL5_{107+ex.16b}$. $hCDKL5_{-ex19}$ is a hypothetical splice variant in which exon 19 is excluded generating alternative C-terminus (light blue). (**C**) Murine CDKL5 isoforms. $mCDKL5_{105}$ harbors a distinct C-terminal region encoded by a mouse specific exon 19 (orange). As in humans, the retention of intron 18 generates the common $CDKL5_{107}$ isoform. (Image taken from [Kilstrup-Nielsen et al. 2012]).*

Although the $CDKL5_{107}$ isoform is the most important CDKL5 splice variant, there are other species-specific CDKL5 splice variants. A previously unidentified CDKL5 splice variant has been described in rat neurons and glial cells [Chen et al. 2010]. It produces a protein product with a variant C-terminus, ending in rat exon 19, and has a specific tissue distribution. Further investigation of CDKL5 in the mouse or rat as a model for human disease must consider these species-specific variants.

2.2.3 Modulation of CDKL5 abundance and localization

Expression studies in human and mouse tissues have shown that CDKL5 mRNA is present mainly in the brain, where the transcripts levels are the highest, but also in a wide range of tissues. Indeed, it can easily be detected in tissues such as testis, lung, spleen, prostate, uterus, and placenta, while it is barely present, or under detection levels, in heart, kidney, liver, and skeletal muscle.

Interestingly, CDKL5 expression in the brain correlates with neuronal maturation. For CDKL5 levels reach the highest in conjunction with the development and differentiation of this organ: CDKL5 is only weakly present during embryogenesis and get strongly induced in the early postnatal stages until P14 in mice, where after it declines. A detailed analysis of CDKL5 expression in adult mouse brain shows that its mRNA levels are particularly high in the forebrain. Higher expression levels are detected in the most superficial cortical layers, particularly involved in the connection of the two hemispheres through the corpus callosum. A slightly higher abundance of mRNA in the frontal cortical areas might suggest a role for CDKL5 in the physiology of such brain districts. Notably, fairly strong staining is detected in the motor cortex and the cingulate cortex, an area of high interest for the origin of a wide plethora of mental diseases. Furthermore, high levels of expression are detected in the pyriform cortex and, possibly, in the entorhinal cortex. Concerning the hippocampus, a brain area that partly shares the same developmental origin as the cortex, very high levels of CDKL5 mRNA have been found in all the CA fields but in the dentate gyrus, possibly in accordance with the establishment of CDKL5 transcription in fully mature neuronal phenotypes, given that the DG neuronal population undergoes adulthood neurogenesis. Considering the fair expression levels of CDKL5 in the striatum, it might be assumed that the glutamatergic and the gabaergic neurons are by far the two cellular types expressing most of the brain CDKL5. Accordingly, very low expression was detected in dopaminergic areas such as the substantia nigra or the ventral tegmental area or in noradrenergic areas such as the locus coeruleus. Interestingly, however, very high levels of CDKL5 transcripts are detected in several thalamic nuclei, including the geniculate nuclei. In the cerebellum, CDKL5 mRNA is expressed in all the lobules and, possibly, in the Purkinje cells; its levels, however, appear significantly lower when compared to the other brain areas [Kilstrup-Nielsen et al. 2012].

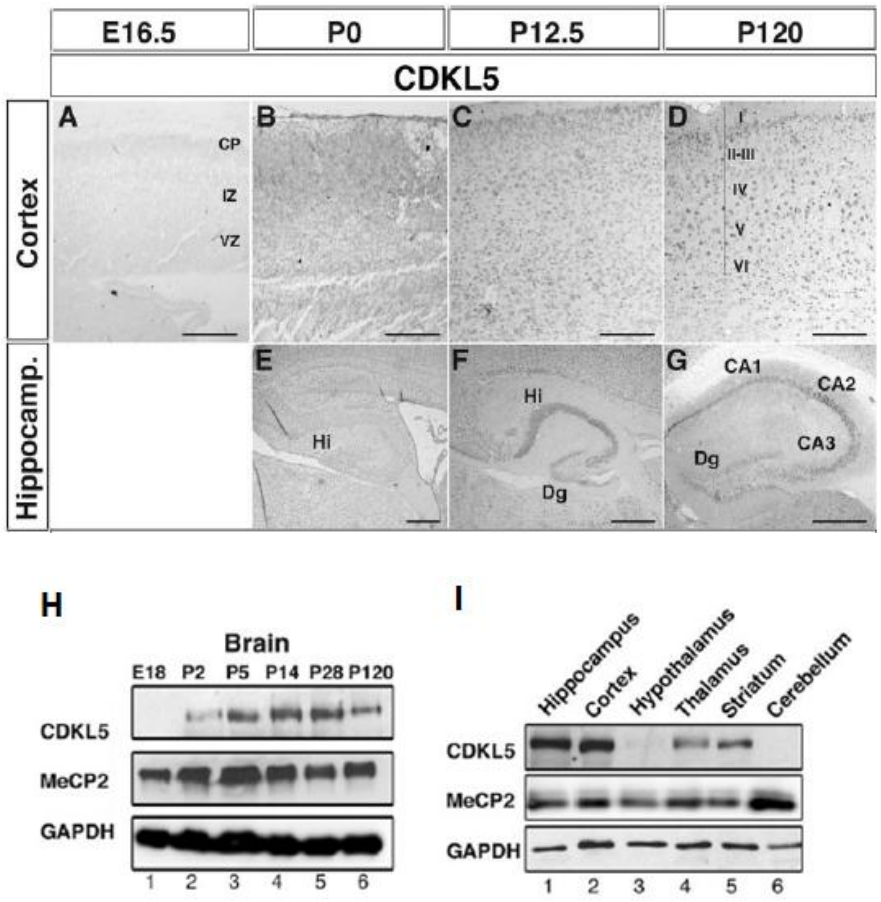

Figure 7. CDKL5 expression is highly induced at early postnatal stages of brain development. *(**A-G**) Immunohistochemistry experiments showing CDKL5 expression in the cortex (**A-D**) and hippocampus (**E-G**) of mouse brains at different embryonic or postnatal stages (**H**) Western blot showing CDKL5 and MeCP2 levels in the total brain at different embryonic and postnatal stages (**I**) Western blot showing CDKL5 and MeCP2 levels in different brain area of adult mice (P120). (Image taken from [Rusconi et al. 2008]).*

Recently, studies on the characterization of CDKL5 transcriptional regulation have been started. In 2010, Carouge and colleagues found in the rat gene a CpG-rich sequence of 0.8 kb, well conserved in the mouse and human counterparts [Carouge et al. 2010]. Interestingly, authors demonstrated that DNA methylation involving this area inhibits CDKL5 expression and the kinase gene is a target of repression mediated by MeCP2. These data apparently contrast earlier reports where CDKL5 mRNA levels were found unaltered in RTT patient lymphocytes or brains of MeCP2-null mice [Mari et al. 2005; Weaving et al. 2004]. However, these contradictory results might stem from the capability of MeCP2 to act on different genes according to the specific cellular type.

CDKL5 transcription appears to be regulated by different stimuli and depending on the specific brain district. For instance, treatment with cocaine, which enhances local serotonin levels, significantly reduces CDKL5 transcription in the striatum of rats, but not in the frontal cortex [Carouge et al. 2010].

Concerning the protein expression, available data suggest that the levels of kinase more or less coincide with those of mRNA in the adult brain. At the cellular level, CDKL5 is easily detectable in neurons while it is expressed at very low levels in the glia. The presence of different CDKL5 splice variants with different relative abundance depending on the localization, indicates that alternative splicing is involved in regulating CDKL5 functions. At the functional level, it still needs to be established whether the different CDKL5 isoforms have distinct functions, whereas the subcellular localization is grossly identical. CDKL5 functions seem to be regulated both through its subcellular localization and through its synthesis and degradation. In brain, CDKL5 is initially predominantly cytoplasmic and progressively accumulates in the nucleus, starting from roughly P14 when approximately 40% of total CDKL5 can be detected in this compartment. However, CDKL5 significantly translocates to the nucleus in certain brain areas: in the cerebellum, for example, more than 80% of CDKL5 remains cytoplasmic while in the cortex it is almost equally distributed between cytoplasm and nucleus. Exogenous CDKL5 shuttles constitutively between the two main compartments in cultured non-neuronal cells through an active nuclear export-dependent mechanism involving the C-terminus of the protein and the CRM1 nuclear export receptor. Interestingly, however, in resting rat hippocampal neurons the protein is not dynamically shuttling and its nuclear exit appears to be regulated by specific stimuli: glutamate treatment induces an active export of CDKL5 leading to its accumulation in the cytoplasm. In the future, it will be interesting to understand whether post-translational modifications or interactions with other proteins are involved in regulating the nuclear export/import of CDKL5, and which other stimuli influence localization and activity of CDKL5 [Kilstrup-Nielsen et al. 2012].

To date, a limited knowledge of the stimuli affecting CDKL5 expression and activities is available. In particular, it has been demonstrated that BDNF, an activity-regulated gene encoding a neurotrophin already involved in several neurological and psychiatric disorders including RTT, induces a transient phosphorylation of CDKL5. For its part the kinase is required for the capability of BDNF to activate Rac1 [Chen et al. 2010]. Rac1 belongs to the Rho GTPase family of proteins and represents a critical regulator of actin remodeling and neuronal morphogenesis, suggesting an involvement of CDKL5 in such processes. Furthermore, it was demonstrated that CDKL5 is transported outside the nucleus into the cytoplasm in response to activation of extrasynaptic NMDA receptors (NMDA-R). Recent publications suggest that extrasynaptic NMDA-Rs have a role in LTD

and dephosphorylation of the transcription factor CREB; alterations in the cross-talk between synaptic and extrasynaptic receptor activities might play an important role in seizures. Of interest, CDKL5 is degraded by the proteasome in response to extended glutamate bath stimulation or other death stimuli. These results, linking CDKL5 to programmed cell death pathways, appear particularly intriguing considering that (i) local cell death and pruning enable proper brain development and (ii) proteolysis by the ubiquitin-proteasome pathway is emerging as a new mechanism controlling synaptic plasticity [Kilstrup-Nielsen et al. 2012].

Concerning this, recent findings show that, at all stages of development, neuronal depolarization induces a rapid increase in CDKL5 levels, mostly mediated by extrasomatic synthesis. In young neurons, this induction is prolonged, whereas in more mature neurons, NMDA-R stimulation induces a protein phosphatase 1-dependent dephosphorylation of CDKL5 that is mandatory for its proteasome-dependent degradation. As a corollary, neuronal activity leads to a prolonged induction of CDKL5 levels in immature neurons but to a short lasting increase of the kinase in mature neurons. Recent results demonstrate that many genes associated with autism spectrum disorders are crucial components of the activity-dependent signaling networks regulating the composition, shape, and strength of the synapse. Thus, it is reasonable to speculate that CDKL5 deficiency disrupts activity-dependent signaling and the consequent synapse development, maturation, and refinement [La Montanara et al. 2015].

2.2.4 CDKL5 kinase targets and critical determinants of substrate recognition

CDKL5 protein is a kinase whose function seems to be very relevant in particular in the central nervous system, by regulating different molecular pathways. However its phosphorylation targets are poorly known.

First MeCP2 protein was identified as a target of CDKL5, at least *in vitro* [Bertani et al. 2006; Mari et al. 2005]. Given the similarities between CDKL5 disorder and Rett syndrome and considering that the cause of RTT has been attributed to mutations in the MeCP2 gene, it is tempting to speculate about the relationship between RTT and CDKL5 disorder on the basis of phosphorylation of MeCP2 by CDKL5. However, due to the fact that phosphorylation of MeCP2 by CDKL5 is relatively weak [Kameshita et al. 2008], it is not reasonable to assume that MeCP2 is a direct substrate of CDKL5. Afterwards, DNA methyltransferase 1 (DNMT1) and netrin-G1 ligand (NGL-1) have been reported to be phosphorylated by CDKL5 [Kameshita et al. 2008; Ricciardi et al. 2012]. DNMT1 is an enzyme that recognizes and methylates hemimethylated CpG after DNA replication to maintain methylation patterns, interacting among other proteins with MeCP2.

Interestingly, NGL-1 plays a crucial role in early synapse formation and subsequent maturation. Furthermore, its phosphorylation by CDKL5 strengthens the NGL1-PSD95 interaction, demonstrating a role for CDKL5 in spine development and synapse morphogenesis [Ricciardi et al. 2012]. In addition, more recently it was identified amphiphysin 1 (AMPH1) as a direct, strongly phosphorylated, CDKL5 substrate in the mouse brain [Sekiguchi et al. 2013]. AMPH1 is a brain specific protein that plays important roles in neuronal transmission and neuronal development, thus suggesting a potential role of CDKL5 in fine control of endocytotic processes in neuronal cells by which neuronal development may be stringently regulated. Furthermore, a lack of AMPH1 is known to cause seizures and striking learning deficits, pointing at AMPH1 as a putative critical molecular component of the pathogenesis underlying CDKL5 neurodevelopmental disorder.

In order to clarify the physiological substrates of CDKL5, it is important to elucidate the detailed molecular mechanisms of substrate recognition by CDKL5. Therefore, the molecular basis of substrate recognition by CDKL5 were recently analyzed by Katayama and colleagues. By using catalytically active CDKL5(1−352) and AMPH1/AMPH2 as model substrates, authors identified the consensus phosphorylation sequence to be RPXSX. Moreover, they reported that CDKL5 recognizes not only the sequence RPXSX around the phosphorylation site (i.e. Ser^{293}) of AMPH1, but also the different region (CLAP domain) as a docking site. These results suggest that CDKL5 shows substrate specificity more restricted than that of other CMGC family protein kinases such as ERK2 and Dyrk1A [Katayama, Sueyoshi, and Kameshita 2015]. Considering that AMPH1 is the most efficient and specific *in vitro* substrate for CDKL5 identified so far and considering its functions in the developing central nervous system, the molecular mechanisms underlying the neurodevelopmental control through phosphorylation of AMPH1 by CDKL5 surely represent an issue to be elucidated.

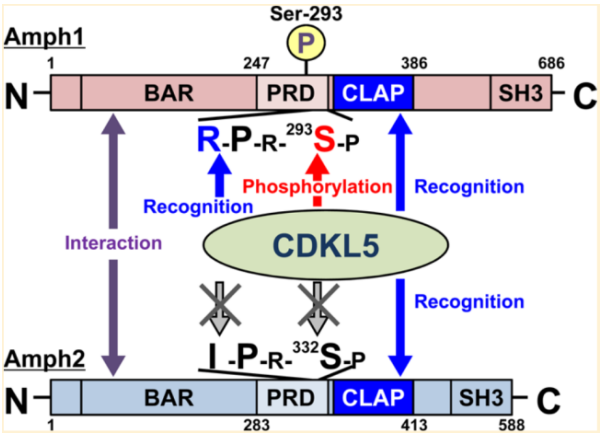

Figure 8. Critical determinants of substrate recognition and phosphorylation site of AMPH1 by CDKL5, as compared to AMPH2 isoform. *Both the phosphorylation site sequence (RPXSX) and the CLAP domain structure in AMPH1 play crucial roles in recognition and phosphorylation by CDKL5. (Image taken from [Katayama, Sueyoshi, and Kameshita 2015]).*

2.3 Molecular mechanisms involved in CDKL5 function

CDKL5 is a ubiquitous protein but is expressed mainly in brain (cerebral cortex, hippocampus, striatum, cerebellum, brainstem), thymus and testes [Lin, Franco, and Rosner 2005]. In the developing mouse brain, CDKL5 expression is strongly induced in early postnatal stages, and in the adult brain CDKL5 is present in mature neurons, but not in astroglia. CDKL5 levels are low in the embryonic cortex and are strongly induced at perinatal and postnatal stages in maturing neurons in the cerebral cortex and hippocampus. This expression profile first suggested a role of CDKL5 protein in neuronal maturation [Rusconi et al. 2008]. CDKL5 shuttles between the cytoplasm and the nucleus, which might reflect a function in both cellular compartments (see e.g. Fig. 9).

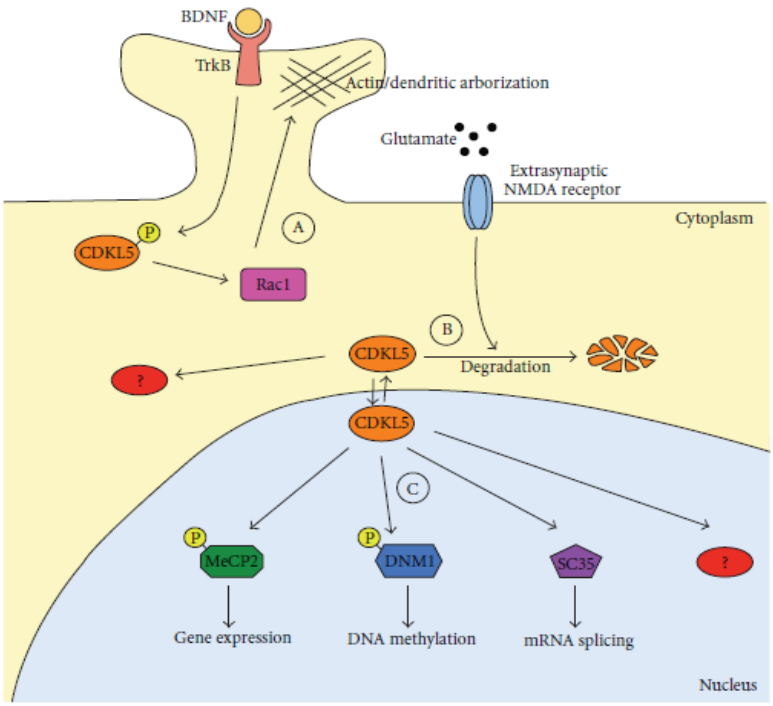

Figure 9. A model depicting some of the CDKL5 functions in cytoplasmic and nuclear compartments. *(**A**) In the cytoplasm CDKL5 is involved in the regulation of actin cytoskeleton and dendritic arborization. This function is mediated by the interaction of CDKL5 with Rac1. (**B**) In the*

*cytoplasmic compartment, the levels of CDKL5 are regulated by degradation. (**C**) In the nucleus, CDKL5 has been proposed capable of interacting and phosphorylating MeCP2 and DNMT1, thereby influencing gene expression and DNA methylation. (Image taken from [Kilstrup-Nielsen et al. 2012]).*

Its presence in the cell nucleus varies at the regional level of the adult brain and is developmentally regulated [Rusconi et al. 2008]. CDKL5 is a kinase, though its phosphorylation targets are poorly known. It is reported that *in vitro* CDKL5 phosphorylates MeCP2, suggesting a common signaling pathway between these two proteins [Mari et al. 2005]. A series of experiments by Chen et al. first provided evidence that CDKL5 plays a critical role in neuronal morphogenesis, and that migratory defects may cause early seizures in patients with CDKL5 mutations. These authors observed that downregulating CDKL5 by RNA interference (RNAi) in cultured cortical neurons inhibits neurite growth and dendritic arborization, whereas overexpressing CDKL5 has opposite effects [Chen et al. 2010]. Knocking down CDKL5 in the rat brain by in utero electroporation resulted in delayed neuronal migration and severely impaired dendritic arborization [Chen et al. 2010]. Recently the first two mouse models for CDKL5-gene–related epileptic encephalopathy have been developed, further shading light on molecular mechanisms regulated by CDKL5. It has been demonstrated that loss of CDKL5 impairs brain development and cognitive behavior in knockout mice. Furthermore, at the molecular level it has been shown that CDKL5 plays a critical role in coordinating multiple signaling cascades, by regulating, among others, the AKT/mTOR/rpS6 and AKT/GSK-3β pathways, important for brain development [Amendola et al. 2014; Wang et al. 2012]. A detailed characterization of CDKL5 mouse models is reported below in a separate section.

2.3.1 CDKL5 regulates the function of epigenetic factors and transcriptional regulators

The first demonstrating the phosphorylation activity of CDKL5 were Mari et al. in 2005. Considering the similar phenotypes caused by mutations in MECP2 and CDKL5, they investigated the expression patterns of both proteins in embryonic and postnatal mouse brains. CDKL5 and the transcriptional repressor MeCP2 show a spatial and temporal overlapping expression during neuronal maturation and synaptogenesis in the brain, in favor of a possible involvement of the two proteins in the same development pathway [Mari et al. 2005]. A schematic representation of MeCP2 mechanism of action as transcriptional regulator is depicted below in Fig. 10.

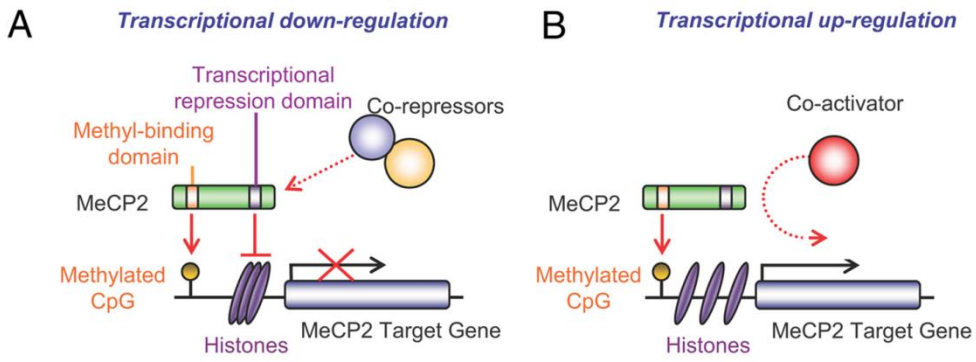

Figure 10. Vignettes of MeCP2 functions as a transcriptional regulator. *MeCP2 binds to methylated CpG regions upstream of the transcriptional start site of target genes and recruits co-factors for repression (**A**) or activation (**B**) of transcription. (Image taken from [Samaco and Neul 2011]).*

Authors also investigated whether MeCP2 and CDKL5 directly interact *in vitro* and *in vivo*. By classical pull-down assays Mari and colleagues demonstrated that MeCP2 and CDKL5 are directly interacting *in vitro* and that a portion on MeCP2, containing the last residues of the TRD and the C-terminal region, is responsible for this association. An analog interaction was demonstrated also in *vivo* by co-immunoprecipitation experiments. Given the interaction between MeCP2 and CDKL5 and the overlapped expression in different brain regions, it was further investigated whether CDKL5 is able to autophosphorylate and to phosphorylate MeCP2. The results demonstrated that CDKL5 is able to phosphorylate itself and to mediate MeCP2 phosphorylation, suggesting that these proteins belong to the same molecular pathway. Nevertheless, there are some controversial results from another research group, which was able to demonstrate the autophosphorylation ability of CDKL5, but not to confirm that CDKL5 directly phosphorylate MeCP2 [Lin, Franco, and Rosner 2005].

Furthermore, a recent report suggested a new link between CDKL5 and MeCP2. Indeed, both proteins have been shown to bind to DNA methyl-transferase 1 (DNMT1), an enzyme that recognizes and methylates hemimethylated CpG dinucleotides after DNA replication in order to maintain a correct methylation pattern [Kameshita et al. 2008]. More recently Carouge and colleagues addressed the question of the transcriptional control of CDKL5 by MeCP2 as a potential link between the two genes, taking advantage of *in vivo* MeCP2 induction by cocaine in rat brain structures [Carouge et al. 2010]. Their data revealed that over-expression of MeCP2 in transfected cells results in the repression of CDKL5 expression and that *in vivo* MeCP2 directly interacts with

CDKL5 gene in a methylation-dependent manner. Taken together these results are consistent with the hypothesis of CDKL5 being a MeCP2-repressed target gene and provide new insights into the mechanism by which mutations in the two genes result in overlapping neurological symptoms [Carouge et al. 2010].

An interesting feature of CDKL5 that distinguishes it from MeCP2 is its subcellular localization. While MeCP2 is only a nuclear protein, CDKL5 shuttles between the nucleus and the cytoplasm. The subcellular localization of CDKL5 within the cell seems to be important for its function. In the nucleus CDKL5 co-localizes and is associated with a number of splicing factors that are stored in specific nuclear foci called nuclear speckles, in both cell lines and tissues. In these structures CDKL5 seems to manage the nuclear trafficking of splicing factors and thus influencing the complex splicing machinery [Ricciardi et al. 2012]. It is already known that phosphorylation of the RS domain of Serine-rich (SR) splicing factors is necessary to release these factors from speckles and to direct them to sites where pre-mRNA processing takes place. Considering that several protein kinases have been described to be able to phosphorylate the RS domain of SR proteins, Ricciardi and colleagues have hypothesized that CDKL5 as well could have a role in nuclear speckles organization. Interestingly, it has been demonstrated that CDKL5 acts on nuclear speckle disassembly determining a redistribution of at least some speckle proteins [Ricciardi et al. 2009]. These results suggest that CDKL5 may play a role in controlling gene expression through phosphorylation of DNMT1 and alteration of CpG methylation, which may affect the transcription of numerous genes. In addition, altering the distribution of the splicing factor machinery within the nucleus may result in alternative splicing of different RNAs leading to a subset of proteins with subtly altered functions.

MeCP2 and DNMT1 are well-known DNA-binding proteins that may function in the nucleus and they both were shown to be phosphorylated by CDKL5 *in vitro*. Nevertheless it is still unclear whether or not these proteins are direct target of CDKL5 in neurons, since the phosphorylation of these proteins is rather weak as the endogenous substrates. Furthermore it is important to mind that CDKL5 is known to be localized not only in the nucleus but also in the cytoplasm. Cellular localization of CDKL5 was reported to change during the process of development: it is mainly expressed in the cytoplasm in the early stages and gradually increased in the nucleus thereafter. Therefore, it is important to increase the knowledge about the endogenous substrates for CDKL5 in the early developing brain in relation to neurodevelopmental disorders resulted from mutations in the CDKL5 gene [Sekiguchi et al. 2013].

2.3.2 CDKL5 affects proliferation and differentiation of cultured neuronal cells

An elegant study carried out by Valli and colleagues in 2012, before the creation of CDKL5 knockout (KO) mouse models, took advantage of neuroblastoma cell cultures (SH-SY5Y and SKNBE cell lines) to study CDKL5 functions *in vitro*. Neuroblastoma cells share several features with normal neurons and thus are considered a good *in vitro* model to study the biochemical and functional properties of neuronal cells, particularly when they are induced to differentiate upon treatment with agents such as retinoic acid. Authors described a correlation between CDKL5 expression and SH-SY5Y differentiation: differentiating SH-SY5Y neuroblastoma cells exhibited strong up-regulation of CDKL5 expression. Conversely, over-expression of CDKL5 protein in SH-SY5Y cells was shown to promote neuronal differentiation (Fig. 11).

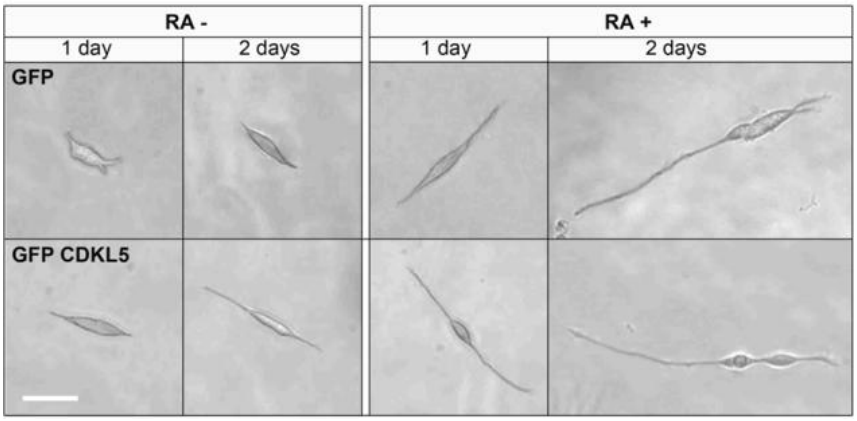

Figure 11. CDKL5 induces differentiation in the SH-SY5Y neuroblastoma cell line. *Contrast phase images show that over-expression of CDKL5 through adenoviral infection induces differentiation in presence or not of retinoic acid (RA). (Image taken from [Valli et al. 2012]).*

Consistently with these data, it was observed that CDKL5 negatively regulates cell proliferation in the SH-SY5Y neuroblastoma cell line, by arresting the cell cycle in the G0/G1 phases. Neuronal proliferation and differentiation represent two closely related processes, primarily important during brain development. Interestingly, CDKL5 expression was shown to be inhibited by MYCN, a transcription factor that promotes cell proliferation during brain development and plays a relevant role in neuroblastoma biology. Indeed, authors showed that MYCN acts as a direct repressor of the CDKL5 promoter [Valli et al. 2012]. These findings not only proposed a cellular mechanism that may explain molecular aspects of the disease phenotype, but also provided a good *in vitro* model to test the activity of a synthetic CDKL5 protein.

Another recent study carried out by University of Siena, Italy, correlates CDKL5 to neuronal differentiation. By using induced pluripotent stem (iPS) cells derived from fibroblasts of MECP2-mutated and CDKL5-mutated patients, authors showed that neurons with CDKL5 mutation and neurons with MECP2 mutation have a common altered gene, GRID1, encoding for glutamate D1 receptor (GluD1). GluD1 is a member of the delta family of ionotropic glutamate receptors which is involved in neuronal maturation. It does not form AMPA or NMDA glutamate receptors, yet it acts like an adhesion molecule by linking the postsynaptic and presynaptic compartments, preferentially inducing the inhibitory presynaptic differentiation of cortical neurons. Results demonstrated that GRID1 expression is down-regulated in both MECP2 and CDKL5-mutated iPS cells and up-regulated in neuronal precursors and mature neurons. Although available data point to a role for GRID1 in neuronal maturation, no data are presently available on which could be the function of GluD1 in neuronal precursor cells. However, both Glutamate and GABA ionotropic receptor subunits and functional receptor channels are expressed very early during brain development in proliferating neuroepitelial cells and are considered important for events such as precursors proliferation, migration, differentiation and survival. It is thus possible that an alteration of GluD1 levels in precursor cells might influence one of these processes and result in alteration of subsequent brain development. Importantly, these data suggest another functional link between MECP2 and CDKL5 genes and provide novel insights into disease pathophysiology, identifying possible new common therapeutic targets for treatment of RTT and CDKL5 disorder [Livide et al. 2015].

2.3.3 CDKL5 affects neuronal development and morphogenesis

As already discussed, CDKL5 expression correlates both *in vitro* and *in vivo* with neuronal maturation, reaching the highest levels of expression when neurons acquire a mature phenotype, thus suggesting an involvement of the kinase in neuronal differentiation and arborization. One of the first *in vivo* studies on the effects of CDKL5 loss-of-function demonstrated that CDKL5 affects neuronal morphogenesis and dendritic arborization in cortical rat neurons subject to RNAi-mediated knockdown of CDKL5 [Chen et al. 2010]. It was proposed a cytoplasmic mechanism as it was found out that in fibroblasts and neurons CDKL5 co-localizes with F-actin in the growth cone and forms a protein complex with Rac1, a critical regulator of actin remodeling and neuronal morphogenesis. In particular, as already mentioned, it was hypothesized that loss of CDKL5 influences neuronal morphogenesis by deregulating the BDNF-Rac1 signaling pathway [Chen et al. 2010].

Recent studies on a CDKL5 KO mouse model confirmed the importance of CDKL5 in neuronal maturation: highly immature pattern and reduced dendritic arborization in cortical and

hippocampal neurons were observed in CDKL5 KO mice [Amendola et al. 2014; Fuchs et al. 2014]. Details are thoroughly discussed below in the text.

Furthermore, one of the very few targets of CDKL5 identified so far is amphiphysin 1 (AMPH1), a brain specific protein involved in neuronal transmission and synaptic vesicle recycling through clathrin-mediated endocytosis [Sekiguchi et al. 2013]. As previously briefly described, in 2013 Sekiguchi and colleagues explored the endogenous substrates of CDKL5 in mouse brains extracts and found AMPH1 as specific cytoplasmic substrate of CDKL5. They demonstrated that CDKL5 phosphorylates AMPH1 exclusively at Ser^{293} and that this phosphorylation is disrupted when mutations in the catalytic domain of CDKL5 occur. It still remains unclear what effect phosphorylation of AMPH1 by CDKL5 has on its function in neuronal development, but interestingly AMPH1 deficient mouse shows major learning difficulties and irreversible seizures, suggesting that AMPH1 is a critical molecular component of the pathogenic pathway of the CDKL5 disorder [Sekiguchi et al. 2013].

2.3.4 CDKL5 contributes to correct dendritic spine structure and synapse activity

Further investigating the role of CDKL5 in neuronal morphogenesis, it was demonstrated that CDKL5 contributes also to correct spine structure and synapse activity. It was shown that CDKL5 localizes almost exclusively at the post synaptic density of excitatory synapses, both *in vivo* and *in vitro*. CDKL5 silencing in rat hippocampal neurons leads to severe deficits in spine density and morphology and similar alterations have been found in neurons established from patient fibroblast-derived pluripotent stem cells (iPSCs), indicating that CDKL5 is required for ensuring a correct number of well-shaped spines. In line with the compromised development of spines, CDKL5-downregulated neurons exhibit a significant decrease in spontaneous miniature excitatory postsynaptic currents (mEPSCs), while there was no significant effect on inhibitory synapse density or any significant changes in miniature inhibitory postsynaptic currents [Ricciardi et al. 2012]. These data suggest that CDKL5 is a key-limiting factor in regulating glutamatergic synapse formation and that changes in excitatory synaptic strength might be responsible, at least in part, for the neurodevelopmental symptoms associated with this disorder.

As previously outlined, at the molecular level CDKL5 interacts and phosphorylates the netrin-G1 ligand (NGL-1), a synaptic cell adhesion molecule (CAMs) that plays a crucial role in synapse homeostasis. NGLs have a conserved C-terminal PDZ-binding domain, which specifically binds to the multidomain protein postsynaptic density (PSD) 95, a protein that plays a significant role in learning and memory. PSD-95 is a major scaffold in the postsynaptic density and has an essential

role in synapse development and maturation. NGL-1 spine-inducing capability is promoted by targeting PSD-95 to new forming dendritic protrusions. CDKL5 phosphorylates NGL-1 on a unique serine (Ser^{631}), which is very close to the PZD-binding domain and this phosphorylation event ensures a stable association between NGL-1 and PSD-95 [Ricciardi et al. 2012]. These data indicate that CDKL5 is critical for the maintenance of synaptic contacts, mainly by regulating the NGL-1 phosphorylated state and thereby its ability to bind PSD-95 and by stabilizing this association.

More recently the critical role of CDKL5 in regulating spine development and synapse activity was further demonstrated by the fact that CDKL5 was shown to directly bind to PSD-95, in a palmitoylation-dependent way. The PSD-95 N-terminal domain is post-translationally modified by palmitoylation, a reversible attachment of 16-carbon palmitate to a cysteine residue. Such palmitate cycling on PSD-95 controls its polarized targeting to synapses, which is essential for its synaptic function. CDKL5 binds to palmitoylated PSD-95 and this binding promotes the targeting of CDKL5 to excitatory synapses. There were proposed two possible ways by which palmitoylated PSD-95 regulates synaptic targeting of CDKL5. First, CDKL5 may bind to palmitoylated PSD-95 at the Golgi apparatus and then the complex moves to the postsynaptic side. Second and more likely important in neurons, free CDKL5 is captured by newly palmitoylated PSD-95 at the dendrites and then trafficked to synapses, to become enriched at the subsynaptic site. Taken together these results demonstrate a critical role of the palmitoylation-dependent CDKL5-PSD95 interaction in localizing CDKL5 to synapses for normal spine development [Zhu et al. 2013].

In particular, PSD-95 is a central element of the postsynaptic architecture of glutamatergic synapses, mediating postsynaptic localization of AMPA and NMDA receptors. PSD-95 is released from postsynaptic membranes in response to Ca^{2+} influx via NMDA receptors and it has been recently shown that Ca^{2+}/calmodulin (CaM) binds at the N-terminus of PSD-95. This N-terminal capping blocks palmitoylation, which is required for postsynaptic PSD-95 targeting and the binding of CDKL5, in turn promoting Ca^{2+}-induced dissociation of PSD-95 from the postsynaptic membrane [Zhang et al. 2014]. Very recently, a further confirmation of the close relationship between CDKL5 and PSD-95 came from a study on a newly generated CDKL5 KO mouse model, which reported that adult mutant mice show a significant reduction in spine density associated with a reduction in PSD-95-positive synaptic puncta [Della Sala et al. 2015].

These data imply that two pathways are important in mediating the cytoplasmic function of CDKL5: first of all CDKL5 is required for BDNF-induced activation of Rac1, which participates in stabilizing the actin cytoskeleton; on the other hand CDKL5, PSD-95 and NGL-1, form a protein complex that functions coordinately to regulate synapse development. These data show that different CDKL5-signaling cascades are involved in synaptic plasticity and learning, acting on spines,

dendritic branching and actin cytoskeleton and elucidate, in part, how the lack of CDKL5 may contribute to the typical neuronal phenotype of the CDKL5 disorder.

2.3.5 Loss of CDKL5 alters lipid serum profile in patients

Very recently, an Italian group lead by Dr. Hayek and Dr. Valacchi demonstrated a cholesterol homeostasis perturbation in CDKL5 patients, similarly to what previously described by the same group for RTT patients [Pecorelli et al. 2011; Sticozzi et al. 2013]. Such alteration was associated with oxidative-mediated loss of the high-density lipoprotein receptor SRB1 (scavenger receptor class B, type 1) and impaired activation of the defensive system Nrf2 (nuclear factor erythroid 2-related factor 2). In addition, CDKL5 fibroblasts showed an increase in 4-hydroxy-2-nonenal– and nitrotyrosine–SRB1 adducts that lead to its ubiquitination and probable degradation.

In particular, authors found a significant increase in HDL and LDL levels in CDKL5 patients. Indeed, SRB1 is involved in the binding of HDL and LDL, thereby promoting selective tissue uptake of cholesterol. Furthermore, SRB1 is also implicated in several other cellular processes, such as recognition of pathogens and apoptotic cells as well as uptake of lipid-soluble antioxidants.

The presence of systemic redox imbalance has been described for both RTT and CDKL5 disorders although the molecular mechanism responsible for increased oxidative stress was not elucidated [Leoncini et al. 2015; Pecorelli et al. 2011]. One of the main mechanisms involved in the cellular antioxidant defense is the activation of the Nrf2 system, a major transcription factor for antioxidant and cytoprotective responses. Upon oxidative stress, Nrf2 translocates into the nucleus and binds to electrophile response elements (EpRE's, also known as antioxidant response elements), increasing transcription of genes related to cellular defense. Impaired Nrf2 activation has been suggested for several pathologies. CDKL5 patients show an increase in both oxidative and nitrosative stress markers and a Nrf2 aberrant activation, all factors that can contribute to cell damage, thus demonstrating a novel mechanism in CDKL5 pathology.

Because of the strictly controlled diet of patients, the reported increase in serum cholesterol levels should be the consequence of an altered lipid metabolism linked to the disease. In addition, cholesterol has multiple roles in the nervous system, from membrane trafficking to myelin formation, along with synapses formation. Therefore, the understanding of cholesterol metabolism has become an emerging area in several neurological diseases. These findings highlights a possible common denominator between RTT syndrome and CDKL5 disorder and a possible common future therapeutic target [Pecorelli et al. 2011].

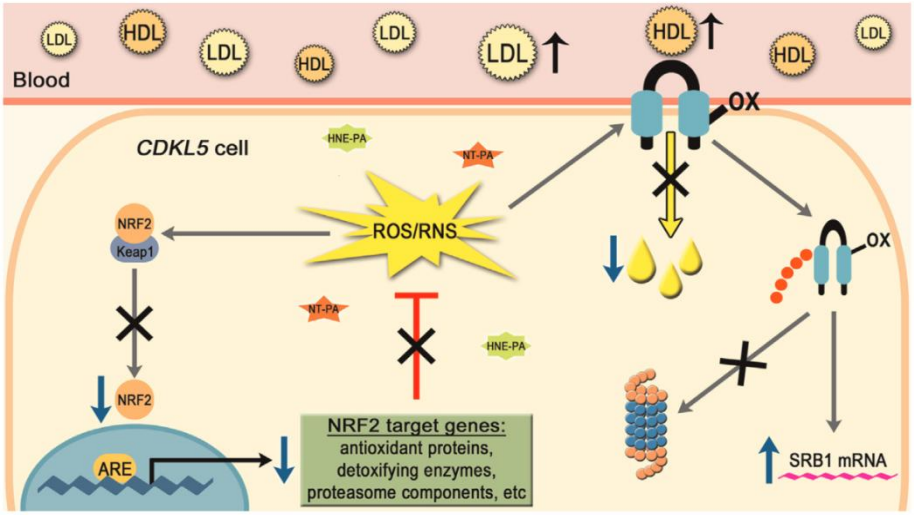

Figure 12. Several mechanisms can play a role in CDKL5 disorder, such as redox imbalance and altered cholesterol pathway. *Owing to a possible Nrf2 aberrant activation with a defective expression of Nrf2 target genes, in CDKL5-defective cells the redox imbalance can contribute to the loss of SRB1 as a consequence of increased oxidative modifications and ubiquitin adduct formation in SRB1 protein. In addition, the decrease in SRB1 levels is associated with the reduction in intracellular lipid uptake and the increase in serum lipoproteins found in CDKL5 patients. Finally, a possible positive feedback loop can be the cause of the SRB1 mRNA overexpression. ARE, antioxidant-response element. (Image taken from [Pecorelli et al. 2011]).*

2.3.6 Oxidative stress and inflammatory status are dysregulated in CDKL5 patients

A complex cytokine dysregulation was recently evidenced in RTT and CDKL5 patients. In CDKL5 disorder in particular, both T helper type 1- (Th1-) related cytokines (IL-1β, TNF-α, IFN-γ, and IL-12p70) and T helper type 2- (Th2-) related cytokines (IL-4, IL-5, IL-6, IL-10, IL-13, and IL-33), except for IL-4, were found to be upregulated. Moreover, increased levels were observed also regarding proinflammatory IL- 22 and regulatory T (T-reg) cytokine TGF-β1. Chemokines were found unchanged. Interestingly, the observed cytokine dysregulation was proportional to clinical severity, inflammatory status, and redox imbalance. Furthermore, 12-month supplementation with ω-3 polyunsaturated fatty acids (PUFAs), in the form of fish oil before food intake, partially counterbalanced cytokine changes, as well as aberrant redox homeostasis and the inflammatory status.

The overall cytokine pattern changes in CDKL5 patients appear to reflect a likely macrophage dysregulation/dysfunction. In particular a strongly increased production of TNF-α and a

strongly increased release of IL-10 and IL-12p70 were evidenced. TNF-α is a proinflammatory cytokine, produced in response to inflammatory stimuli. Elevated levels of TNF-α have been reported in rheumatoid arthritis, ankylosing spondylitis, irritable bowel disease, and psoriasis. Actually, none of the clinical features observed in these associated pathologies are usually present in CDKL5 disorder. Upregulation of both Th1- and Th2-related cytokines in CDKL5 disorder does not translate into increased inflammatory marker levels, likely due to a bulk increase in the anti-inflammatory IL-10 (about 21-fold), a key regulator cytokine of immune response. The clinical translation for the observed changes remains to be elucidated. Nevertheless, cytokine dysregulation in RTT appears to be associated with a proinflammatory status, as evidenced by raised erythrocyte sedimentation rate (ESR) values, as nonspecificmarker of inflammation, and an acute phase protein response. On the other hand, the final result in CDKL5 remains unclear, given that ESR was found to be slightly higher than control values, although not statistically different. To date, no information concerning immunological response, inflammatory status, or defense against infections is available for this condition. Overall, the observed cytokine dysregulation does not appear to translate into a primary immunodeficiency, nor in a classical autoimmune disease. Although the reasons behind to date observed cytokine dysregulation are unknown, possible explanations may include either a defective genetic/epigenetic control on target genes or an aberrant redox imbalance.

Oxidation of polyunsaturated fatty acids, with consequent enhanced formation of isoprostanes and neuroprostanes (markers of brain grey matter oxidative injury), is one of major features of oxidative stress. Analysis of the redox status in both RTT and CDKL5 disorder evidenced oxidative imbalance, mirrored by a strong decrease in reduced/oxidized glutathione (GSH/GSSG) ratio in both conditions.

Therefore, a complex interplay exists between cytokines, redox homeostasis, and inflammatory status in RTT and CDKL5 disorder. Statistically, cytokine levels were found to explain a very consistent fraction of the observed variance for subclinical inflammation and redox abnormality, thus indicating that the aberrant immune response, as regulated by cytokine signalling, is intimately related to redox imbalance and both are likely responsible for modulating phenotype severity.

A beneficial effect of ω-3 PUFAs, in the form of fish oil containing mainly eicosapentaenoic acid (EPA) and docosahexaenoic acid (DHA), partially counterbalance cytokine changes, aberrant redox homeostasis and proinflammatory status. In particular, a consistent number of the investigated cytokines appear to be rescued following a 12-month high dosage supplementation. Target cytokines for ω-3 PUFAs include TNF-α, IL-4, IL-5, IL-13, IL-17A, IL-8, IP-10, and I-TAC in CDKL5

patients. These data appear to further support and extend prior reports on the immunomodulatory effects of DHA and EPA in biological systems.

These findings indicate that RTT and CDKL5 disorders are associated with a subclinical immune dysregulation, as a likely consequence of a defective inflammation regulatory signaling system. This abnormal regulation of the inflammatory response appears to be an unrecognized hallmark feature of such diseases, intimately related to oxidative stress imbalance and likely contributing to disease expression [Leoncini et al. 2015].

2.3.7 CDKL5 is overexpressed in Adult T-cell Leukemia (ATL) cells

Another involvement of CDKL5 in peripheral processes was found by chance in Adult T-cell Leukemia (ATL) biology. In 2007 Kawahara and colleagues attempted a comprehensive analysis of human leukocyte antigen (HLA) class I-bound peptides presented on ATL cells. They took advantage of the latest technology of mass spectrometry combined with reversed phase liquid chromatography (LC/MS) to identify novel tumor-associated antigens. The sequenced peptides for those compatible with the motives of the respective HLA class I alleles were screened and then the candidate peptides were narrowed down according to the differential expression of their source proteins between ATL cells and normal CD4+ T cells. Interestingly, among these candidates, authors found CDKL5 protein to be highly expressed in several ATL cell lines and some ATL clinical samples, but not in normal CD4+ T cells. Therefore, they focused on CDKL5 as a putative novel target of immunotherapy for ATL. They furthermore induced cytotoxic T-lymphocytes from a donor that specifically killed CDKL5+ ATL cells [Kawahara et al. 2007]. The identification of CDKL5 as tumor-associated antigen indicates for the first time *in vivo* an involvement of CDKL5 in tumor biology. While in neuroblastoma cells over-expression of CDKL5 inhibits proliferation and induces differentiation, indicating a sort of anti-tumor effect of CDKL5, no tumor development has been reported so far in CDKL5-deficient patients, but it should be kept in mind that reported patients are all young. Interestingly, on the contrary of what happens in neuroblastoma cells, the kinase was found to be over-expressed in ATL. Kawahara and colleagues did not investigate the specific role of CDKL5 in ATL pathogenesis, but its function in blood cells represents an interesting cue to study.

2.4 CDKL5 KO mouse models

CDKL5 is an X-linked gene associated with early infantile epileptic encephalopathy 2 (EIEE2), atypical Rett syndrome (RTT), and autism spectrum disorders (ASDs). Patients with

CDKL5 mutations display a heterogenous array of clinical phenotypes, the most prominent of which include early-onset seizures and intellectual disability with autistic features. CDKL5 is a serine/threonine (S/T) kinase that is highly expressed in the brain [Kilstrup-Nielsen et al. 2012] and *in vitro* studies demonstrated that it may mediate the phosphorylation of MeCP2 [Mari et al. 2005], DNMT1 [Kameshita et al. 2008], NGL-1 [Ricciardi et al. 2012] and AMPH1 [Sekiguchi et al. 2013]. RNAi-mediated knockdown studies showed that CDKL5 can regulate neuronal outgrowth and synapse stability [Chen et al. 2010; Ricciardi et al. 2012]. Despite these proposed functions, the exact role of CDKL5 in the brain functions remains unclear, and thus requires further investigation. The limited understanding of CDKL5 mechanisms of action and its associated signal transduction pathways has hindered the development of therapeutics for CDKL5-related disorders. For this reason, in order to investigate the functions of CDKL5 in a disease model and identify potential avenues of therapeutic intervention, two different CDKL5 KO mouse models have been recently developed.

2.4.1 The Wang model: deletion of exon 6

In 2012 Wang and colleagues from the University of Pennsylvania, with Dr. Zhou coordinating the research group, generated the first CDKL5 KO mouse. It models a splice site mutation found in a CDKL5 patient. This mutation results in the skipping of human CDKL5 exon 7, generating a premature termination codon and causing an early truncation of CDKL5 in its N-terminal kinase domain, thereby disrupting kinase activity. To mimic the effects of this splice site mutation, it was deleted mouse CDKL5 exon 6 through homologous-mediated recombination in embryonic stem cells. Deletion of CDKL5 exon 6 leads to a similar shift in the reading frame and premature truncation within the N-terminal kinase domain, likely representing a loss-of-function mutation (Fig. 13). Experimental mice have been backcrossed onto the C57BL/6 background for at least six generations and knockout mice resulted viable, fertile, and with normal appearance, growth, and overall brain morphology. Since CDKL5 is localized on X chromosome, the genotypes deriving from deletion of CDKL5 gene are: homozygous females (-/-), heterozygous female (+/-) and hemizygous males (-/Y).

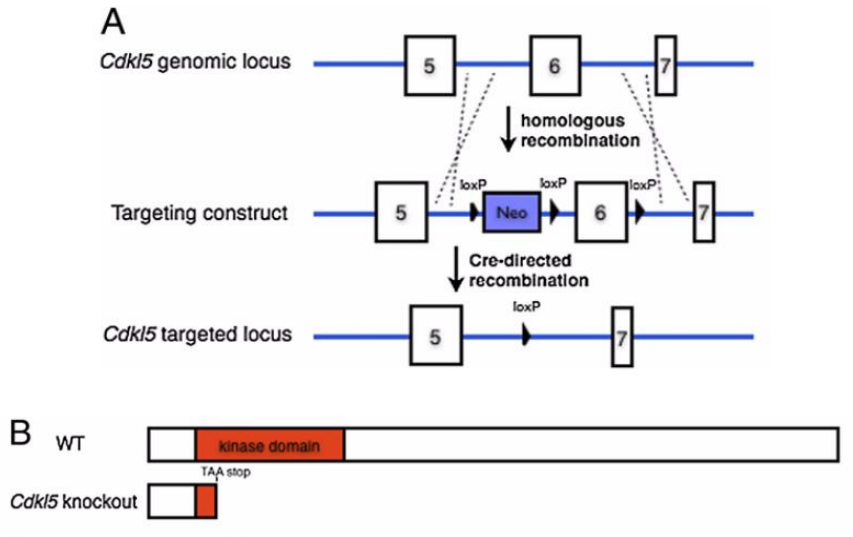

Figure 13. Generation of CDKL5 KO mice in the Wang model. *(**A**) Targeting strategy. Three loxP sites and a neomycin positive selection cassette (Neo) were inserted surrounding the genomic locus of CDKL5 exon 6 via homologous recombination. Upon Cre-directed recombination, both the Neo cassette and exon 6 were excised. (**B**) Schematic of CDKL5 protein in WT and KO. The excision of exon 6 causes a reading frame shift, resulting in a TAA stop codon in the 5' end of exon 7, leading to truncation of CDKL5 in its kinase domain (red). (Image taken from [Wang et al. 2012]).*

Core characteristics of CDKL5-related disorders include early-onset seizures, severe intellectual disability, and autistic-like features. In the behavioral analysis, the Wang model mirrors the latter features, but not early-onset seizures. Despite the large degree of homology between the murine and human CDKL5 protein, the absence of spontaneous seizures observed in the CDKL5 KO mice may reflect a distinct function or modification of CDKL5 in humans that is absent in lower organisms. Moreover, the C57BL/6 genetic background is known to confer increased seizure resistance, thus potentially occluding spontaneous seizures in the CDKL5 KO mice. CDKL5 KO mice display hyperactivity, motor defects, reduced anxiety, decreased sociability, and impaired learning and memory. These phenotypes have been described in other ASD and RTT mouse models and may mimic the absence of hand skills, intellectual disability, hyperactivity, and poor response to social interactions that have been described in CDKL5 patients.

Sensory information processing measured as an event-related potential (ERP) has recently been proposed as a biomarker to monitor neural circuit function in ASD and RTT animal model. In the Wang model ERP analysis showed attenuated and delayed ERP polarity peaks in the KO compared to WT mice, suggestive of impaired neuronal connectivity, which is consistent with

findings in ASD and RTT patients and animal models.

Given the highly conserved S/T kinase domain in CDKL5, the CDKL5 loss-of-function disrupts phosphorylation profile of CDKL5 kinase substrates and related signaling pathways, thereby mediating deficits in neuronal network communication and autistic-like behaviors. Therefore, to investigate the signaling networks affected by the absence of CDKL5 *in vivo*, Wang and colleagues surveyed the S/T kinome profile in CDKL5 KO mice, assessing the consequence of CDKL5 loss-of-function on overall S/T phosphorylation events. Interestingly, the S/T kinome study revealed that many signal transduction pathways are disrupted in CDKL5 KO mice. Of these, many pathway components, including the AKT–mTOR pathway, have been implicated in the etiology of ASDs. Given that mTOR is a known regulator of cell growth, proliferation, motility, and neural plasticity, one consequence of reduced AKT–mTOR activity in the absence of CDKL5 is the disruption of neuronal development. Accordingly, RNAi-mediated knockdown of CDKL5 results in impaired dendritic outgrowth, neuronal migration, and spine maturation. Together, these data suggest a mechanism by which CDKL5 regulates AKT–mTOR-mediated cellular development, thus implicating the AKT–mTOR pathway as a potential therapeutic target for treatment of patients with CDKL5-related disorders.

In addition to the AKT–mTOR pathway, authors found that the phosphorylation profiles of kinases involved in synaptic plasticity, including PKA, PKC and PKD, as well as kinases involved in cellular metabolism, including AMPK, ATM/ATR, and casein kinase (CK) were also decreased in CDKL5 KO mice. Notably, links between these signaling pathways have been previously described, as CK regulates glutamatergic synaptic transmission, ATM mediates AKT S^{473} phosphorylation, and mutations in ATM cause the neurodegenerative movement disorder ataxia telangiectasia. Although many of these signaling changes may be indirect effects of CDKL5 loss-of-function, these data suggest that CDKL5 plays a critical role in coordinating multiple signaling cascades. It is possible, therefore, that CDKL5 may serve to mediate cross-talk between these signaling pathways [Wang et al. 2012].

2.4.2 The Amendola model: deletion of exon 4

At the same time, in parallel to the previously described model, another CDKL5 KO mouse model was created by the EMBL in Monterotondo (Italy), by the group lead by Dr. Gross. A constitutive knockout allele of CDKL5 was produced by germline deletion of exon 4 of a CDKL5 conditional knockout allele produced by standard gene targeting in embryonic stem cells. Stem cell clones were injected into C57BL/6N host embryos. A loxP site was inserted upstream of the exon 4

and positive offspring were further crossed to C57BL/6J congenic Cre-deleter mice to generate the CDKL5 null allele. Similarly to the Wang model, knockout mice have no differences in viability, body weight and brain weight compared to wild type littermates. Furthermore, in order to better define the role of CDKL5 in neurons, authors also used a conditional knockout approach to map the behavioral features identified to distinct populations of forebrain neurons [Amendola et al. 2014].

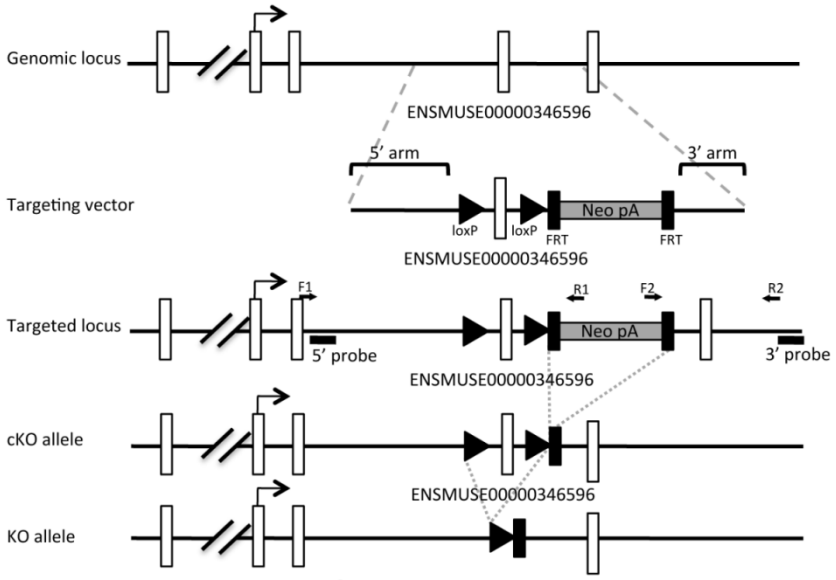

Figure 14. Generation of CDKL5 conditional KO mice in the Amendola model. *Figure shows genomic organization of the CDKL5 locus showing critical exon 4 (ENSMUSE00000346596), the targeting construct, successfully targeted CDKL5 locus (genotyping primers indicated by arrows), FRT-deleted conditional CDKL5 KO allele, and Cre-deleted constitutive CDKL5 KO allele. (Image taken from [Amendola et al. 2014]).*

Behavioral features

Behavioral characterization on constitutive CDKL5 KO mice revealed abnormal clasping of hind-limbs in a significant fraction of heterozygous and homozygous female as well as hemizygous male mice while no, or very low levels of clasping were seen in wild type littermates (Fig. 19). Home cage activity showed a significant decrease in locomotion, not seen when mice were placed in a novel open arena, suggesting that the deficit did not reflect a reduced capacity for locomotion (Fig. 19, graph). Furthermore, loss of CDKL5 impairs hippocampus-dependent learning and memory, assessed with Y-maze, Morris Water Maze and Passive Avoidance tasks. This finding is consistent with neuroanatomical defects seen in the hippocampus of knockout mice, reported below [Fuchs et al. 2015; Fuchs et al. 2014].

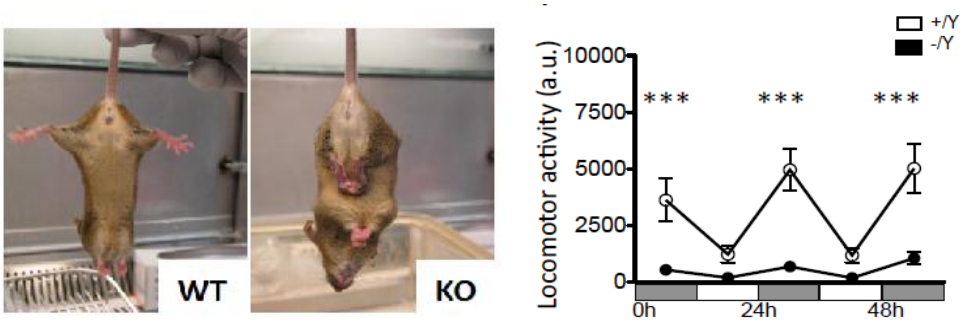

Figure 15. Behavioral impairments in the CDKL5 KO mice*. Image shows clasping behavior (on the left) and locomotor activity (on the right). Image taken from [Amendola et al. 2014].*

Neurophysiological features

Several physiological substrates were examined, including spontaneous and convulsant-induced electroencephalograph (EEG) activity and visual evoked potentials (VEPs). The visual drum test showed that CDKL5 KO mice have a significant decrease in the number of head tracks responses to a continuously moving visual stimulus compared to wild type littermates and VEP analysis indicated deficient visual processing in the mutant mice. Although early onset seizures are a prominent feature of CDKL5 disorder, no evidence for spontaneous seizures emerged during videotaped observations. By backcrossing consitutive CDKL5 KO mice onto the DBA/2J background, Amendola and colleagues demonstrated that the C57BL/6 genetic background, known to have high seizure resistance, was not masking an epileptic phenotype as no evidence of spontaneous seizures in knockout mice emerged on the DBA/2J genetic background. While CDKL5 KO mice do not exhibit spontaneous seizures or increased seizure susceptibility, they do show abnormal EEG response to pro-convulsant (kainic acid) treatment [Amendola et al. 2014].

Neuroanatomical features

Anatomical analysis was carried out in order to identify aberrant morphological features of neurons, including cortical neuron dendritic arborization reported following the developmental knockdown of CDKL5 in rat [Chen et al. 2010]. Reduced dendritic arborization in CDKL5 KO mice was observed in layer V cortical and CA1 hippocampal pyramidal neurons: total length of apical dendritic arbors was significantly reduced in homozygous (-/-) female and hemizygous (-/y) male CDKL5 KO mice compared to wild type littermates, while dendritic arbor length of cortical neurons in heterozygous (-/+) female CDKL5 KO mice showed an intermediate mean distribution. Reduced dendritic arborization was associated with a significant reduction in cortical thickness and in the

thickness of hippocampal layers, including CA1, stratum oriens and the molecular layer of both the upper and lower blades of the dentate gyrus [Amendola et al. 2014].

A further characterization of hippocampus features in the Amendola CDKL5 KO mouse model was carried out by our laboratory. In the early postnatal period, CDKL5 brain expression exhibits a peak [Ricciardi et al. 2012; Zhu et al. 2013], suggesting its potential importance in brain maturation and function. We mainly focused our study on the hippocampal dentate gyrus as it is a region that largely develops postnatally, thus representing an ideal model to study neurogenesis and brain development.

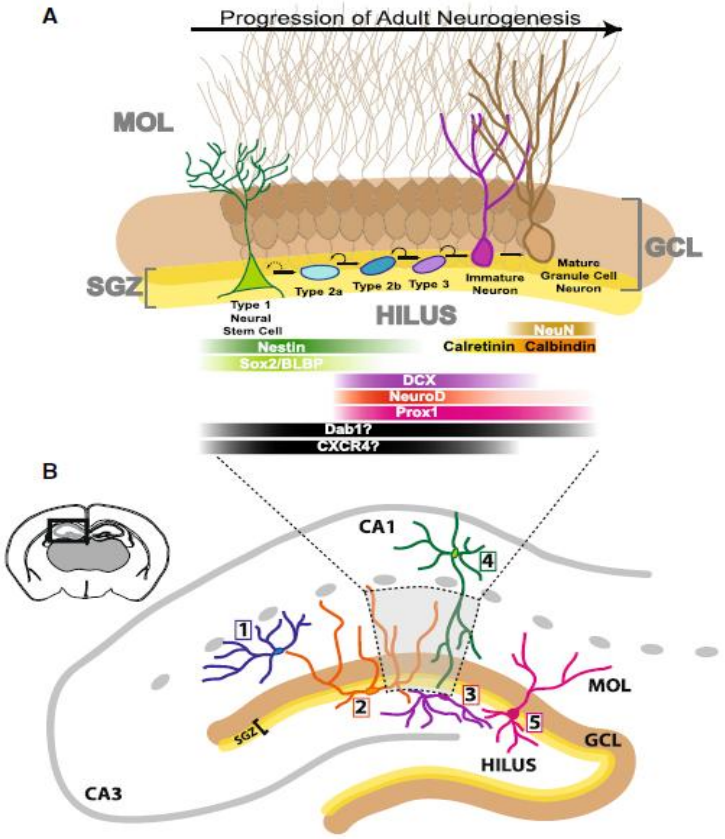

Figure 16. An overview of hippocampal neurogenesis. *(Image taken from [Masiulis, Yun, and Eisch 2011]).*

We found a higher proliferation rate of neural precursors in CDKL5 KO mice in comparison with wild type mice. However, there was an increase in apoptotic cell death of postmitotic granule neuron precursors, resulting in a reduction in total number of granule cells. Looking at dendritic development, we found that in CDKL5 KO mice the newly-generated granule cells exhibited a dendritic tree with a highly immature pattern, evidenced by little branching and elongation (See Fig. 17). These data suggest that CDKL5 plays a fundamental role on postnatal hippocampal

neurogenesis, by affecting neural precursor survival and maturation of newborn neurons [Fuchs et al. 2014].

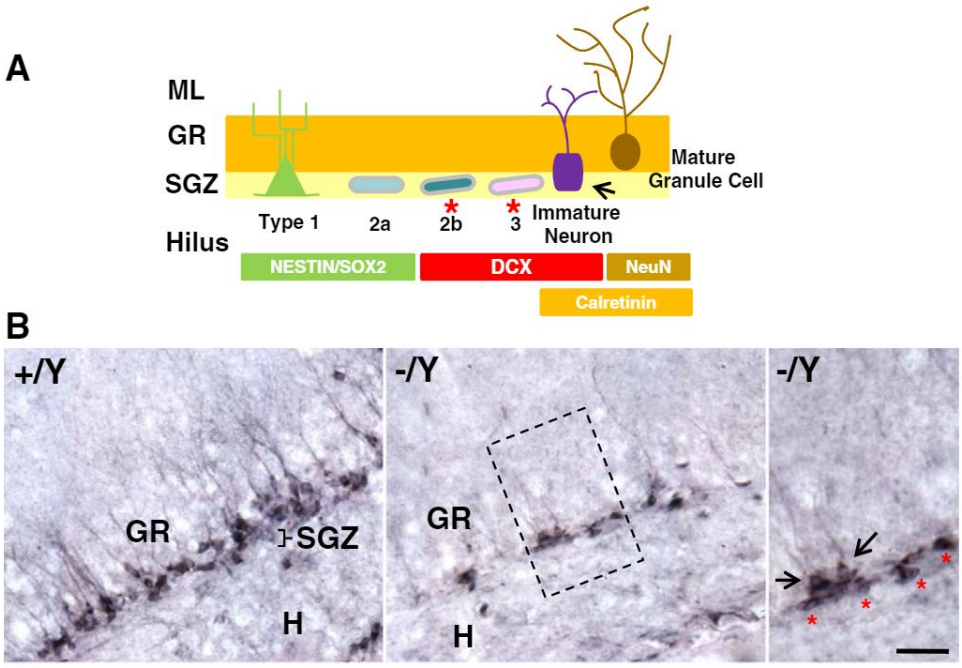

Figure 17. Post-mitotic neurons in the dentate gyrus of CDKL5 KO mice. *(**A**) Schematic representation of adult hippocampal neurogenesis. The subgranular zone (SGZ) of the dentate gyrus (DG) is inhabited by a heterogonous population of cells which go through a series of stages associated with proliferative activity: from stem cell (type 1 cells, expressing Nestin and SOX2) over intermediate progenitor stages (type 2a/b and type 3) to postmitotic maturation. Doublecortin (DCX) is widely expressed by the actively dividing type 2b and type 3 intermediate progenitor cells and also by immature granule neurons and these two cell types can be distinguished based on their morphology: while type 2b/3 cells are orientated parallel to the SGZ (red asterisks), immature granule neurons have a vertical orientation and extend long apical processes into the granule cell layer (GR). (**B**) Examples of sections processed for DCX immunostaining from the DG of wild-type (+/Y) and hemizygous male (-/Y) CDKL5 KO mice. The high magnification photomicrograph show immature DCX-positive neurons (vertical orientation with apical processes; black arrows) in the innermost portion of the GR and type 2b/3 DCX-positive granule cells (orientated parallel to the GR; red asterisks) in the SGZ. (Image taken from [Fuchs et al. 2014]).*

Besides the dendritic arborization, dendritic spines of knockout mice were analyzed. It has been recently shown that rodent neurons silenced for CDKL5 and iPSC-derived neurons from

patients with CDKL5 mutations exhibit aberrant dendritic spines. Furthermore, CDKL5 was shown to interact with synaptic proteins *in vitro* [Chen et al. 2010; Ricciardi et al. 2012]. A first *in vivo* dendritic spine analysis in the CDKL5 KO mouse model demonstrated that CDKL5 plays a crucial role in the organization and maintenance of synaptic structure. Physiologically adult dendritic spines maintain a significant degree of plasticity undergoing different processes such as formation, elongation, stabilization, and retraction. Thus, to understand the role of CDKL5 in these processes, the dynamical changes of dendritic spines in CDKL5 KO mice were analyzed, both during postnatal development and adulthood. Taking advantage of *in vivo* two photon imaging, evidence showed that CDKL5 absence results in a specific deficit of dendritic spines stabilization that is prominent in juvenile mice and that persists in the adult. Consistently, the density of dendritic spines is greatly reduced. Moreover, spine deficits are accompanied by molecular and functional synaptic alterations, consisting in a reduction of synaptic PSD-95, impaired LTP maintenance, and reduced spontaneous EPSC frequency [Della Sala et al. 2015].

Molecular features

Molecular analyses of CDKL5 KO mice brains were carried out on several signaling pathways identified to be altered in MeCP2 knockout mice and thought to be relevant to Rett syndrome. A first screening revealed that no change in MeCP2 protein levels and BDNF immunoreactivity, reported to be reduced in MeCP2 knockout brain, occurred in CDKL5 KO mice.

Looking at the molecular mechanisms whereby loss of CDKL5 may alter brain development, it was identified a central role of activated protein kinase B (PKB/AKT), a critical component of neurotrophin signaling and up-stream modulator of different signaling pathways. Decreased levels of phosphorylated AKT were observed in extracts of hippocampus from CDKL5 KOs when compared to wild type littermates. Moreover, as reported in MeCP2 mutant mice, levels of $Ser^{240/244}$-phosphorylated ribosomal protein S6 (rpS6), a ribosomal regulatory subunit and modulator of protein translation, were significantly reduced in somatosensory cortex of CDKL5 KO mice. Phosphorylation of $Ser^{240-244}$ residues of S6 ribosomal protein is specifically induced by the action of the mTOR/PI3K pathway. These findings suggest that down-regulation of the rpS6 pathway may be a common signaling deficit in CDKL5 disorder and Rett Syndrome and point to defective translational regulation as a potential core mechanisms for common pathological features of these disorders [Amendola et al. 2014].

Besides disruption of AKT/mTOR/rpS6 signaling cascade, it was observed also disruption of the AKT/GSK3β signaling pathway in neural precursor cells of CDKL5 KO mice, leading to reduced phosphorylation at Ser^{9} of GSK-3β. Glycogen synthase kinase 3 (GSK-3β) is a ubiquitously active

serine/threonine kinase which is inhibited upon phosphorylation at Ser^{9} by AKT. AKT/GSK-3β signaling is known to regulate diverse developmental events in the brain, including neurogenesis, neuron survival and differentiation. Further evaluation of phosphorylation levels of proteins involved in the AKT/GSK-3β pathway showed lower phosphorylation levels of: i) PDK1 (PDK1 stands upstream by phosphorylating AKT), ii) AKT, at its two critical residues Thr^{308} and Ser^{473}, iii) GSK-3β at Ser^{9}, and iv) CREB at Ser^{133} in CDKL5 KO in comparison with wild type mice. While CREB phosphorylation and consequent DNA binding is inhibited by activated (Ser^{9}-dephosphorylated) GSK-3β, collapsin response mediator protein-2 (CRMP2) is phosphorylated and consequently inactivated by GSK-3β. In contrast, GSK-3β controls the amount of β-catenin by negatively regulating β-catenin protein stability. In line with an increased activity of GSK-3β, there were found higher phosphorylation levels of CRMP2 and lower levels of β-catenin. No differences were found between CDKL5 KO and wild type mice in the phosphorylation levels of ERK, suggesting a specific alteration of the AKT/GSK-3β pathway in the absence of CDKL5. These findings strongly suggest a putative mechanism by which loss of CDKL5 impairs neuron survival and maturation by disrupting the AKT/GSK-3β signaling pathway [Fuchs et al. 2014].

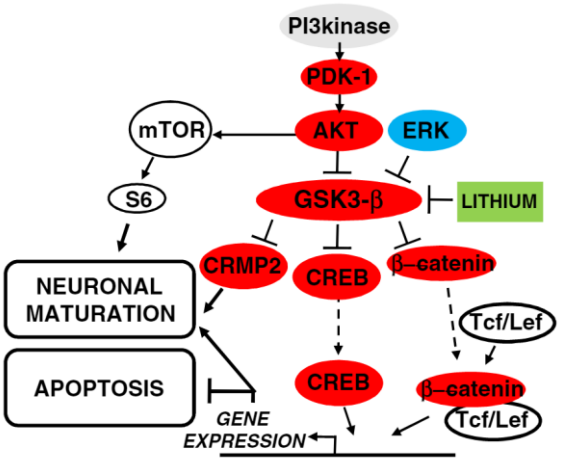

Figure 18. Diagram of AKT/GSK-3β signaling cascade. *Proteins emphasized in red showed significantly altered phosphorylation or expression whereas proteins emphasized in blue did not show significantly alteration in CDKL5 KO mice in comparison to wild-type littermates. Lithium, an inhibitor of GSK-3β, is green colored. Image taken from [Fuchs et al. 2014].*

In conclusion, these data indicate a central role of the AKT/mTOR/rpS6 and AKT/GSK-3β signaling pathways in the pathogenesis of CDKL5 disorder and point toward such pathways as potential therapeutic targets for the treatment of neurological symptoms of the disease. A first

investigation of treatments targeted to these molecular pathways is reported below in the text.

***Ex vivo* neuronal culture analysis**

An *ex vivo* analysis of neuronal precursor cells (NPCs) derived from CDKL5 KO mice was carried out by our laboratory. Cultures of NPCs from the subventricular zone (SVZ) of CDKL5 KO mice were observed to exhibit the same defects observed *in vivo* in granule cell precursors. Namely, in cultures of neuronal precursor cells derived from wild type mice there were more neurons (β-tubulin III positive cells) than in cultures of neuronal precursor cells derived from CDKL5 KO mice. This suggests that the loss of CDKL5 decreases the survival of postmitotic neurons. Assessment of neurite outgrowth in β-tubulin III positive cells demonstrated that neurons generated from CDKL5 KO NPCs were less differentiated compared to wild type neurons. These results indicate that postmitotic NPCs from CDKL5 KO mice have an intrinsic defect, not only in cell survival, but also in neuronal maturation. Furthermore, disruption of the AKT/GSK3β signaling pathway in neural precursor cells of CDKL5 KO mice, leading to reduced phosphorylation at Ser^{9} of GSK-3β, was observed. As shown in Fig. 19, pharmacological normalization of GSK-3β phosphorylation levels restored neuron survival and maturation, suggesting a potential therapeutic strategy to test *in vivo [Fuchs et al. 2014]*.

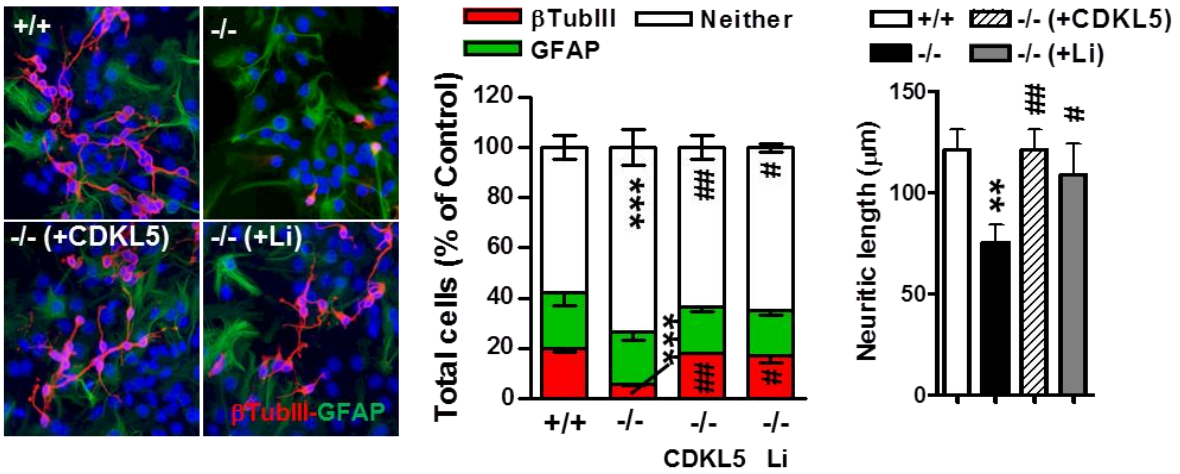

Figure 19. AKT/GSK3-β pathway immunoreactivity in NPCs from CDKL5 KO mice. *Representative double-fluorescence images of NPCs after 6 days of differentiation. Cells with neuronal phenotype are immunopositive for β-tubulin III (red) and cells with astrocytic phenotype are immunopositive for GFAP (green). Cell nuclei were stained using Hoechst dye (blue). NPC cultures from KO mice treated with Litium, a GSK-3β inhibitor, exhibit restored maturation. (Image taken from [Fuchs et al. 2014]).*

Conditional CDKL5 KO models

To help identify the cell-types in which CDKL5 deletion drives pathological phenotypes, Amendola and colleagues examined mice carrying a Cre-conditional knockout (cKO) allele of CDKL5. The CDKL5 conditional knockout allele was crossed with the Dlx5/6::Cre transgene or with the Emx1::Cre transgene respectively for deletion in forebrain GABAergic neurons (e.g. cortical interneurons, striatal medium spiny neurons) or in cortical glutamatergic neurons (e.g. cortical and hippocampal pyramidal neurons).

Both Dlx5/6 and Emx1 cKO mice appeared outwardly normal at birth and showed normal body weight and viability when compared to littermate controls. A general behavioral screen revealed abnormal clasping of hind-limbs in a significant fraction of Emx1-conditional, but not in Dlx5/6-conditional CDKL5 KO mice. Continuous monitoring of home cage activity revealed a significant decrease in locomotion in hemizygous male Dlx5/6-conditional, but not Emx1-conditional CDKL5 KOs. Finally, measurement of head tracking responses to a continuously moving visual stimulus in the visual drum test showed that Emx1 cKO mice showed a trend for decreased head tracking, while Dlx5/6 cKO did not show deficits.

Taken together these data argue that the behavioral phenotypes seen in CDKL5 KOs can be mapped to diverse forebrain neuronal populations, with defects in limb clasping and head tracking associated with glutamatergic neurons and hypolocomotion associated with GABAergic neurons. These findings reveal a double dissociation of behavioral phenotypes and have several implications. First, they suggest that behavioral deficits in CDKL5 disorder derive from the localized absence of the kinase in forebrain neurons. Second, they suggest that the limb control and eye tracking phenotypes depend on cortical motor and visual circuit deficits that are separable from those underlying hypotonia. Whether the later phenotype depends on deficits in cortical interneuron function or deficits in subcortical circuits cannot be determined at this point, although the double dissociation observed in Emx1- and Dlx5/6-conditional mice suggests that non-cortical regions control the hypolocomotion phenotype. Basing on these findings, it is reasonable to hypothesize that therapies aimed at re-expression of CDKL5 in cortical pyramidal neurons may have success in reversing the most debilitating behavioral phenotypes of the disorder [Amendola et al. 2014].

2.5 Current perspectives of treatment for CDKL5 disorder

2.5.1 Pharmacological therapies

CDKL5 disorder is a chronic debilitating condition associated with severe intellectual disability. The neurodevelopmental delay associated with mutations in the CDKL5 gene leads to gross motor impairment, autistic-like features and intractable epileptic seizures from the very first months of life. No cure is currently available for CDKL5 patients given the complexity of this disease, thus having a strong impact on patients' families and on health-care system. Current treatments focus only on managing symptoms and reducing seizure frequency, but have limited effectiveness [Bahi-Buisson and Bienvenu 2012].

The analysis of genetic models of CDKL5 deletion enabled the identification of signaling pathways involved in the brain action of CDKL5. There were reported deficits in the activation of several kinases, suggesting them as potential targets for symptomatic therapies. Below there are reported the few treatments that have been attempted so far to modulate specific aspects of the neurological phenotype of CDKL5 KO mice.

GSK-3β inhibitor SB216763

Exploiting one of the newly generated CDKL5 KO mouse models, our laboratory recently described important defects in the hippocampus of knock-out mice. As CDKL5 expression is higher in the developing brain and seems to be very important in neurogenesis processes, we focused a great part of our work on the hippocampus, a region characterized by ongoing postnatal neurogenesis, that plays a key role in learning and memory. We found that loss of CDKL5 impairs postnatal hippocampal development with a reduction in neuronal precursor survival and maturation. At the molecular level, these defects are accompanied by increased activity of the kinase GSK-3β, a crucial inhibitory regulator of many neurodevelopmental processes [Fuchs et al. 2014]. As a consequence, the following step of our study was to establish whether pharmacological inhibition of GSK-3β could correct hippocampal developmental defects due to CDKL5 loss. We found that treatment with the GSK-3β inhibitor **SB216763** fully rescues hippocampal development and behavioral deficits in a mouse model of CDKL5 disorder. In particular, treatment in developing mice (P20-P45) with SB216763 restored neuronal precursor survival, dendritic maturation and connectivity in term of synapse maturation. Parallel to these structural effects, pharmacological inhibition of GSK-3β restored hippocampus-dependent learning and memory in the CDKL5 KO mouse. Importantly, all these structural and functional effects were retained one month after treatment cessation (P75).

At present, there are no therapeutic strategies to improve the neurological defects of subjects with CDKL5 disorder. Current results point at GSK-3β inhibitors as potential therapeutic tools for the improvement of abnormal brain development in CDKL5 disorder [Fuchs et al. 2015].

AKT/mTOR/rpS6 pathway activator IGF-1

Very little is known about the function of CDKL5 in brain cells. In mice, CDKL5 is expressed at low levels at embryonic stages and its expression is markedly up-regulated during postnatal brain development. Expression analysis suggested that CDKL5 can be localized in postsynaptic structures where RNA interference and mutation analysis showed that it can regulate dendritic spine density and morphology and modulate excitatory synaptic function. The synaptic localization of CDKL5 seems to be regulated by its direct interaction with the palmitoylated form of PSD-95, or by the formation of a complex involving PSD-95 and its interacting protein NGL-1, a target of CDKL5 kinase activity. Considering the strong impairment in dendritic spine stability observed in juvenile CDKL5 KO mice, this phenotype was used by Della Sala and colleagues to evaluate the effects of a treatment aimed at ameliorating CDKL5 KO mice condition.

Furthermore, among the other kinases whose activation was found altered in the CDKL5 KO mouse model, phosphorylation of $Ser^{240-244}$ of S6, a specific target of the AKT-mTOR pathway, is downregulated in CDKL5 mutants. The AKT-mTOR pathway is an important molecular cascade involved in several neurodevelopmental disorders and it is hypofunctional also in RTT models carrying MeCP2 deletion. **Insulin-like growth factor 1** (IGF-1) is an activator of the AKT-mTOR pathway and treatment with IGF-1 was found to ameliorate spine dynamics and behavioral phenotype in murine models of RTT. For, a clinical trial on the use of IGF-1 in MeCP2 patients is currently ongoing and the results of the phase 1 study have been recently published [Khwaja et al. 2014].

Basing on these considerations, Della Sala and colleagues treated young (P24-P27) and adult (P120-P124) CDKL5 KO mice, showing that IGF-1 is able to rescue S6 phosphorylation, spine deficits and defective PSD-95 expression also in this mouse model. In particular, authors found that systemic IGF-1 treatment restored spine density and spine elimination rate. Interestingly, the increased spine density induced by IGF-1 was still present 20 days after the end of IGF-1 treatment, suggesting that the spines induced by IGF-1 are long-lasting and thus candidating IGF-1 as a treatment for synaptic deficits in CDKL5 disorder [Della Sala et al. 2015].

2.5.2 Gene therapy

Gene therapy - the replacement of a mutated gene that causes disease with a healthy and functioning copy of the gene - has becoming a realistic treatment option for genetic based neurologic disorders over the past year. A decade ago, strategies for gene delivery to the brain were limited mostly to stereotaxic injection of viral vectors to the brain and any measure of widespread gene delivery was achieved by the use of multiple injections to create pockets of transgene expression throughout the brain. Recently, advancements in viral vector design and the exploration of alternative routes of administration have made global Central Nervous System (CNS) gene delivery a possibility. The most prominent CNS gene delivery vector is currently **adeno-asscociated virus (AAV)**. Several features make AAV vector an ideal gene delivery vehicle to the CNS. Although AAV naturally infects humans, it is nonpathogenic and is classified as a dependovirus, because infection by AAV occurs only in the presence of a helper virus, either adenovirus or herpesvirus. In addition to its safety, AAV can infect both dividing and non-dividing cells and has the ability to confer long-term stable gene expression without causing associated inflammation or toxicity. Additionally, rapidly evolving vector production and purification methods facilitate both basic research applications as well as the ability to produce the large quantities needed for some clinical trials. Using AAV, advancements in global CNS gene delivery have accelerated to the point that treatments for neurodevelopmental disorders, such as Fragile X Syndrome, Rett Syndrome and CDKL5 disorder, seem within the reach.

The expectation for gene therapy in the treatment of genetic brain disease is high, because much has been promised with this technology and scientific community interest on gene therapy is increasing. However, gene delivery efficacy and genome transduction safety problems have not been completely overcome to enable easy translation from animal models to patients. Anyway no treatments are currently available to improve the neurological phenotype of patients with CDKL5 disorder, thus investigating the possibility of developing a gene therapy to compensate for the lack of CDKL5 in the CDKL5 KO mouse model, in parallel to basic research studies on other therapeutic interventions, surely represents an interesting option to consider.

2.5.3 Protein replacement therapy

Recently, a new alternative approach to gene therapy, named “protein transduction” or “protein therapy” has emerged that enables the trans-vascular delivery of an exogenous protein to the brain following a simple systemic injection. Lately, it has been discovered that certain proteins and

peptides exhibit the unique property of efficient translocation across cell membranes. This unique translocation is usually due to the presence of a Protein Transduction Domain (PTD) in these molecules. PTDs are small peptides that are able to ferry even large molecules into cells independently of classical endocytosis. This property makes PTDs ideal tools to transfer proteins and other molecules into living cells for therapeutic purposes. The mechanism by which this internalization takes place is poorly understood. Although the exact mechanism of transduction is unknown, internalization of these proteins is not receptor- or transporter-mediated. It is therefore likely that all cell types are transducible by these PTDs. PTDs are valuable research tools, as they can be used to deliver molecules into living cells under physiological conditions.

The first proteins to be described to have transduction properties were of viral origin. These proteins are still the most commonly accepted models for PTD action. The HIV-1 Transactivator of Transcription (TAT) protein is the best characterized viral PTD containing protein. The minimal PTD of TAT has been identified as a 9 amino acid protein sequence [Wender et al. 2000]. Earlier experiments with the TAT-PTD protein domain demonstrated successful transduction of fusion proteins up to 120 kDa into murine cells [Nagahara et al. 1998; Schwarze et al. 1999; Xia, Mao, and Davidson 2001]. Schwarze et al. reported that a recombinant TAT-β-galactosidase protein, injected intraperitoneally into mice, was distributed to all tissues including the brain and retained its biological activity [Schwarze et al. 1999]. Importantly, no toxic effect and immunogenicity problems of the TAT-PTD have been reported so far [Verdurmen and Brock 2011].

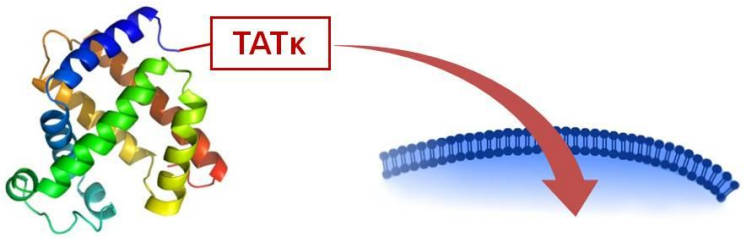

Figure 20. Schematic representation of TAT protein transduction domain ability to carry cargo molecules through cell membranes.

TAT-MECP2 fusion protein

Recently Prof. Franco Laccone (a genetist presently at the Institute of Medical Genetics, University of Vienna) has developed a synthetic MeCP2 sequence for a protein substitution therapy (Patent WO/2007/115578; University of Göttingen, Germany). The invention relates to codon-

optimized nucleic acid sequences for the expression of the MeCP2 protein in heterologous expression systems (i.e. human protein in *Escherichia coli*) fused to the TAT-PTD domain. Prof. Laccone demonstrated that the purified TAT-MeCP2 fusion protein retains its biological activity and is efficiently delivered into the brain. He demonstrated that daily injections of the purified TAT-MeCP2 improved motor learning and extended lifespan of a mouse model of Rett syndrome (see website: WIPO, Search International and National Patent Collections). This is the first demonstration of a possible therapeutic use of a TAT-fusion protein in the nervous system to ameliorate the course of a genetic disease.

Synthetic TATκ-PTD

The trans-acting activator of transcription (TAT) protein transduction domain (PTD) mediates the transduction of peptides and proteins into target cells. The TAT-PTD has an important potential as a tool for the delivery of therapeutic agents. The production of TAT fusion proteins in bacteria, however, is often problematic because of protein insolubility and the absence of eukaryotic post-translational modifications. An attractive alternative, both for *in vitro* protein production and for *in vivo* applications, is the use of higher eukaryotic cells for secretion of TAT fusion proteins. However, the ubiquitous expression of furin endoprotease (also called PACE or SPC1) in the Golgi/endoplasmic reticulum of cells, and the presence of furin recognition sequences within TAT-PTD, results in the cleavage and loss of the TAT-PTD domain during its secretory transition through the endoplasmic reticulum and Golgi, via the costitutive pathway. Detailed analysis of TAT sequence revealed the presence of two furin cleavage sites, characterized by the amino acid sequences RXRR or RXKR (where X can be any amino acid). To overcome this problem, in 2008 Flinterman and colleagues successfully developed a synthetic TATκ-PTD in which mutation of the furin recognition sequences, but retention of protein transduction activity, allows secretion of recombinant proteins, followed by successful uptake of the modified protein by the target cells. In particular, authors introduced mutations into the HIV-TAT within amino acid 47-57 sequence YG**RKKRRQRR**R (furin sites: RKKR and RQRR in bold) to generate a synthetic modified TAT, which lacked the furin sites but retained the protein transduction ability. The resulting sequence is YARKAARQARA and this novel TAT was named TATκ [Flinterman et al. 2009]. This novel strategy for sure has important potential for the efficient delivery of therapeutic proteins. Given its advantages, the TATκ sequence has been used in the present study, where we fused this modified transduction domain to CDKL5, obtaining a TATκ-CDKL5 fusion protein.

3 MATERIALS AND METHODS

3.1 Constructs

3.1.1 TAT-CDKL5 fusion protein for bacterial expression

E. coli codon-optimized TAT-CDKL5$_{115}$ open reading frame was cloned into the pET-28a expression vector. The pET-28a-TAT-CDKL5 plasmid was transformed into *E. Coli BL21(DE3)* cells and recombinant clones were grown in TYP medium at 37°C until OD_{600} around 0.4–0.8. Expression was induced with 1.0 mM IPTG (Isopropyl β-D-1-thiogalactopyranoside) for 3 hours at 37°C. Cells were harvested and protein extracts were obtained by sonication. Expression was checked either by Coomassie stained protein gel or western blot in both the total cell extract (soluble + insoluble) and the soluble fraction only.

3.1.2 TAT-CDKL5 fusion protein for expression in mammalian cells

TAT-CDKL5$_{115}$ fusion gene was cloned into the expression plasmid pTriEx-1.1 with two purification tags, Strep-tag and 6xHis-tag, added at the C-terminal region. HEK 293T cells were transfected with pTriEx-1.1-TAT-CDKL5 plasmid. Cells were grown for 24 hours and TAT-CDKL5 protein was recovered from the cell lysate with a lysis buffer containing 50 mM Tris/HCl pH=8, 500 mM NaCl, 20mM imidazole and EDTA-free protease inhibitors. Extraction was obtained by sonication and 0.25% Nonidet-P40 was then added. After an additional hour of incubation with lysis buffer on ice, supernatant was filtered and added to NiNTA agarose beads (buffer exchanged with lysis buffer) in order to purify TAT-CDKL5 from the total proteins extract. Binding was performed in a rotating wheel at room temperature for 30 minutes. Beads were washed twice (washing buffer contained 50 mM Tris/HCl pH=8, 500 mM NaCl, 50 mM imidazole) and TAT-CDKL5 was eluted for 30 minutes (elution buffer contained 50 mM Tris/HCl pH=8, 500 mM NaCl, 500 mM imidazole). Imidazole was removed with overnight dialysis with PBS at 4°C and TAT-CDKL5 purification was checked with western blot analysis.

3.1.3 Secretable TATκ-CDKL5 fusion proteins

CDKL5$_{115}$, CDKL5$_{107}$ and CDKL5$_{115}$-3xFLAG-2xSTOP cDNAs were cloned into the XhoI

site of the secretable vector pPTK-GFP kindly provided by Dr. Tavassoli. As described by authors [Flinterman et al. 2009], this plasmid carries a modification of TAT linked to GFP (TATκ-GFP), cloned in frame with a signal peptide (Igκ-chain leader sequence) present in a modified mammalian pSecTag2 eukaryotic expression vector (Invitrogen) in which the zeocin selectable marker had been replaced by puromycin. The murine Ig κ-chain V-J2-C signal peptide directs the product to the constitutive secretion pathway. The vector contained also two successive tags (myc-tag and 6xHis-tag) and the resulting constructs were TATκ-GFP-myc-6xHis (original plasmid), TATκ-GFP-CDKL5$_{115}$-myc-6xHis, TATκ-GFP-CDKL5$_{107}$-myc-6xHis and TATκ-CDKL5$_{115}$-3xFLAG (which was cloned AgeI/XhoI to eliminate the GFP sequence). For each construct, insert was PCR-amplified and purified with gel-extraction. The following primers were used: CCGCTCGAGCGAAGATTCCTAACATTGG (forward for TATκ-GFP-CDKL5, both isoforms), CCGCTCGAGCGGACTTGCCCGTCAGTGCC (reverse for TATκ-GFP-CDKL5$_{115}$), CCGCTCGAGCGGACAAGGCTGTCTCTTTTAAATC (reverse for TATκ-GFP-CDKL5$_{107}$), GCACCGGTGAAGATTCCTAACATTGG (forward for TATκ-CDKL5$_{115}$-3xFLAG), CCGCTCGAGCGGATCACTACTTGTCATCGTCATCC (reverse for TATκ-CDKL5$_{115}$-3xFLAG). All primers were purchased by Sigma-Aldrich.

3.2 Production and Purification of the TATκ-CDKL5 Protein

3.2.1 Transient transfection

Human embryo kidney 293T cells were seeded to be 70-90% confluent at transfection. The following day cells were transfected with Metafectene EASY+ (Biontex) or Lipofectamine 3000 (Invitrogen) according to the supplier's instructions. The culture medium was changed immediately before and after 4 hours from transfection with DMEM high glucose culture medium without serum.

3.2.2 Stable clones selection

5’000’000 293T cells were seeded in 10-cm culture dishes and transfected the following day with 20 μg of TATκ-GFP, TATκ-GFP-CDKL5 and TATκ-CDKL5-3xFLAG constructs using Metafectene EASY+ (Biontex) or Lipofectamine 3000 (Invitrogen) according to instructions. After 3 days cells were put under selection with 5 μg/ml puromycin. Selection medium was changed every 3–4 days and clones were picked after 3 weeks.

3.2.3 Concentration/Purification of supernatant

At 48 hours after transfection or stable clones seeding, serum-free culture medium was collected, centrifuged to pellet cell debris and filtered through 0,2 µm syringe filters in order to avoid subsequent clogging of centrifugal filters. The culture medium was then transferred to Amicon Ultra Centrifugal Filters (Millipore) with 50 kDa molecular weight cut-off and was centrifuged at 4 °C resulting in a 20 or 480-fold concentration (for *in vitro* and *in vivo* studies respectively). For *in vivo* treatments the preparation underwent buffer exchange with 80 volumes of saline (NaCl 0.9% sterile solution).

3.3 Cell cultures

3.3.1 HEK 293T cell line

Human embryo kidney 293T cell line was cultured in Dulbecco's modified Eagle's medium (DMEM) supplemented with 10% heat-inactivated fetal bovine serum (FBS), 2 mM of glutamine and antibiotics (penicillin, 100 U/ml; streptomycin, 100 µg/ml), in a humidified atmosphere of 5% of CO_2 in air at 37 °C.

For evaluation of protein transduction activity, 75'000 293T cells per well were seeded onto poly-D-lysine coated slides in 24 well plates. 24 hours after plating, medium was replaced with 100 µL of fresh DMEM with 20% FBS and 100 µL of 40x serum-free concentrated medium containing either vehicle (i.e. 48 hours serum-free culture medium from 293T cells) or TATκ-GFP-CDKL5 protein. After different times (30 min – 1 hour – 2 hours) cells were gently washed with PBS and fixed with a 4% paraformaldehyde solution for 20 minutes at room temperature, and immunocytochemistry anti-GFP was performed.

3.3.2 Neuroblastoma SH-SY5Y cell line

Human neuroblastoma cell line SH-SY5Y, obtained from ATCC (Manassas, VA, USA) were maintained in Dulbecco's Modified Eagle Medium (DMEM) supplemented with 10% heat-inactivated FBS, 2 mM of glutamine and antibiotics (penicillin, 100 U/ml; streptomycin, 100 µg/ml), in a humidified atmosphere of 5% of CO_2 in air at 37 °C. Cell medium was replaced every 3 days and the cells were sub-cultured once they reached 90% confluence.

Neuroblastoma SH-SY5Y cells were treated with TATκ-CDKL5 fusion proteins. The day before treatment SH-SY5Y were plated onto poly-D-lysine coated slides in 24 well plates at density

of 150’000, 60’000 or 10’000 cells/well for protein transduction assay, proliferation assay and differentiation assay respectively. The following day cells medium was replaced with 100 µL of fresh DMEM with 20% FBS and 100 µL of 40x serum-free concentrated medium containing vehicle (i.e. 48 hours serum-free culture medium from 293T cells), TATκ-GFP, TATκ-GFP-CDKL5$_{115}$, TATκ-GFP-CDKL5$_{107}$ or TATκ-CDKL5$_{115}$-FLAG. The treatment was left for either 1 hour or overnight respectively for protein transduction assay and proliferation assay, while it was left overnight and replaced every day for three days for differentiation assay. At the end of each treatment cells were gently washed with PBS and fixed with a 4% paraformaldehyde 4% glucose solution for 20 minutes at room temperature, and the relative analysis were performed.

3.3.3 Neuronal Precursor Cells

Cells were isolated from the subventricular zone (SVZ) of newborn (P1–P2) CDKL5 KO +/Y and CDKL5 KO −/Y male mice. To obtain neurospheres, cells were cultured in suspension in DMEM/F12 (1:1) containing B27 supplements (2%), FGF-2 (20 ng/ml), EGF (20 ng/ml), heparin (5 µg/ml), penicillin (100 units/ml), and antibiotics. Primary neurospheres were dissociated at days 7–8 using Accutase (PAA, Pasching, Austria) to derive secondary neurospheres. The subculturing protocol consisted of neurosphere passaging every 7 days with whole culture media change (with freshly added FGF-2 and EGF). All experiments were done using neurospheres obtained after one to three passages from the initially prepared cultures. Cell cultures were kept in a humidified atmosphere of 5% CO_2 at 37 °C.

For differentiation analysis, neurospheres obtained after three passages *in vitro* were dissociated and plated on cover slips coated with 15 µg/ml poly-l-ornithyine (Sigma) at density 20’000 cells/well. Cells were grown for 2 days and then transferred to a differentiating medium (EGF and FGF free plus 1% foetal bovine serum) from day 3 for 7 days. TATκ-CDKL5 fusion proteins were daily administered at a final 10x concentration after buffer exchange with DMEM-F12, avoiding complete change of culture medium. Every 3 days, half of the medium was replenished with fresh differentiating medium. Differentiated cells were fixed with a 4% paraformaldehyde 4% glucose solution at room temperature for 30 minutes and incubated with anti-glial fibrillary acidic protein (1:400; GFAP mouse monoclonal, Sigma) and anti-β-tubulin III (1:100; rabbit polyclonal, Sigma), as primary antibodies, and with anti-mouse FITC-conjugated (1:100; Sigma) and anti-rabbit Cy3-conjugated (1:100; Jackson Laboratories), as secondary antibodies. Samples were counterstained with Hoechst-33258.

3.4 Biochemical Assays

3.4.1 Kinase Assay

Protein kinase activity results in the incorporation of radiolabeled phosphate from [γ^{32}P]-ATP into a peptide or protein substrate. As a substrate we used TATκ-GFP-CDKL5 itself, exploiting the autophosphorylation activity of CDKL5. TATκ-GFP-CDKL5 and TATκ-GFP concentrated media underwent buffer exchange with a 50 mM Tris/HCl (pH=8) - 500 mM NaCl solution and were subject to purification with Ni-NTA resin exploiting the 6xHis-tag at the C-terminus. The buffer used contained a high saline concentration in order to minimize protein precipitation and, PMSF protease-inhibitor added, it was used also to wash Ni-NTA beads before and after the protein binding. After the overnight binding, Ni-NTA slurry beads were buffer exchanged with a proper buffer (aqueous solution containing: Hepes-NaOH 20 mM (pH=7.4), NaCl 10 mM, $MgCl_2$ 1 mM) and were subject to a kinase assay with 2mM cold ATP and 10 μCi radioactivity from [γ^{32}P]-ATP for 1 hour at 32°C. The reaction was stopped by adding SDS-PAGE loading buffer and boiling for 5 minutes at 100°C. The mix was then immediately loaded onto a polyacrylamide gel and transferred to a nitrocellulose membrane. The radioactivity incorporated into TATκ-GFP-CDKL5 as a consequence of autophosphorylation was assessed by exposing an autoradiographic film to the western blot membrane for 4 days. Radioactive signal on the film was then confirmed by western blot anti-CDKL5 (1:1000; Sigma).

3.4.2 Immunocytochemistry

For immunofluorescence studies the following antibodies were used. Primary antibodies: anti-GFP rabbit polyclonal (1:500, Invitrogen) and anti-FLAG M2 mouse monoclonal (1:1000; Sigma) were used in order to detect the fusion protein inside target cells; anti-β-tubulin III rabbit polyclonal (1:500, Sigma) and anti-glial fibrillary acidic protein (1:400; GFAP mouse monoclonal, Sigma) were used in order to discriminate neurons (β-tubulin III positive) from glia in NPC cultures. Secondary antibodies: Cy3-conjugated anti-rabbit antibody (1:200, Jackson Immuno Research Laboratories), Cy3-conjugated anti-mouse antibody (1:200, Jackson Immuno Research Laboratories), FITC-conjugated anti-rabbit antibody (1:200, Jackson Immuno Research Laboratories). Cells were counterstained with Hoechst-33258, which allowed the identification of mitotic and apoptotic nuclei. Fluorescence images were taken on an Eclipse TE 2000-S microscope (Nikon, Tokyo, Japan) equipped with a digital camera Sight DS-2MBW (Nikon).

3.4.3 Confocal analysis

Confocal microscopy was used to confirm TATκ-GFP-CDKL5 localization inside target cells, after immunofluorescence and western blot analysis. Images immunoprocessed for rabbit anti-GFP antibody (1:500, Invitrogen) were acquired on a Nikon Ti-E fluorescence microscope coupled with an A1R confocal system (Nikon, Tokyo, Japan). Pictures were taken as Z-stack with slices of 0.4 μm.

3.4.4 Analysis of neurite outgrowth

Phase contrast photographs of neuroblastoma cell cultures for differentiation analyses were taken at various time intervals with an Eclipse TE 2000-S microscope (Nikon, Tokyo, Japan) equipped with an AxioCam MRm (Zeiss, Oberkochen, Germany) digital camera. Different areas were randomly selected and neurite outgrowth was measured using the image analysis system Image Pro Plus (Media Cybernetics, Silver Spring, MD 20910, USA). Only cells with neurites longer than one cell body diameter were considered as neurite-bearing cells. The total length of neurites was divided for the total number of cells counted in the areas.

3.4.5 Western blot assay

For the preparation of total cell extracts, cells were lysed in RIPA lysis buffer (Tris–HCl 50 mM, NaCl 150 mM, Triton X-100 1%, sodium deoxycholate 0.5%, SDS 0.1%, protease and phosphatase inhibitors cocktails 1%; Sigma). Protein concentration was estimated by the Lowry method and 30 μg of total proteins were subjected to electrophoresis on a 4–12% NuPAGE Bis-Tris Precast Gel (Novex, Life Technologies, Ltd, Paisley, UK) and transferred to a Hybond ECL nitrocellulose membrane (Amersham Life Science). The following primary antibodies were used to reveal the presence of TATκ-CDKL5 fusion proteins in transfected or treated cells: anti-CDKL5 (1:1000; Sigma), anti-GFP (1:1000, Invitrogen), anti-FLAG M2 (1:1000; Sigma).

3.5 Animal handling

3.5.1 Animal housing and Genotyping

Mice for testing were produced by crossing CDKL5 KO +/− females with CDKL5 KO Y/− males and CDKL5 KO +/− females with Y/+ males. Littermate controls were used for all experiments. Animals were karyotyped by PCR on genomic DNA using the following primers: 108 F: 5′-ACGATAGAAATAGAGGATCAACCC-3′, 109R: 5′-CCCAAGTATACCCCTT TCCA-3′; 125R: 5′-CTGTGACTAGGGGCTAGAGA-3′ [Amendola et al. 2014]. The day of birth was designed as postnatal day (P) zero and animals with 24 hours of age were considered as 1-day-old animals (P1). After weaning, mice were housed three to five per cage on a 12-hours light/dark cycle in a temperature-controlled environment with food and water provided *ad libitum*. Experiments were performed in accordance with the Italian and European Community law for the use of experimental animals and were approved by Bologna University Bioethical Committee. In this study all efforts were made to minimize animal suffering and to keep the number of animals used to a minimum.

3.5.2 Intracerebroventricular cannula implantation and microinjections

Adult mice (3 to 6 months old) were anesthetized with ketamine (100-125 mg/kg) and xylazine (10-12.5 mg/kg). Intracerebroventricular (ICV) guide cannula (diameter 22 G, C313G, Plastics One, USA) was implanted in mice basing on the following stereotaxic coordinates: 0,6 mm posterior and 1,2 mm lateral to bregma, 2 mm depth from the bone surface. Seven days after implantation mice were infused by using a Hamilton syringe connected to a motorized nanoinjector (at a rate of 0.5 l/min). An internal cannula (diameter 26 G, C312I, Plastics One, USA) was used for ICV injections. TATκ-GFP-CDKL5 or TATκ-GFP in saline were injected with the mouse anesthetized at light on. Each mouse received 5 or 10 daily injections with protein in 10 µL bolus volume. Infusion rate was always set at 1 µL/min. The correct cannula position was verified by histology after ink injection (2 µL) at sacrifice.

3.5.3 Intravenous injections

Adult mice (3 to 4 months old) were anesthetized with ketamine (100-125 mg/kg) and xylazine (10-12.5 mg/kg) and dilation of the tail veins was stimulated by placing the tail in a warmer environment (40 ºC water bath) for several minutes. Body temperature was maintained by means of a heated stage. A small-volume sterile insulin syringe with a permanently attached needle (27 gauge) was used in order to have the lower dead volume possible. Being careful not to introduce any air into the syringe, 200 µL of protein preparation were withdrawn. The needle was then inserted 5 mm into the tail vein and verification of the needle to be in vein was ensured by pullback. Being careful not to

perforate the vein, preparation was slowly injected. The needle was then removed and ehanol swab was applied directly to the injection site for 5-10 seconds to stop any bleeding. Each mouse received 5 daily injections.

3.5.4 Subcutaneous injections

Mouse pups (P7) were injected with up to 1 mL vehicle (i.e. 48 hours serum-free culture medium from 293T cells), TATκ-GFP or TATκ-GFP-CDKL5 concentrated media administered subcutaneously. Animals were sacrificed 4 hours after the injection, brains were fixed with a 4% paraformaldehyde solution and immunohistochemistry anti-GFP, followed by a tyramide-based signal amplification, was performed to detect the protein in the brain.

3.6 Behavioral testing

3.6.1 Morris Water Maze Test

Mice were trained in the Morris Water Maze task to locate a hidden escape platform in a circular pool. The apparatus consisted of a large circular water tank (1 m diameter, 50 cm height) with a transparent round escape platform (10 cm^2). The pool was virtually divided into four equal quadrants identified as north-east, north-west, south-east, and south-west. The tank was filled with tap water at a temperature of 22 °C up to 0.5 cm above the top of the platform and the water was made opaque with milk. The platform was placed in the tank in a fixed position (in the middle of the north-west quadrant). The pool was placed in a large room with a number of intra- (squares, triangles, circles and stars) and extra-maze visual cues. After training, each mouse was tested for two sessions of 4 trials each per day, for 5 consecutive days with an inter-session interval of 40 min (acquisition phase). A video camera was placed above the center of the pool and connected to a video-tracking system (Ethovision 3.1; Noldus Information Technology B.V., Wageningen, Netherlands). Mice were released facing the wall of the pool from one of the following starting points: North, East, South, or West and allowed to search for up to 60 s for the platform. If a mouse did not find the platform, it was gently guided to it and allowed to remain there for 15 s. During the inter-trail time (15 s) mice were placed in an empty cage. The latency to find the hidden platform was used as a measure of learning. Retention was assessed with one trial without platform (probe trial), on the sixth day, 24 h after the last acquisition trial, using the same starting point for all mice. Mice were allowed to search for up to 60 s for the platform. For the probe trial, the percentage of

time spent and the frequency of entrances into the quadrant in which the platform had been located during training, the percentage of time spent in the other quadrants and the latency of the first entrance in the former platform quadrant were employed as measures of retention of acquired spatial preference.

3.6.2 Y-Maze Test

Y-Maze Spontaneous Alternation task was used to measure the willingness of mice to explore new environments and hippocampus dependent spatial reference memory. Each mouse was placed at the distal part of one arm facing the center of the maze. Each of the three arms was 34 cm × 5 cm × 10 cm height, angled 120° from the others and made of gray opaque plastic. After introduction into the maze, the animal is allowed to freely explore the three arms for 8 min. Over the course of multiple entries into the arm, the subject should show a tendency to enter a less recently-visited arm. Arm entries were defined by the presence of all four paws in an arm. The 8-min trial was recorded and scored via the ANY-maze video tracking software (Stoelting). The maze was cleaned with 50% ethanol after each trial. The percentage of spontaneous alternations is defined as: (total alternations/total arm entries − 2) × 100. One alternation is defined as consecutive entries into three different arms.

3.6.3 Passive Avoidance Test

For the Passive Avoidance test we used a tilting-floor box (47 × 18 × 26 cm) divided into two compartments by a sliding door and a control unit incorporating a shocker (Ugo Basile, Italy). This classic instrument for Pavlovian conditioning exploits the tendency in mice to escape from an illuminated area into a dark one (step-through method). On the first day mice were individually placed into the illuminated compartment. After 60 s of habituation period, the connecting door between the chambers opened. In general, mice step quickly through the gate and enter the dark compartment due to their innate tendency to prefer dark areas and avoid bright ones. Upon entering the dark compartment, mice received a brief foot shock (2 mA for 3 s) and were removed from the chamber after 15 s of latency. If the mouse remained in the light compartment for the duration of the trial (358 s), the door closed and the mouse was removed from the light compartment. The chambers were cleaned with 70% ethanol between testing of individual mice. After a 24 hour retention period, mice were placed back into the light compartment and the time it took them to re-enter the dark compartment (latency) was measured up to 358 s.

3.6.4 Clasping behavior

Mice were suspended by their tail 1 m above the ground for 2 min. Hind-limb clasping was assessed from video recordings and the total time spent in the clasping position was measured. A clasping event is defined by the retraction of limbs into the body and toward the midline. Data are presented as percentage of time spent in the clasping position in the 2 minutes.

Clasping is a typical behavior of CDKL5 KO mice [Amendola et al. 2014]. Nevertheless a small variability between CDKL5 KO mice leads a small percentage of knockouts not to show clasping behavior. Therefore each animal was tested both before and after the treatment to reduce intra-strain variability and animals not exhibiting clasping behavior before the treatment were excluded by the analysis.

3.7 Histological Procedures

3.7.1 Tissue fixation

Some animals were deeply anesthetized and transcardially perfused with phosphate buffered saline (PBS), followed by a 4% solution of paraformaldehyde in 100 mM PBS, pH 7.4. Brains were stored in the fixative for 24 h, cut along the midline and kept in 20% sucrose in phosphate buffer for an additional 24 h. Hemispheres were frozen and stored a −80°C. The right hemisphere was cut with a freezing microtome into 30-µm-thick coronal sections that were serially collected in antifreeze solution containing sodium azide.

Some animals were deeply anesthetized and the brain was removed and cut along the midline. One hemisphere was Golgi-stained using the FD Rapid Golgi Stain™ Kit (FD NeuroTechnologies, Inc., Columbia, MD, USA) according to instructions and subsequently cut into 80-µm-thick coronal sections. Hippocampus and cortex from the other hemisphere and the cerebellum were rapidly frozen with dry ice and stored a −80°C for subsequent total protein extraction.

3.7.2 Immunohistochemistry

One out of 12 serial brain sections from the region of interest were used for immunohistochemistry with the following antibodies: anti-GFP rabbit polyclonal (1:500, Invitrogen), anti-doublecortin (goat polyclonal, 1:100, sc-8066, Santa Cruz Biotechnology), anti-cleaved caspase-

3 (rabbit polyclonal, 1:200, 9661, Cell Signaling Technology), anti-synaptophysin (SY38 mouse monoclonal Ab, 1:1000, MAB 5258, Merck Millipore), anti-AIF1 (rabbit polyclonal, 1:1000, Thermo Scientific). For anti-GFP and anti-cleaved caspase-3 immunohistochemistry procedures the signal was amplified through TSA cyanine-3 plus evaluation kit (Perkin Elmer), according to instructions.

3.7.3 Number of DCX-positive cells

DCX-positive type 2b/3 cells (parallel-oriented to the subgranular zone), and DCX-positive immature granule neurons (vertically-oriented cells with long apical processes), were separately counted in one out of 12 hippocampal sections. The count was done within an area that included the subgranular zone and the deepest two rows of cells in the granular layer. DCX-positive cells were expressed as number of cells/mm^2.

3.7.4 Measurement of the dendritic tree

Dendritic trees of DCX-positive granule cells sampled in the inner part of the granule cell layer close to the subgranular zone, and Golgi-stained granule cells and CA1 pyramidal neurons were traced with a dedicated software, custom-designed for dendritic reconstruction (Immagini Computer, Milan, Italy), interfaced with Image Pro Plus. The dendritic tree was traced live, at a final magnification of 500×, by focusing into the depth of the section. The operator starts with branches emerging from the cell soma and after having drawn the first parent branch (order 1, primary dendrite) goes on with all daughter branches of the next order in a centrifugal. At the end of tracing, the program reconstructs the number and length of individual branches of each order, the mean length of branches of each order, total number of branches and total dendritic length.

3.7.5 Spine density/morphology

In Golgi-stained sections, spines of granule cells were counted using a 100× oil immersion objective lens. Dendritic spine density was measured by manually counting the number of dendritic spines on dendritic segments in the inner and outer half of the molecular layer and expressed as the number of dendritic spines per 20 μm dendritic length. The dendritic spine length was measured by manually drawing a vertical line from the tip of the protrusion to the point where it met the dendritic shaft. The number of spine clusters was counted manually on dendritic segments in the inner and

outer half of the molecular layer and expressed as number of spine clusters per 50 μm dendritic length.

3.7.6 Synaptophysin densitometry

One out of 12 free-floating coronal sections from the DG of animals were processed for immunohistochemistry as previously described [Guidi et al. 2013]. Intensity of SYN immunoreactivity was determined by optical densitometry of immunohistochemically stained sections. Fluorescence images were captured using a Nikon Eclipse E600 microscope equipped with a Nikon Digital Camera DXM1200 (ATI system). Densitometric analysis in the molecular layer and cortex was carried out using the Image Analysis System Image Pro Plus (Media Cybernetics, Silver Spring, Md. 20910, USA). A box of 4000 μm^2 was placed in the cortical layers II, III and IV-VI and a box of 400 μm^2 was placed in stratum radiatum of CA1 and stratum moleculare of the dentate gyrus. Measurements were taken in each region of interest, normalized to background. In particular, for each image the intensity threshold was estimated by analyzing the distribution of pixel intensities in the areas that did not contain immunoreactivity and this value was subtracted to calculate the optical density of each sampled area.

3.7.7 Number of apoptotic cells

Apoptotic cells (cleaved caspase 3-positive cells) were counted in one out of 12 sections. The count was done in the hippocampal granular layer. The total number of apoptotic cells in the granular layer was estimated by multiplying the number of cells counted in the series of sampled sections by the inverse of the section sampling fraction (ssf = 1 / 12).

3.8 Statistical analysis

Data from single animals were the unity of analysis. Results are presented as mean ± standard error of the mean (±SE). The software SPSS was used for statistical analysis. Statistical testing was performed using a two-way analysis of variance (ANOVA) with genotype (CDKL5 +/Y; CDKL5 −/Y) and treatment (vehicle, TATκ-CDKL5 protein) as fixed factors and mouse as random factor, or using a one-way ANOVA followed by Fisher LSD post hoc test or Duncan's test. A p-value < 0.05 was considered to be statistically significant.

4 RESULTS

4.1 TAT-CDKL5 can be efficiently produced as secretable fusion protein in mammalian cells

4.1.1 TAT-CDKL5 recombinant protein cannot be produced in bacteria

To develop a protein therapy for CDKL5 disorder the first step was to produce and purify a TAT-CDKL5 fusion protein. The low cost and simplicity of cultivating bacteria make the bacterial expression system a preferable choice for the production of therapeutic proteins, both on a lab scale and in industry. The most commonly used bacterium for recombinant protein production is *Escherichia coli*, an enteric bacterium that has a long pedigree of safe use in laboratories and industry. *E. coli* is a particularly suitable host because it is well characterized physiologically and metabolically; it was among the first organisms to have its entire genome sequenced and many molecular biology tools are available for engineering its DNA sequences to generate novel functionality [Overton 2014]. Bacteria have not developed sophisticated mechanisms for performing posttranslational modifications, such as glycosylation, which are present in higher organisms. As a consequence, an increasing number of protein therapeutics is expressed in mammalian cells. However, for proteins that are not required to be synthesized in a glycosylated or extensively post-translationally modified form, bacteria are an excellent expression system because of their relative simplicity.

Given these premises, the first attempt to produce a recombinant TAT-CDKL5 fusion protein was carried out using a common bacterial expression system. An *E. coli* codon-optimized TAT-CDKL5 open reading frame was cloned into the pET-28a vector. pET-28a-TAT-CDKL5 plasmid was transferred into *E. Coli BL21* cells and recombinant clones were grown in TYP medium at 37°C. Following a 3-hr expression induced with 1.0 mM IPTG, cells were harvested, sonicated and protein extracts were obtained. No TAT-CDKL5 protein expression was detected in *E. Coli* protein extracts (Fig. 21), suggesting the absence, or very low levels, of TAT-CDKL5 expression.

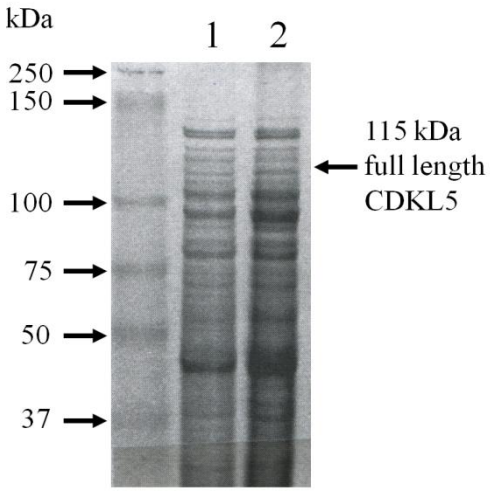

Figure 21. TAT-CDKL5 full-length recombinant production in E. coli BL21. *Image shows result of Coomassie blue staining of a gel loaded with E.coli lysate prior to IPTG induction (lane 1) and after 3 hours of IPTG induction (lane 2).*

Indeed, the difficulty in obtaining a constitutively active full-length CDKL5 through *E. coli* expression systems has been reported by various authors in the past few years [Katayama, Sueyoshi, and Kameshita 2015].

Furthermore, it has recently been demonstrated that CDKL5 is almost completely degraded in *E. coli* bacterial cells (unpublished observation by Dr. Tutino). In particular, *E. coli* insoluble fraction (i.e. bacterial pellet) contains TAT-CDKL5 products whose size is compatible with either aggregated (higher molecular weight) or proteolytically cleaved (lower molecular weight) forms. On the other hand, the soluble fraction, namely the only fraction from which the protein can be recovered, does not contain full-length TAT-CDKL5 protein.

Taken together, such observations hinder the production of TAT-CDKL5 fusion protein through the classical bacterial expression systems.

4.1.2 Inefficient TAT-CDKL5 protein purification from mammalian cells

Due to the impossibility of producing the recombinant TAT-CDKL5 protein in bacteria, we set up expression of the recombinant protein in mammalian cells. This method is less efficient, but has the great advantage of ensuring exactly the same post-translational modifications carried by the endogenous protein. For this reason about half of all recombinant therapeutic proteins currently on the market are produced in mammalian cells.

Hence, the TAT-CDKL5 fusion gene was cloned into the expression plasmid pTriEx-1.1. This plasmid is designed to allow expression of genes in multiple expression systems and high expression levels of target proteins. In order to purify the TAT-CDKL5 protein, we added two successive tags, Strep-tag and 6xHis-tag, at the C-terminal region of the TAT-CDKL5 gene. HEK 293T cells were transfected with TAT-CDKL5 plasmid. Cells were grown for 24 hours and TAT-CDKL5 protein was recovered from the cell lysate and purified using an immobilized-metal affinity chromatography that is based on the proven 6xHis-tag-Ni-NTA interaction. We found that the starting quantity of soluble recombinant TAT-CDKL5 protein obtained from HEK 293T cell extract was very low (Fig. 22-A). It should be noted that purification of a large protein like CDKL5 (115 kDa) may be inefficient due to insolubility of the protein. After trying various buffer conditions, we found that the best condition to enhance TAT-CDKL5 protein solubility and stability requires a lysis buffer with high ionic strength (500 mM NaCl) (data not shown). However very little purified protein was eluted from the column (Fig. 22-A), and the dialysis or diafiltration process to remove the imidazole led to an even lower quantity of protein (Fig. 22-B).

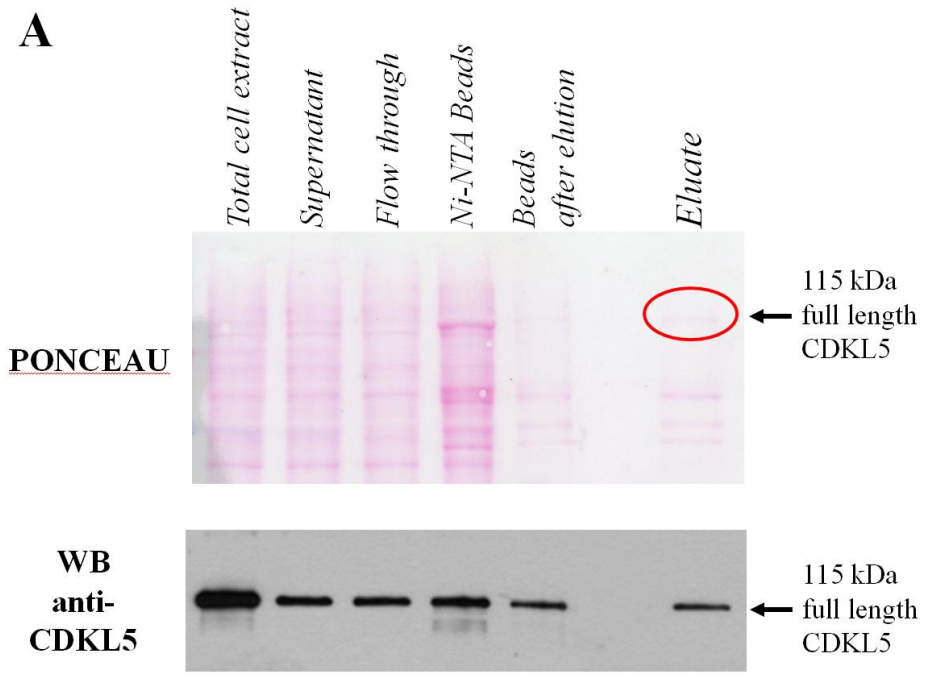

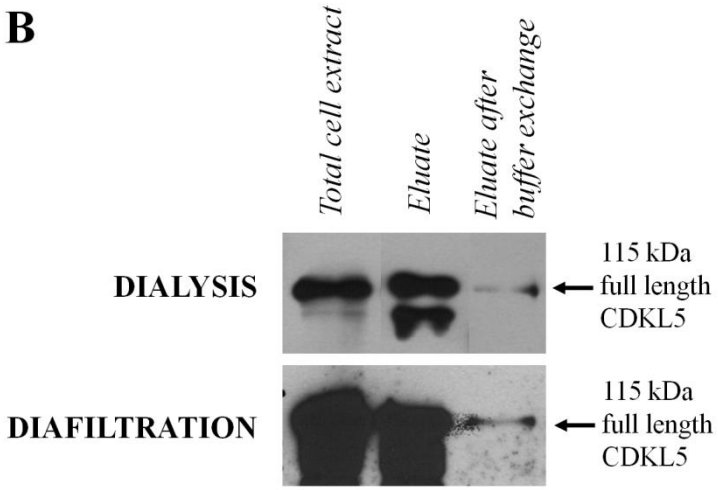

Figure 22. TAT-CDKL5 fusion protein expression and purification in HEK 293T mammalian cells. *(**A**) Taking advantage of a 6xHis-tag, TAT-CDKL5 protein was purified from cell extract using Ni-NTA beads. We found that the starting quantity of protein produced in 293T cells is low (Total cell extract) and a consistent fraction of protein is lost at every purification step, so that very few purified (Eluate) protein is obtained. (**B**) After purification the eluate underwent dialysis or diafiltration to remove mobile phase containing imidazole, leading to a very small amount of purified protein.*

4.1.3 Efficient expression pattern and purification of secretable TATκ-CDKL5 fusion proteins

In order to overcome purification problems and enhance protein recovery, we took advantage of a novel system for the secretion of TAT recombinant proteins from mammalian cells. The success of this system is due to the identification and modification of the two furin sites present in the TAT peptide. Furin is the best-characterized mammalian enzyme from the subtilisin-like convertases and is an endoprotease that recognizes and cleaves the amino acid sequences RXRR or RXKR, where X can be any amino acid. Furin is mainly localized in the trans-Golgi network but can translocate between the trans-Golgi network and the cell surface (Denault JB 1996). Therefore, the presence of these furin sites in the TAT moiety results in the TAT peptide being cleaved from fusion proteins that are secreted via the constitutive pathway. Recently, Flinterman and colleagues introduced mutations to destroy the two furin cleavage sites without affecting TAT protein transduction ability. The modified TAT was named TATκ [Flinterman et al. 2009].

A TATκ-CDKL5 fusion gene containing a human CDKL5 was cloned into the expression plasmid pSecTag2 (Life Technologies). This plasmid is designed to allow expression of genes in mammalian hosts and high expression levels of target proteins. Proteins expressed from pSecTag2 are fused at the N-terminus to the murine Igκ chain leader sequence for protein secretion in culture medium. Due to the absence of a suitable anti-CDKL5 antibody, the TATκ-CDKL5 fusion protein was tagged with a GFP protein to monitor the expression levels and localization of the TATκ-CDKL5 fusion protein. Furthermore, to facilitate protein purification, the TATκ-CDKL5 fusion protein was configured to include a myc-tag and 6xHis tag at the C-terminal region of the TATκ-GFP-CDKL5 gene.

HEK 293T cells were transfected with the TATκ-GFP-CDKL5 expression plasmid and grown in serum-free medium (High glucose Dulbecco's Modified Eagle Medium, DMEM). After 48 hours the medium was collected, diafiltered and concentrated with 50 kDa cut-off Amicon ultra centrifugal filters (Fig. 23-A exemplifies the procedure). This method allows high recovery of the secreted TATκ-GFP-CDKL5 protein.

Fig. 23-B demonstrates western blot analysis results from TATκ-GFP-CDKL5 protein expression in transfected HEK 293T cells. Western blot image on the left demonstrates TATκ-GFP-CDKL5 fusion protein expression in cell homogenates from transfected HEK 293T cells, while western blot image on the right demonstrates TATκ-GFP-CDKL5 fusion protein accumulation in concentrated (20×) cell culture medium from transfected HEK 293T cells.

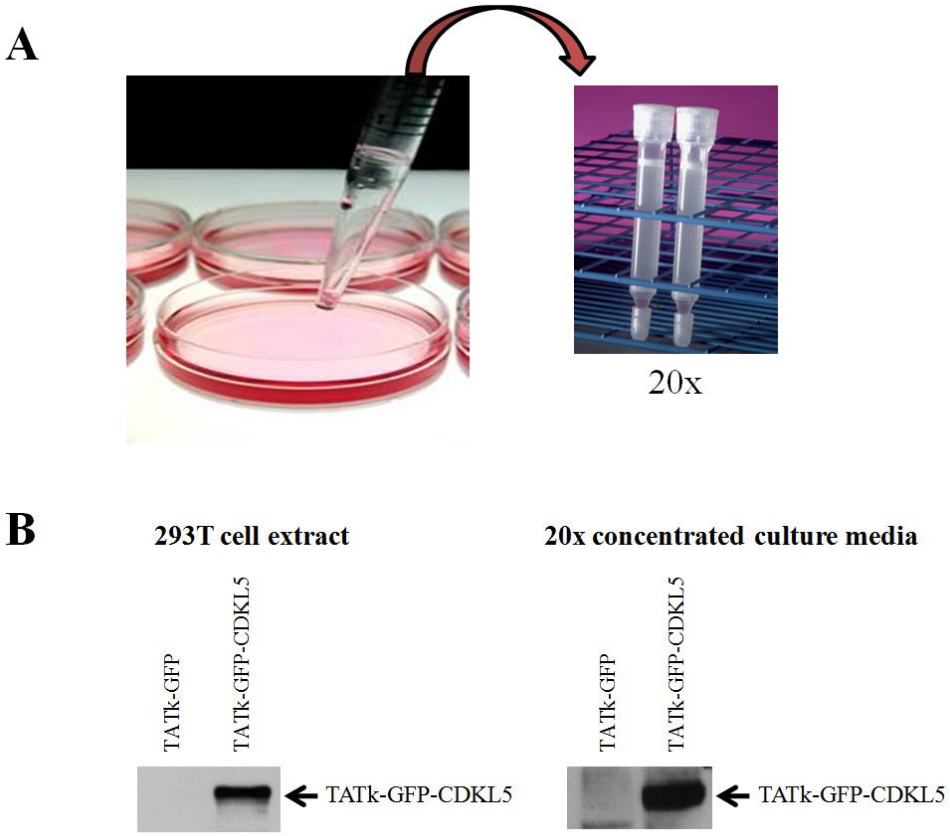

Figure 23. TATκ-CDKL5 Production method. *(**A**) Scheme of the production and purification of the fusion protein TATκ-GFP-CDKL5. TATκ-CDKL5 protein was GFP tagged in order to identify CDKL5. (**B**) Western blot analysis with anti-CDKL5 antibody confirmed TATκ-CDKL5 protein expression in transfected 293T cells (left panel) and accumulation in the concentrated culture medium (right panel).*

The main advantages of using this production method instead of recovering the protein from cell lysate consist in higher recovery of protein together with the advantage of avoiding the use of strong chemicals for lysis and purification. Indeed, physiological buffers are used during the whole process.

4.2 Target cells are efficiently transduced by TATκ-CDKL5

To evaluate the efficiency of transduction of TATκ-GFP-CDKL5 protein, HEK 293T cells were incubated with the purified/concentrated fusion protein. After different incubation times, cells were lysed and total protein extracts were transferred to a nitrocellulose membrane for immunoblotting for TATκ-GFP-CDKL5 protein quantification. As shown in Fig. 24-C, TATκ-GFP-

CDKL5 is internalized by cells after only about 30 minutes of incubation. Other cultures were treated in parallel and were fixed and immunostained with an anti-GFP specific antibody to visualize the transduced TATκ-GFP-CDKL5 protein. As demonstrated in Fig. 24-A, TATκ-GFP-CDKL5 protein was efficiently translocated into the cells.

The internalization in target cells was confirmed by confocal microscopy (Fig. 24-B). SH-SY5Y neuroblastoma cells were incubated for 30 minutes with the supernatant collected from 293T cells expressing TATκ-GFP-CDKL5. Fig. 24-B shows serial confocal images (1-12) of TATκ-GFP-CDKL5 transduced SH-SY5Y cells, demonstrating that TATκ-GFP-CDKL5 protein is internalized by target cells and localized both in the nucleus and cytoplasm of SH-SY5Y cells (Fig. 24-B), consistently with CDKL5 cellular distribution [Rusconi et al. 2008].

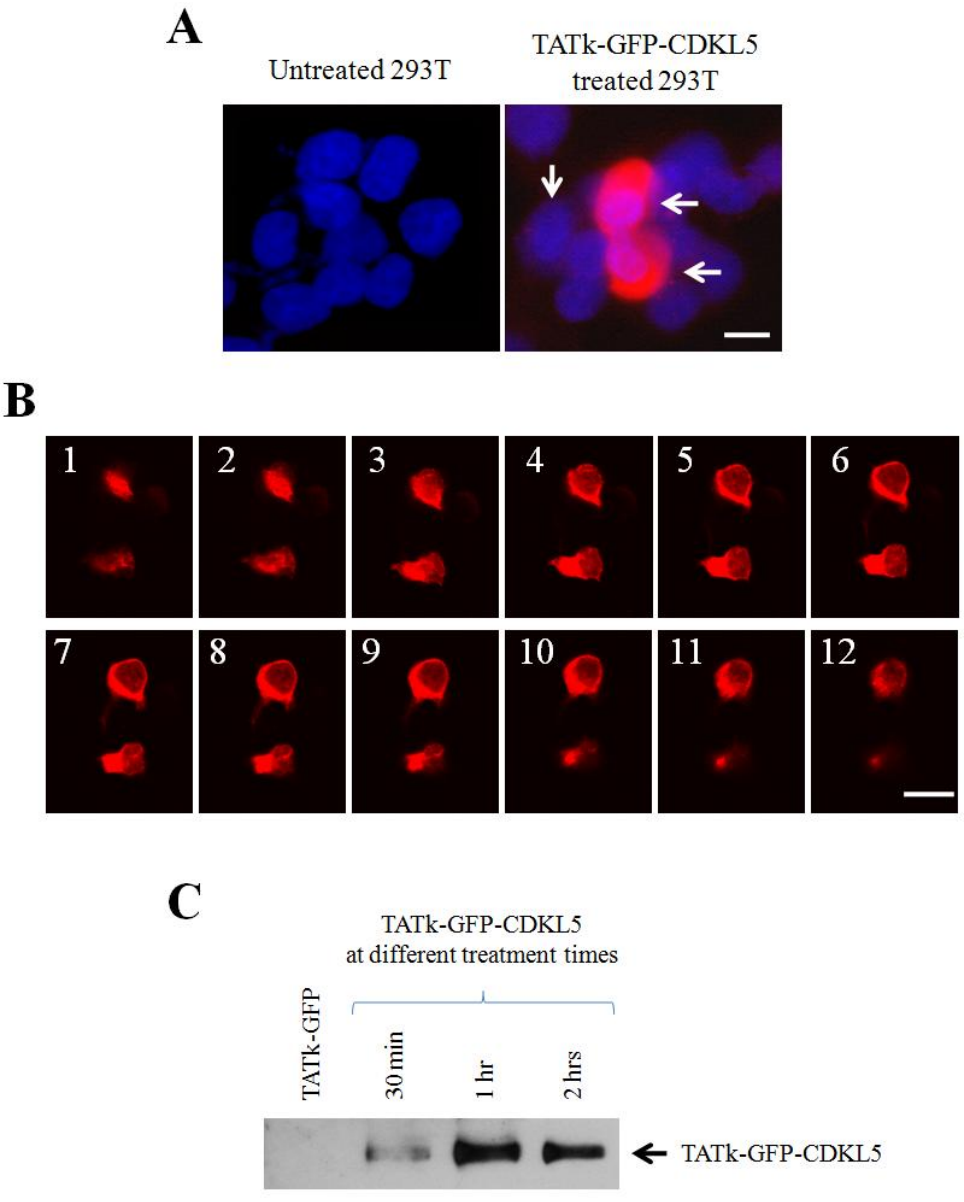

Figure 24. Internalization of TATκ-CDKL5 by target cells. *(**A**) 293T target cells treated with concentrated culture medium with or without TATκ-GFP-CDKL5. Cells were stained for GFP expression using a primary antibody to GFP and a secondary antibody labeled with Cy3 (red). All cells were CDKL5 positive to a variable degree. (**B**) Confocal microscopy showing TATκ-GFP-CDKL5 expression in target cells. SH-SY5Y cells were treated with TATκ-GFP-CDKL5 for 30 minutes and examined by confocal microscopy (Z stack size 0.4 µm). (**C**) Western blot analysis of homogenates of 293T cells treated for different times with concentrated medium containing TATκ-GFP-CDKL5. Note that TATκ-GFP-CDKL5 protein is internalized by target cells.*

4.3 TATκ-CDKL5 retains wild type activity

4.3.1 TATκ-CDKL5 retains kinase activity

TATκ-GFP-CDKL5 fusion protein was purified from culture medium on a Ni-NTA resin, exploiting the 6xHis purification tag at the C-terminus. It has been shown that the CDKL5 kinase has a high autophosphorylation activity [Lin, Franco, and Rosner 2005; Mari et al. 2005]. As shown in Fig. 25, which show the results from an *in vitro* kinase activity assay with radioactive [γ^{32}P]-ATP, purified TATκ-GFP-CDKL5 protein preserves its autophosphorylation activity. This demonstrates that the purified fusion protein retains its kinase activity.

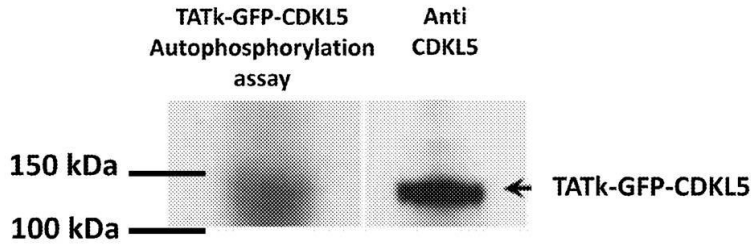

Figure 25. Kinase activity assay. *Panel on the left shows results from the kinase assay demonstrating that TATκ-GFP-CDKL5 fusion protein retains CDKL5 autophosphorylation activity. Band corresponding to CDKL5 was confirmed by western blot analysis using an anti-CDKL5 antibody, shown in the right panel.*

4.3.2 TATκ-CDKL5 inhibits proliferation and induces differentiation of SH-SY5Y neuroblastoma cells

As previously described, the CDKL5 gene affects both the proliferation and differentiation of neural cells [Valli et al. 2012]. Therefore, neuroblastoma cells were employed to study the TATκ-CDKL5 function *in vitro.* SH-SY5Y cells were treated with purified TATκ-GFP-CDKL5 or TATκ-GFP (as a control) the day after seeding. In particular, cells were incubated with the concentrated media containing the concentrated/purified protein for about 24 hours. Cell proliferation was evaluated as a mitotic index (the ratio between the number of cells in a population undergoing mitosis to the number of cells) using Hoechst nuclear staining. Differentiation was evaluated by examining neurite growth, which is a sign of neuronal differentiation. For this analysis, cells were grown for an additional 2 days and neurite outgrowth was measured using an image analysis system.

The increase of CDKL5 protein levels within neuroblastoma cells (through TATκ-GFP-CDKL5 protein treatment) caused a strong inhibition of cell proliferation (Fig. 26) with no increase in apoptotic cell death (data not shown) compared to controls. Furthermore, as shown in Fig. 27, TATκ-GFP-CDKL5 promotes neuroblastoma cell differentiation as indicated by neurite outgrowth in SH-SY5Y cells. These results demonstrate that synthetic TATκ-CDKL5 is functional in an *in vitro* neuronal model.

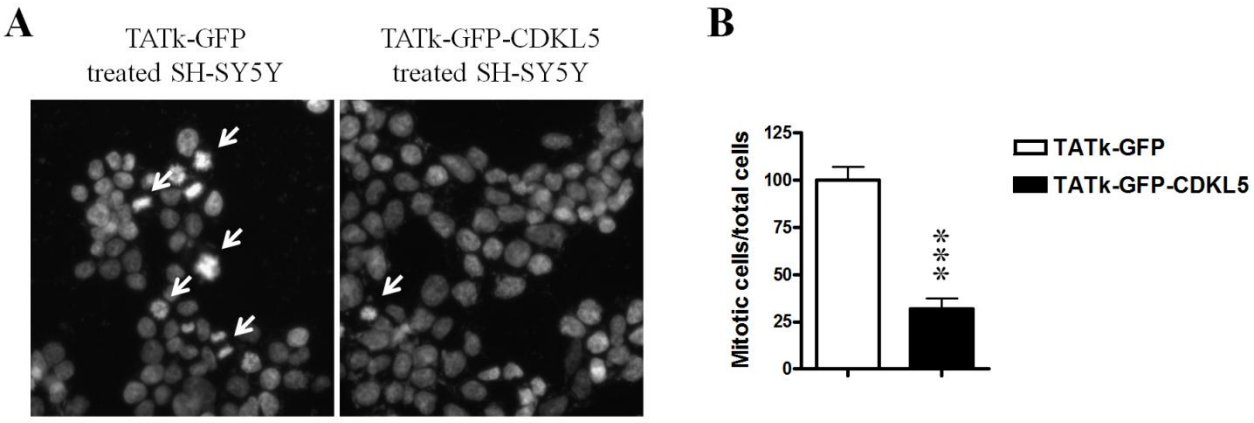

Figure 26. Effect of TATκ-GFP-CDKL5 on neuroblastoma cell proliferation. *(**A**) Images of Hoechst stained nuclei of SH-SY5Y cells treated with TATκ-GFP-CDKL5 or TATκ-GFP for 24 hours. Examples of mitotic (i.e. proliferating) cells are indicated by an arrow. (**B**) Quantification of the mitotic index evaluated as number of mitotic cells on total cell number. Note the large reduction in the number of proliferating cells. Values represent percentage of mean ± SEM. *** $p < 0.001$ as compared to TATκ-GFP treated cells (T-test).*

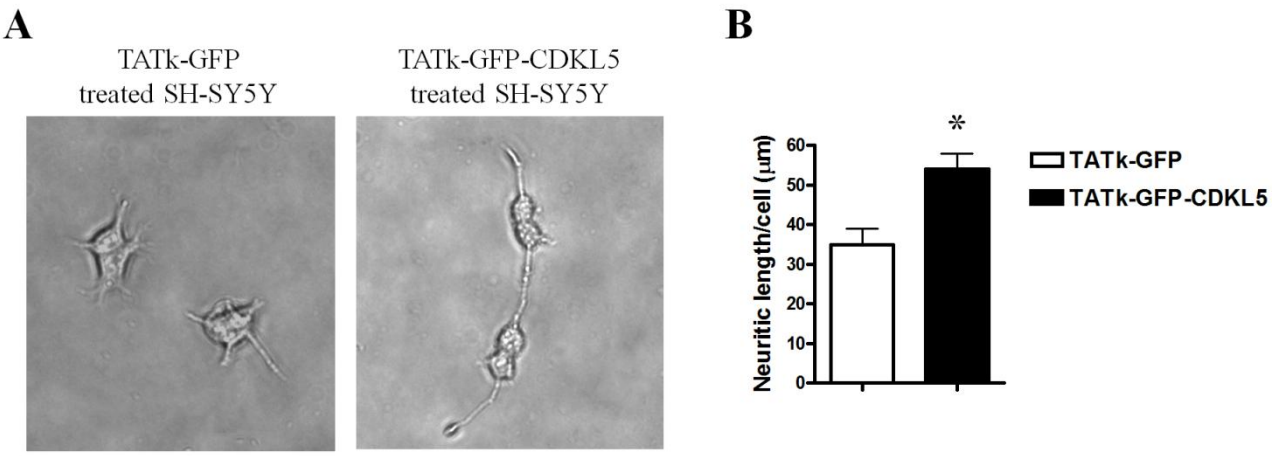

Figure 27. Effect of TATκ-GFP-CDKL5 on neuroblastoma cell differentiation*. (**A**) Representative phase-contrast images of SH-SY5Y cells treated with TATκ-GFP or TATκ-GFP-CDKL5 and cultured for 72 hours. Note that cells treated with TATκ-GFP-CDKL5 have longer processes. (**B**) Quantification of neurite outgrowth of SH-SY5Y cells treated with TATκ-GFP or TATκ-GFP-CDKL5. Values represent mean ± SE. * p < 0.05 (T-test).*

4.3.3 Expression and activity comparison between secretable TATκ-CDKL5 constructs

In order to simplify biochemical analysis of TATκ-CDKL5, we added a GFP-tag sequence in frame with CDKL5, given that no good anti-CDKL5 antibodies are available to date. Therefore we created TATκ-GFP-CDKL5$_{115}$ and TATκ-GFP-CDKL5$_{107}$ constructs, and a TATκ-GFP construct to be used as negative control. Considering that a GFP-tagged protein might have different activity compared to the native protein [Stevens et al. 2010], we tested the *in vitro* activity of TATκ-GFP-CDKL5$_{115}$ in parallel to a TATκ-CDKL5$_{115}$ with only a small 3xFLAG-tag at the C-terminus. As shown in Fig. 28, we demonstrated that both the proteins have the same effect on SH-SY5Y neuroblastoma cells in term of inhibition of proliferation, indicating that the GFP-tag does not alter CDKL5 activity.

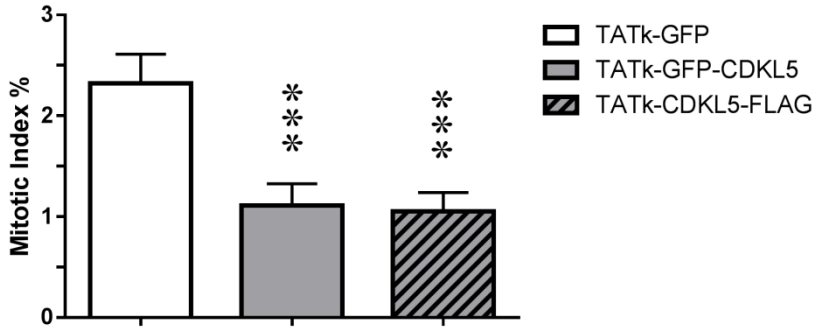

Figure 28. Comparison between the effect of TATκ-GFP-CDKL5 and TATκ-CDKL5-FLAG on neuroblastoma cell proliferation*. SH-SY5Y cells were treated with TATκ-GFP, TATκ-GFP-CDKL5 or TATκ-CDKL5-FLAG for 24 hours and the mitotic index was evaluated as number of mitotic cells on total cell number. Note that the two fusion proteins show a similar activity of inhibition of SH-SY5Y mitosis compared to TATκ-GFP treated control cells. Values represent mean ± SEM. *** p < 0.001 as compared to TATκ-GFP treated cells (T-test).*

4.3.4 TATκ-CDKL5 restores neurite development of Neuronal Precursor Cells derived from CDKL5 KO Mice

In order to further confirm the functionality of the recombinant protein before starting *in vivo* experiments, an *ex vivo* treatment was performed on Neuronal Precursor Cells (NPCs) derived from mouse brains. NPC cultures from CDKL5 KO (−/Y) mice and wild type (+/Y) mice were treated with TATκ-GFP-CDKL5 or TATκ-GFP. Neuronal maturation was evaluated by measuring the total neuritic length of differentiated neurons (positive for β-tubulin III). An evaluation of neurite length was performed using the image analysis system Image Pro Plus (Media Cybernetics, Silver Spring, Md. 20910, USA). The average neurite length per cell was calculated by dividing the total neurite length by the number of cells counted in the areas. As shown in Fig. 29, the absence of CDKL5 in KO NPCs causes a reduction in the maturation of new neurons, but treatment with TATκ-CDKL5 restores neurite development.

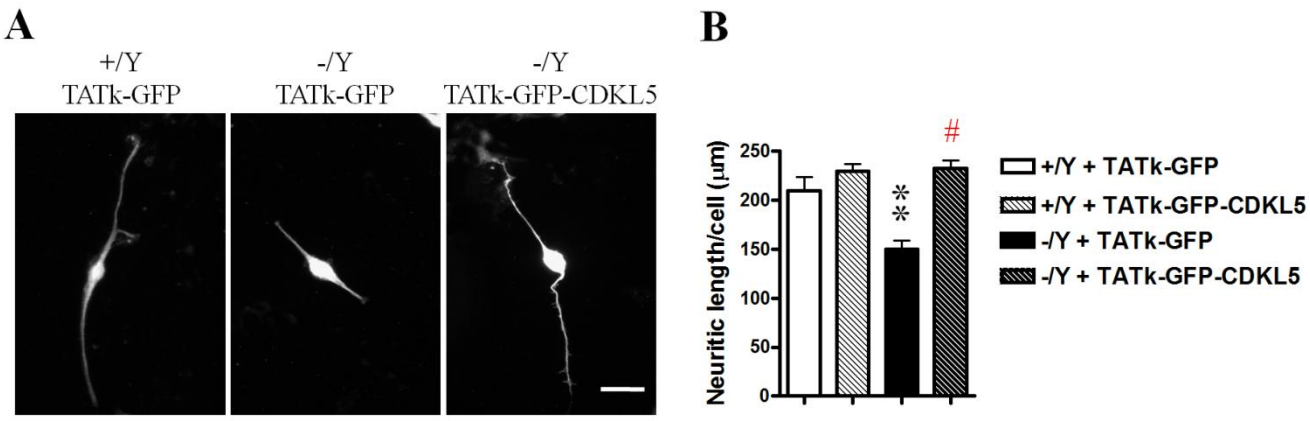

Figure 29. Effect of TATκ-GFP-CDKL5 on NPCs cultures*. (**A**) Images of β-tubulin III stained neuronal precursor cells from the CDKL5 KO (-/Y) and wild type (+/Y) mouse. Cultures were treated with TATκ-GFP-CDKL5 or TATκ-GFP during differentiation. (**B**) Neuronal maturation was evaluated by measuring the total neuritic length of differentiated neurons (positive for β-tubulin III). Values represent mean ± SE. ** p < 0.01 as compared to +/Y; # p < 0.05 as compared to the -/Y samples (Bonferroni's test after ANOVA).*

4.4 TATκ-CDKL5 production optimization for *in vivo* treatments

4.4.1 Creation of mammalian stable clones expressing different TATκ-CDKL5 isoforms

Based on the promising results obtained *in vitro*, we started planning *in vivo* studies, in order to set up a reproducible TATκ-CDKL5 protein production. The generation of stably-transfected cell lines is essential for a wide range of applications, such as gene function studies, drug discovery assays, or the production of recombinant proteins [Wurm 2004]. In contrast to transient expression, stable expression allows long term, as well as defined and reproducible, expression of the gene of interest. Therefore we created 293T cell lines that stably express the recombinant TATκ-GFP-CDKL5 protein as well as TATκ-GFP protein as a negative control.

Alternative splice isoforms for the *CDKL5* gene have been described (Kilstrup-Nielsen, 2012). The original CDKL5 transcript generates a protein of 1030 amino acids ($CDKL5_{115}$; 115 kDa). While $CDKL5_{115}$ is the first characterized CDKL5 isoform, a recently identified transcript, characterized by an altered C-terminal region, is likely to be relevant for CDKL5 brain functions ($CDKL5_{107}$; 107 kDa) [Williamson et al. 2012]. To compare the levels of production and activity of the two CDKL5 isoforms, we created different 293T cell lines that express either TATκ-GFP-$CDKL5_{115}$ or TATκ-GFP-$CDKL5_{107}$ isoform. Consistently with the reported higher stability of the

107 kDa isoform to proteasomal degradation [Williamson et al. 2012], we found that the recovery of TATκ-GFP-CDKL5$_{107}$ fusion protein from culture medium was higher than that of TATκ-GFP-CDKL5$_{115}$ (Fig. 30).

Importantly, at a functional level, we found that the two isoforms have a comparable inhibition effect on neuroblastoma cell proliferation (FIG R12), indicating a similar enzymatic activity.

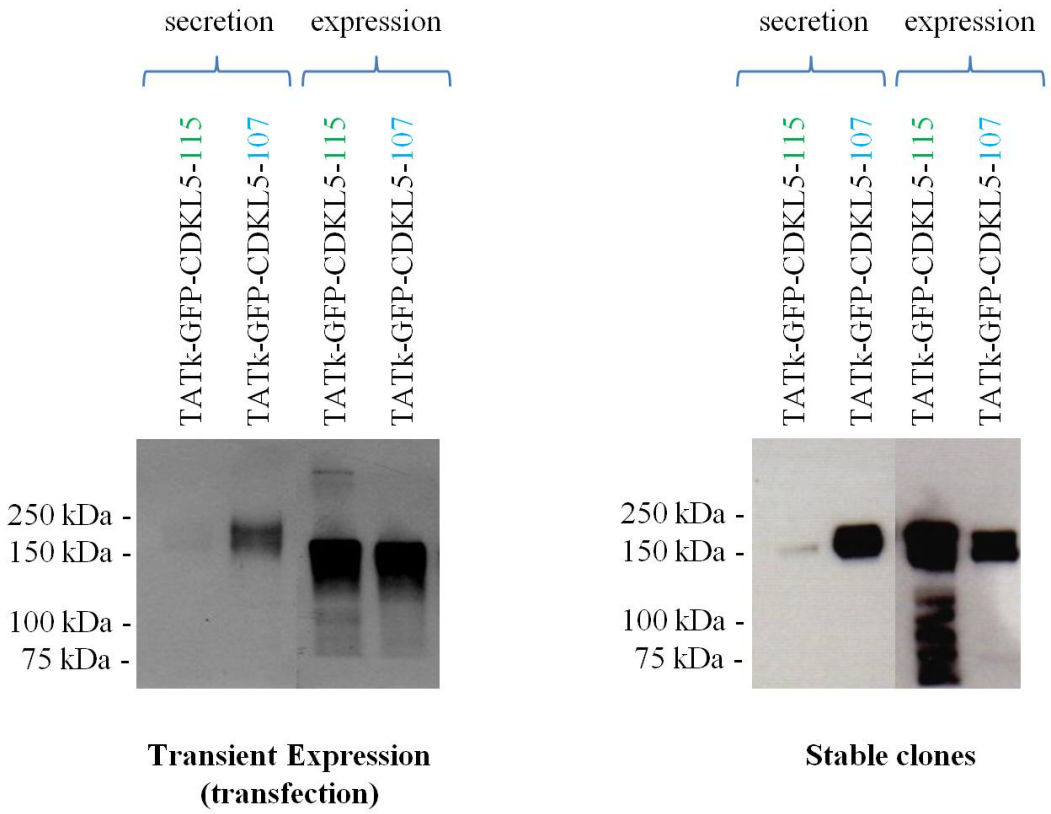

Figure 30. Comparison of the expression and secretion pattern of TATκ-GFP-CDKL5$_{115}$ and TATκ-GFP-CDKL5$_{107}$. *Images show western blots of 20-fold concentrated culture medium of transfected 293T cells (panel on the left) or in stable clones (panel on the right) expressing TATκ-GFP-CDKL5.*

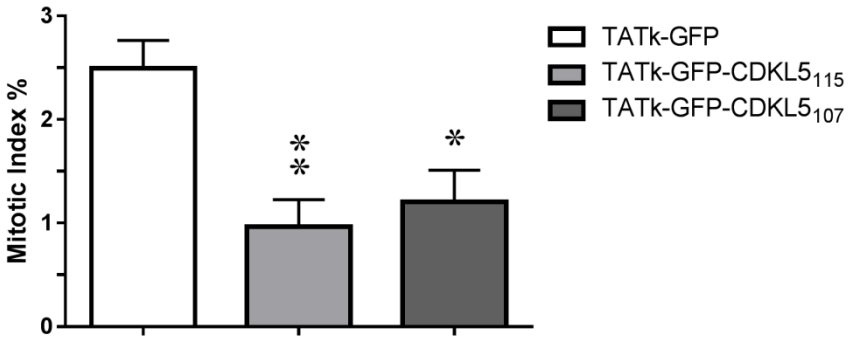

Figure 31. Effect of TATκ-GFP-CDKL5$_{115}$ and TATκ-GFP-CDKL5$_{107}$ isoforms on SH-SY5Y neuroblastoma cells proliferation. *SH-SY5Y cells were treated with TATκ-GFP, TATκ-GFP-CDKL5$_{115}$ or TATκ-GFP-CDKL5$_{107}$ for 24 hours and the mitotic index was evaluated as number of mitotic cells on total cell number. Note that the two CDKL5 isoforms show a similar activity of inhibition of SH-SY5Y mitosis compared to TATκ-GFP treated control cells. Values represent mean ± SEM. * p < 0.05 and ** p < 0.01 as compared to TATκ-GFP treated cells (T-test).*

4.4.2 TATκ-CDKL5 fusion protein in culture medium can be concentrated up to 480×

In order to formulate a more suitable preparation for *in vivo* treatments, TATκ-GFP-CDKL5 proteins were purified from serum-free culture medium at increasing concentrations (40- 60-120-240- 480- fold). Starting from the 20-fold medium concentration used for *in vitro* studies, we reached a maximum of 480-fold concentration without protein precipitation (Fig. 32). Once the highest concentration that did not cause protein precipitate had been found, the concentrated medium was subjected to buffer exchange with sterile saline.

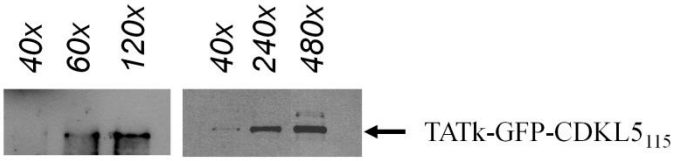

Figure 32. Increasing concentration of culture medium containing TATκ-CDKL5. *Image shows an anti-CDKL5 western blot analysis of conditioned media from 293T cells expressing TATκ-GFP-CDKL5. Note that the protein does not precipitate at 480-fold concentration.*

4.4.3 Quantification of the purified TATκ-CDKL5 protein

The established formulation for *in vivo* treatments takes into account different variables among which the most important is protein concentration. Therefore, we quantified the purified TATκ-CDKL5 protein. Using a purified GFP protein at a known concentration as reference standard, we quantified TAT-GFP-CDKL5$_{115}$ and TAT-GFP-CDKL5$_{107}$ proteins through western blot analysis using an anti-GFP antibody. We calculated that in 480-fold purified medium the 115-kDa isoform is about 0.5 ng/µL concentrated while the 107-kDa isoform can be more efficiently produced with a final concentration of 8-10 ng/µL.

The first *in vivo* treatments were performed with intracerebroventricular injections. Such a technique limits the volume of bolus to 10-15 µL per injection. We started experiments with the lower concentration, treating adult animals with 10 µL of TAT-GFP-CDKL5$_{115}$ preparation, corresponding to 5 ng/day of protein. As described in detail in the text below, treatment did not cause evident side effects and, as a matter of fact, improved various aspects of brain functionality. Therefore, we performed the following treatments with a higher protein concentration using the TAT-GFP-CDKL5$_{107}$ preparation, maintaining the same bolus volume of 10 µL, and thus injecting about 80 ng of protein per day. Even though a more precise quantification is required, results demonstrated a dose-dependent improvement of the analyzed neurophysiological aspects.

4.4.4 Temperature and time of storage do not affect TATκ-CDKL5 protein stability

Purified proteins often need to be stored for an extended period of time, still retaining their original activity. Stability is an inherent property of the protein(s) of interest. Not all proteins behave similarly under the same storage conditions. We evaluated the stability of the purified TATκ-GFP-CDKL5 protein after a long period at -80°C and a freezing-thawing cycle. We treated SH-SY5Y neuroblastoma cells with a freshly-produced protein, in parallel with a protein stored at -80°C for one month. We performed a proliferation assay evaluating the mitotic index as previously described and observed that the stored protein maintained the same anti-proliferative activity of the freshly-produced protein (Fig. 33), indicating that storage in freezing conditions did not alter CDKL5 activity.

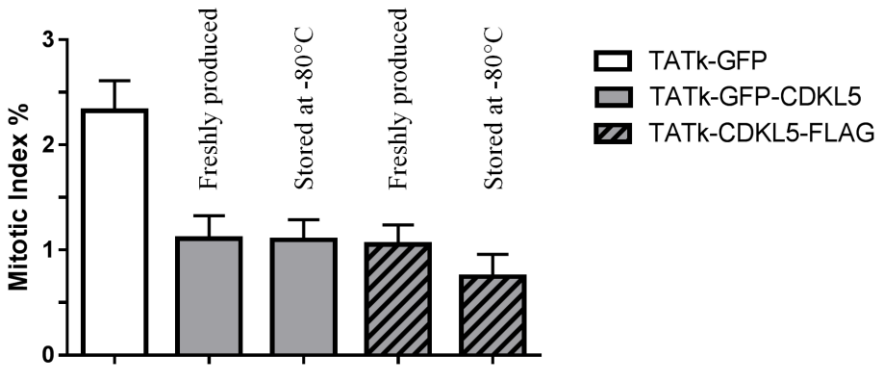

Figure 33. Histogram showing the activity of purified TATκ-GFP-CDKL5$_{115}$ and TATκ-CDKL5$_{115}$-FLAG tested immediately after production or after a freeze-thaw cycle. *Protein activity was evaluated as ability to inhibit SH-SY5Y neuroblastoma cells proliferation. SH-SY5Y cells were treated with TATκ-GFP, TATκ-GFP-CDKL5$_{115}$ or TATκ-CDKL5$_{115}$-FLAG freshly produced or freezed-thawed proteins for 24 hours and the mitotic index was evaluated as number of mitotic cells on total cell number. Values represent mean ± SEM.*

Furthermore, we evaluated the stability of TATκ-CDKL5-FLAG (data not shown) and TATκ-GFP-CDKL5 at 37°C, in order to assess the protein stability at a physiological temperature. Thus we kept aliquots of purified proteins at 37°C for different periods, starting from 24 hrs to one week. Through western blot analysis we demonstrated that a substantial amount of both proteins remains in the preparation after 3 days of storage at 37°C (Fig. 34) and it is still detectable after one week (data not shown). Such information enables the use of reservoir-based therapeutic systems in future preclinical studies and drug development, in view of clinical trials which need patient compliance and controlled release.

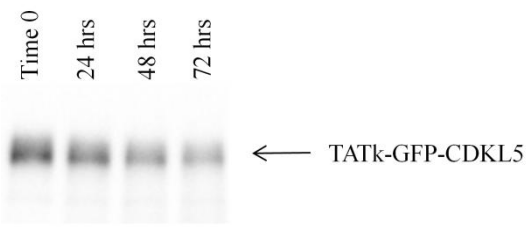

Figure 34. Western blot analysis showing degradation on time of TATκ-GFP-CDKL5 at physiological temperature. *Aliquots of protein were kept in the incubator at 37°C for different times. After three days of incubation a consistent amount of the full-length protein is revealed with an anti-CDKL5 antibody in the western blot membrane.*

4.5 Intracerebroventricular treatment with TATκ-CDKL5 restores neuronal maturation and survival

4.5.1 TATκ-CDKL5 restores dendritic arborization

The first *in vivo* study was scheduled with TATκ-GFP-CDKL5$_{115}$ or vehicle injected directly to the third cerebral ventricle of adult mice (4-6 months of age) for 5 consecutive days (experimental schedule in Fig. 35).

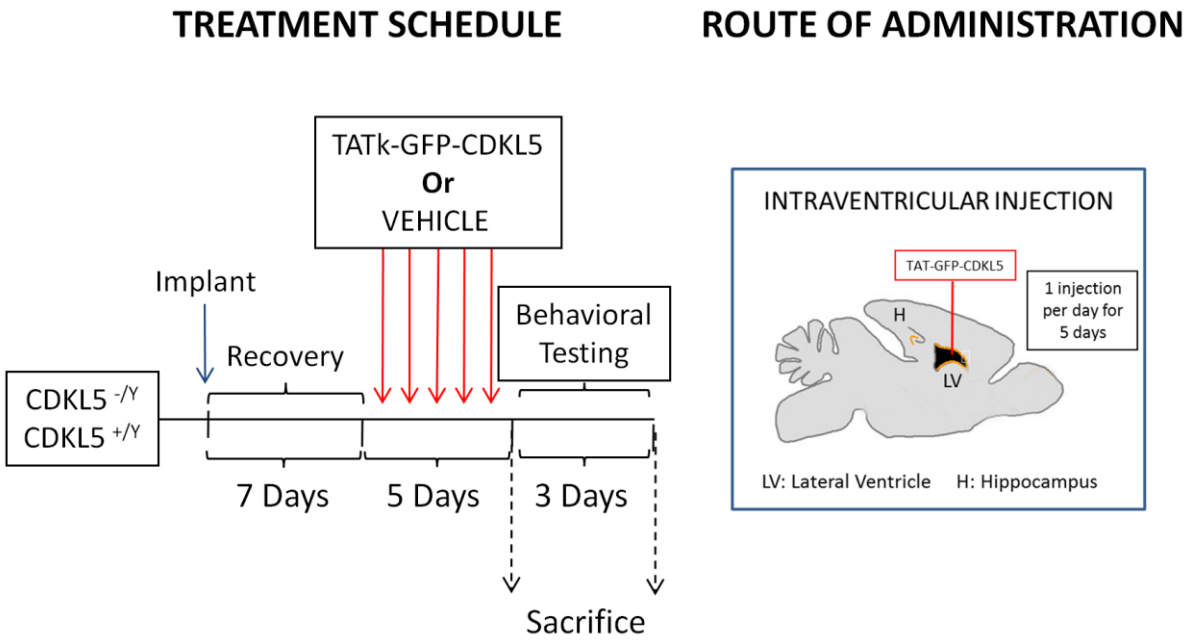

Figure 35. ICV short-treatment schedule. *Male CDKL5 WT (CDKL5$^{+/Y}$) and CDKL5 KO (CDKL5$^{-/Y}$) mice received treatment with vehicle (n=6) or TATκ-GFP-CDKL5$_{115}$ (n=6) as indicated above. Treatment period consisted of a single daily intraventricular injection for 5 consecutive days. Animals were sacrificed 1 hour after the last injection or after 3 days. Some animals from each experimental group were behaviorally tested as indicated.*

In this study we initially used the CDKL5$_{115}$ isoform since from *in vitro* studies CDKL5 isoform is the best known from a functional point of view. Twenty-four hours after the last injection animals were sacrificed, and the dendritic morphology of newborn hippocampal granule cells was analyzed with immunohistochemistry for doublecortin (DCX), a microtubule-associated protein

expressed by neuronal precursor cells and immature neurons. As previously described [Amendola et al. 2014; Fuchs et al. 2014], the hippocampal region shows major structural and functional defects in CDKL5 KO mice, representing a brain structure that is well suited for the study of the effects of therapies on CDKL5 KO mice. Indeed Fig. 36-A demonstrates that DCX positive neurons of CDKL5 KO mice exhibit shorter processes than those of their wild type counterparts. Importantly, TATκ-GFP-CDKL5$_{115}$ fusion protein administered intraventricularly was observed to increase neurite length and branch number in CDKL5 KO mice to levels similar to wild type (Fig. 36-A,B). Fig. 36-C shows examples of the reconstructed dendritic tree of newborn granule cells of wild type (+/Y), hemizygous CDKL5 KO (−/Y) mice, and their relative counterparts treated with TATκ-GFP-CDKL5$_{115}$ fusion protein. Quantification of the dendritic size of DCX positive cells demonstrated that, while untreated CDKL5 KO (−/Y) mice had a shorter dendritic length and a reduced number of segments than wild type mice, TATκ-GFP-CDKL5$_{115}$ treated knockout (−/Y) mice showed an increase in both parameters that became even larger in comparison with +/Y mice (Histograms in Fig. 36-B).

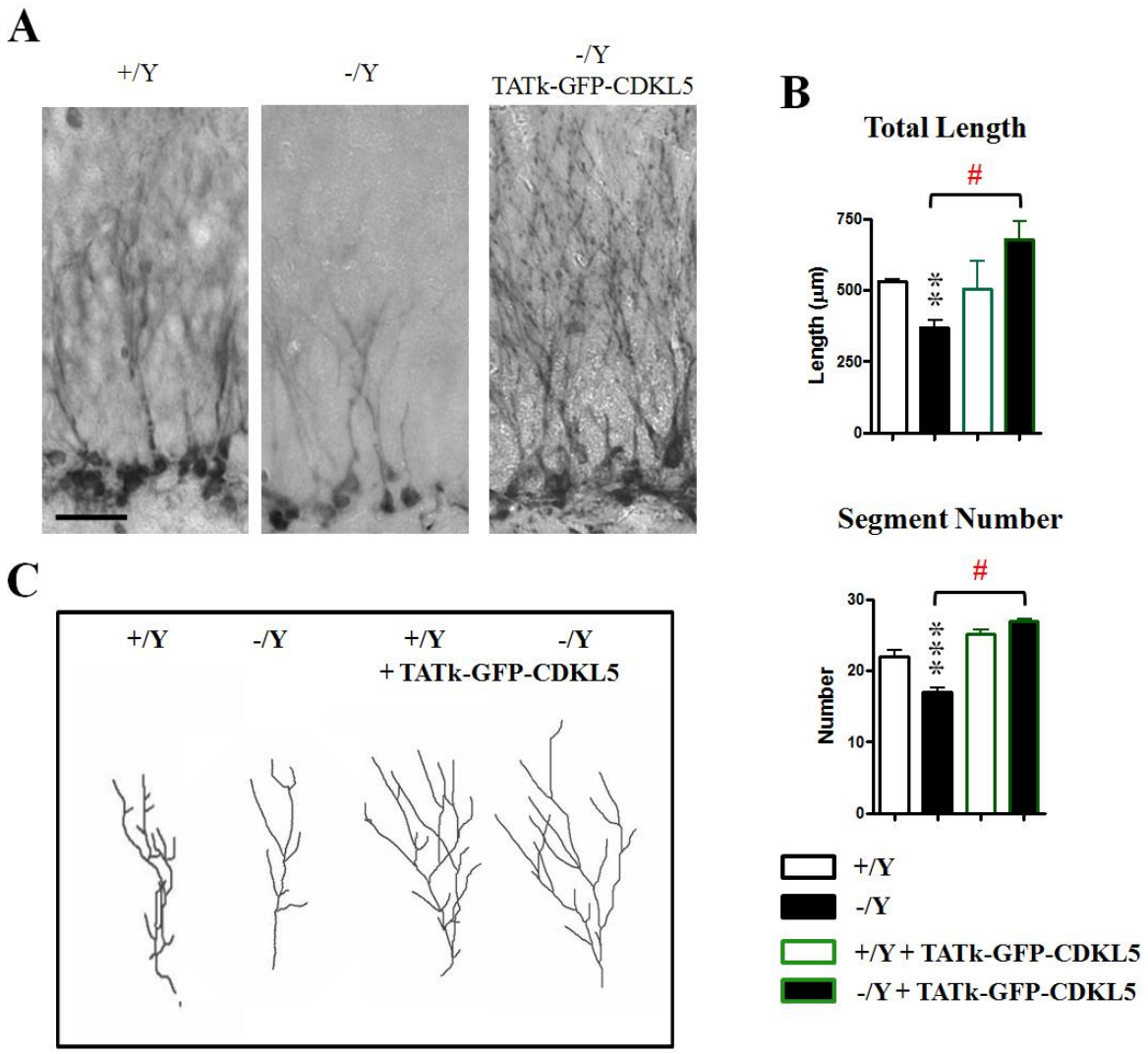

Figure 36. Effects of 5-days treatment with TATκ-GFP-CDKL5$_{115}$ on immature neurons. *(**A**) Images of hippocampus (dentate gyrus) sections immunostained for DCX of WT male mice (+/Y) and CDKL5 KO male mice (-/Y). Note the reduced neurite length and number of newborn granule cells in CDKL5 KO (-/Y) as compared to WT mice (+/Y). TATκ-GFP-CDKL5 administered once daily by intraventricular injection for five consecutive days was observed to increase neurite length and number of newborn granule cells in CDKL5 KO mice to levels similar to wild-type. Scale bar = 60 mm. (**B**) Quantification of the mean total dendritic length (upper panel), and mean number of dendritic segments (lower panel) of newborn granule cells (DCX-positive cells) of the hippocampus (dentate gyrus). Values represent mean ± SE. ** p < 0.01; *** p < 0.001 as compared to +/Y; # p < 0.05 as compared to the -/Y samples (Bonferroni's test after ANOVA). (**C**) Examples of the reconstructed dendritic tree of newborn granule cells.*

The effects of TATκ-GFP-CDKL5$_{115}$ treatment on the dendritic architecture were further examined by evaluating each dendritic order separately. A striking feature of CDKL5 KO mice is the absence of branches of higher orders (Fig. 37; red arrows). While wild type (+/Y) mice have up to 10 orders of branches, CDKL5 KO (−/Y) mice lack branches of orders 8-10. In addition, CDKL5 KO (−/Y) mice show a reduced branch length of orders 5-8 (Fig. 37-A) and a reduced number of branches of orders 6-8 (Fig. 37-B). These data indicate that in CDKL5 KO mice the dendritic tree of the newborn granule cells is hypotrophic and that this defect is due to a reduction in the number and length of branches of intermediate orders and a lack of branches of higher orders. It was observed that all these defects were completely rescued by TATκ-GFP-CDKL5$_{115}$ treatment (FIGS. 37-A,B), indicating that protein therapy has a positive impact on the dendritic development of newborn neurons.

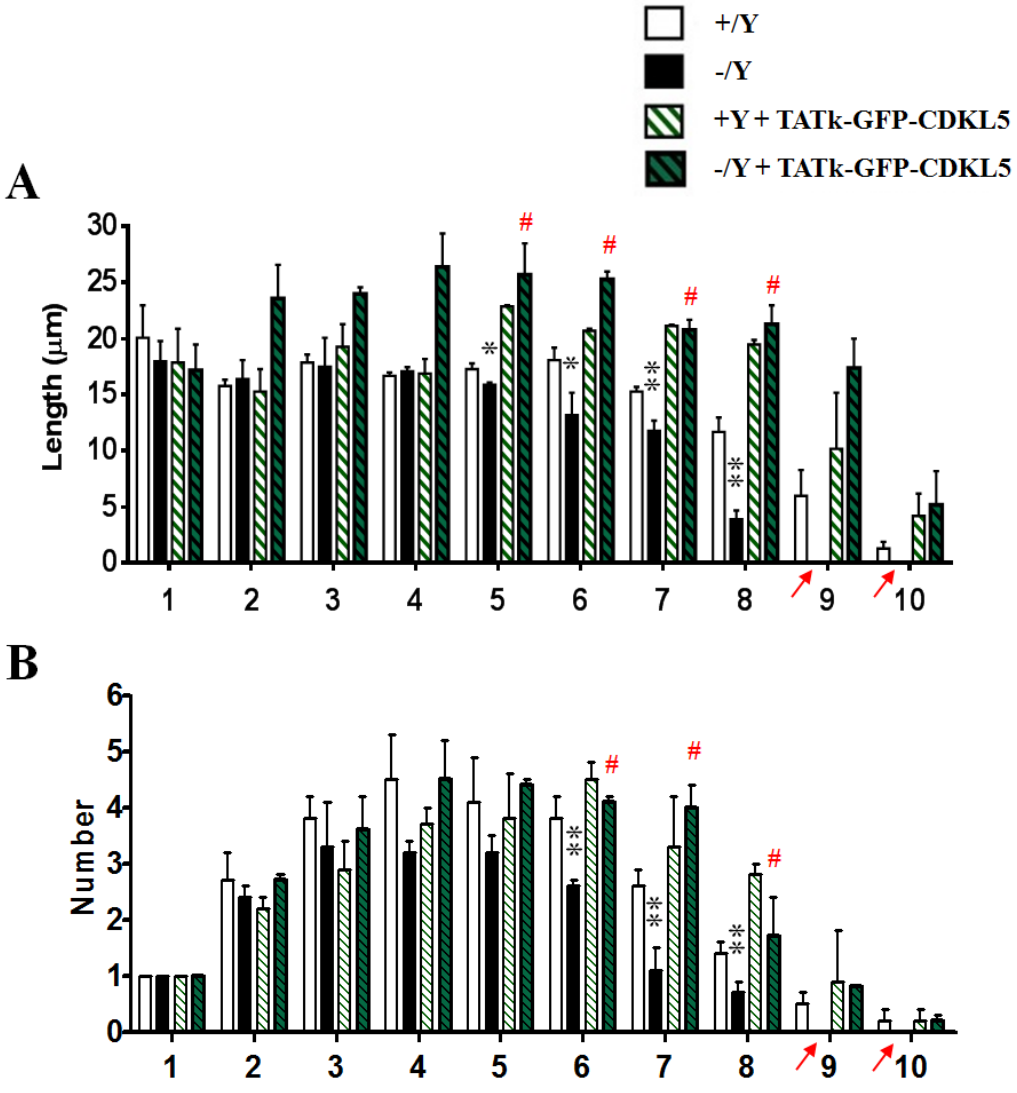

Figure 37. Effects of 5-days treatment with TATκ-GFP-CDKL5$_{115}$ on dendritic arborization. *Quantification of the mean length (**A**) and mean number (**B**) of branches of the different orders of newborn granule cells of the dentate gyrus of WT male mice (+/Y) and CDKL5 KO male mice (-/Y) treated for 5 consecutive days with vehicle or TATκ-GFP-CDKL5. Arrows indicate the absence of branches in CDKL5 KO male mice (-/Y) treated with vehicle. Values represent mean ± SE. * p < 0.05; ** p < 0.01 as compared to +/Y; # p < 0.05 as compared to the -/Y samples (Bonferroni's test after ANOVA).*

Furthermore, we analyzed the effects of treatment on the dendritic architecture of mature neurons. To this end we examined Golgi-stained granule neurons located in the middle portion of the granule cell layer. While CDKL5 KO (−/Y) mice show a shorter length of dendritic branches compared to wild-type (+/Y) mice, these defects were completely rescued by treatment with TATκ-GFP-CDKL5 (Fig. 38-A). In both treated −/Y and +/Y mice total dendritic length became even larger in comparison with untreated +/Y mice. These results show that the impaired dendritic architecture of mature granule neurons observed in CDKL5 −/Y mice was restored by treatment with TATκ-GFP-CDKL5 protein.

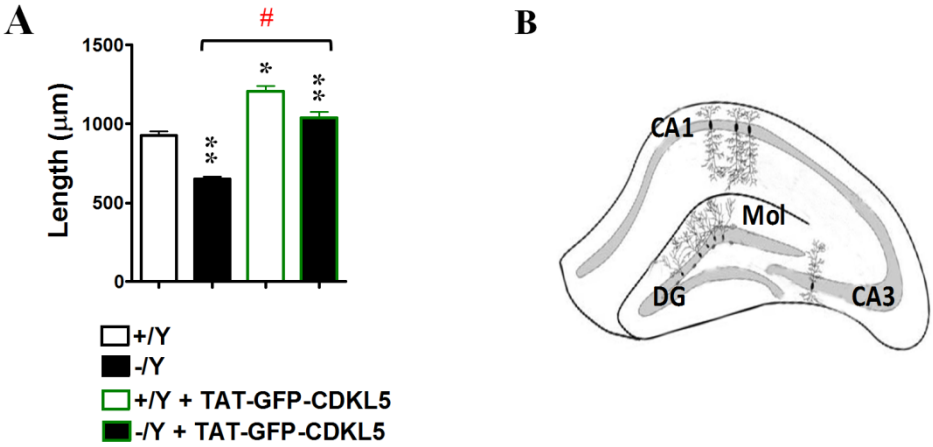

Figure 38. Effects of 5-days treatment with TATκ-GFP-CDKL5$_{115}$ on mature neurons. *(**A**) Mean total dendritic length of Golgi-stained granule cells in wild-type male mice (+/Y) and CDKL5 KO male mice (-/Y) treated with vehicle or TATκ-GFP-CDKL5 via intraventricular injections given once a day for 5 consecutive days. (**B**) Scheme of a hippocampal slice showing the different layers and the position of CA1 pyramidal cells and granule cells. The molecular layer (Mol) of the dentate gyrus (DG) contains the granule cell dendrites. Values represent mean ± SE. * p < 0.05; ** p < 0.01 as compared to +/Y; # p < 0.05 as compared to the -/Y samples (Bonferroni's test after ANOVA).*

4.5.2 TATκ-CDKL5 restores neuronal survival

It was observed that CDKL5 KO mice (−/Y) mice have fewer postmitotic neurons (DCX-positive cells) than wild type (+/Y) mice in the hippocampal dentate gyrus [Fuchs et al. 2014]. Importantly, as shown in Fig. 39-A, the number of postmitotic neurons in TATκ-GFP-CDKL5$_{115}$ treated CDKL5 KO mice underwent an increase, becoming similar to that of wild type (+/Y) mice.

In order to evaluate the effects of TATκ-GFP-CDKL5$_{115}$ treatment on apoptotic cell death, we counted the number of apoptotic cells expressing cleaved caspase-3 in the hippocampal dentate gyrus. As previously discussed, neural precursors of CDKL5 −/Y mice exhibit an abnormally high proliferation rate. Quantification of cleaved caspase-3 cells showed that TATκ-GFP-CDKL5 treatment completely normalized apoptotic cell death in CDKL5 KO mice (Fig. 39-B). This indicates that the increased death of postmitotic immature granule cells, a characteristic of CDKL5 KO mice, is rescued by TATκ-GFP-CDKL5 treatment.

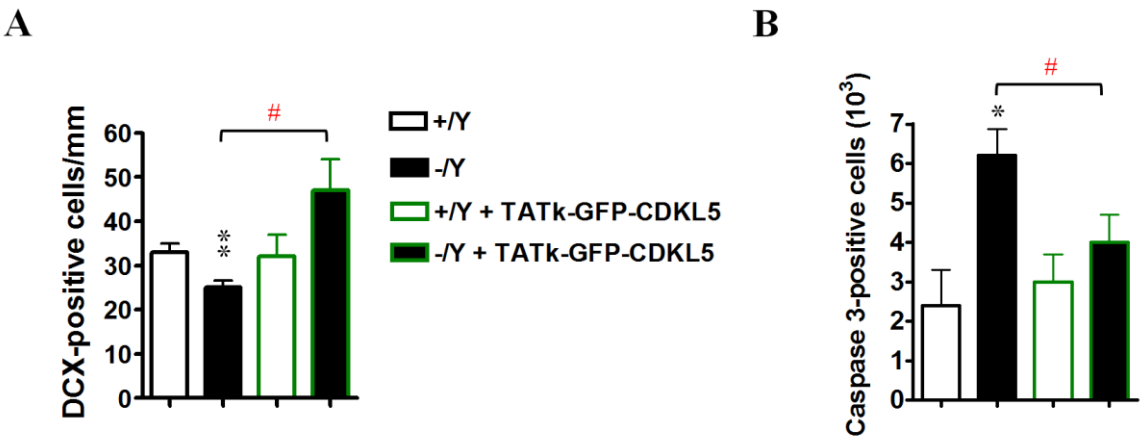

Figure 39. Effects of 5-days treatment with TATκ-GFP-CDKL5$_{115}$ on survival. *(**A**) Quantification of DCX positive cells in the dentate gyrus of WT male mice (+/Y), CDKL5 KO male mice (-/Y) with vehicle or TATκ-GFP-CDKL5. Treatment period consisted of one daily intraventricular injection given daily for 5 consecutive days. (**B**) Quantification of apoptotic cells (cleaved caspase-3 positive cells) mice treated as in A. Values represent mean ± SE. * p < 0.05; ** p < 0.05 as compared to +/Y; # p < 0.05 as compared to the -/Y samples (Bonferroni's test after ANOVA).*

Taken together, these data demonstrate that treatment with TATκ-GFP-CDKL5$_{115}$ in CDKL5 KO mice increased neurite length and survival of newborn cells in the hippocampus, indicating that

injected TATκ-GFP-CDKL5$_{115}$ diffused from the lateral ventricle to the hippocampus and restored maturation and survival of postmitotic granule cells.

4.6 Intracerebroventricular treatment with TATκ-CDKL5 restores connectivity

4.6.1 TATκ-CDKL5 restores synaptic molecules expression

A reduction in connectivity may be the counterpart of the dendritic hypotrophy that characterizes the newborn granule cells of CDKL5 KO mice. Synaptophysin (SYN; also known as p38) is a synaptic vesicle glycoprotein that is a specific marker of presynaptic terminals. We previously reported that in CDKL5 KO mice the optical density of SYN in the molecular layer of the hippocampus is significantly lower than in wild type mice [Fuchs et al. 2014], suggesting that CDKL5 KO mice have fewer synaptic contacts in the dentate gyrus. Furthermore, dendritic arborization is significantly reduced in cortical pyramidal neurons of CDKL5 KO mice compared to their wild type counterparts [Amendola et al. 2014]. At the same time, similar lower levels of SYN immunoreactivity in the layer III of the neocortex were observed. In CDKL5 KO (−/Y) mice treated with TATκ-GFP-CDKL5$_{115}$ these defects were fully rescued (Fig. 40), suggesting that the positive impact of treatment with TATκ-GFP-CDKL5$_{115}$ on dendritic structure was paralleled by restoration of the input to neurons.

Fig. 40-A shows representative images demonstrating brain sections processed for SYN immunofluorescence from the molecular layer (Mol) of the dentate gryrus (DG) from a wild type (+/Y) mouse, a hemizygous CDKL5 KO (−/Y) mouse, and a hemizygous CDKL5 KO mouse treated with TATκ-GFP-CDKL5$_{115}$ protein via intraventricular injections given once a day for 5 consecutive days (−/Y + TATκ-GFP-CDKL5).

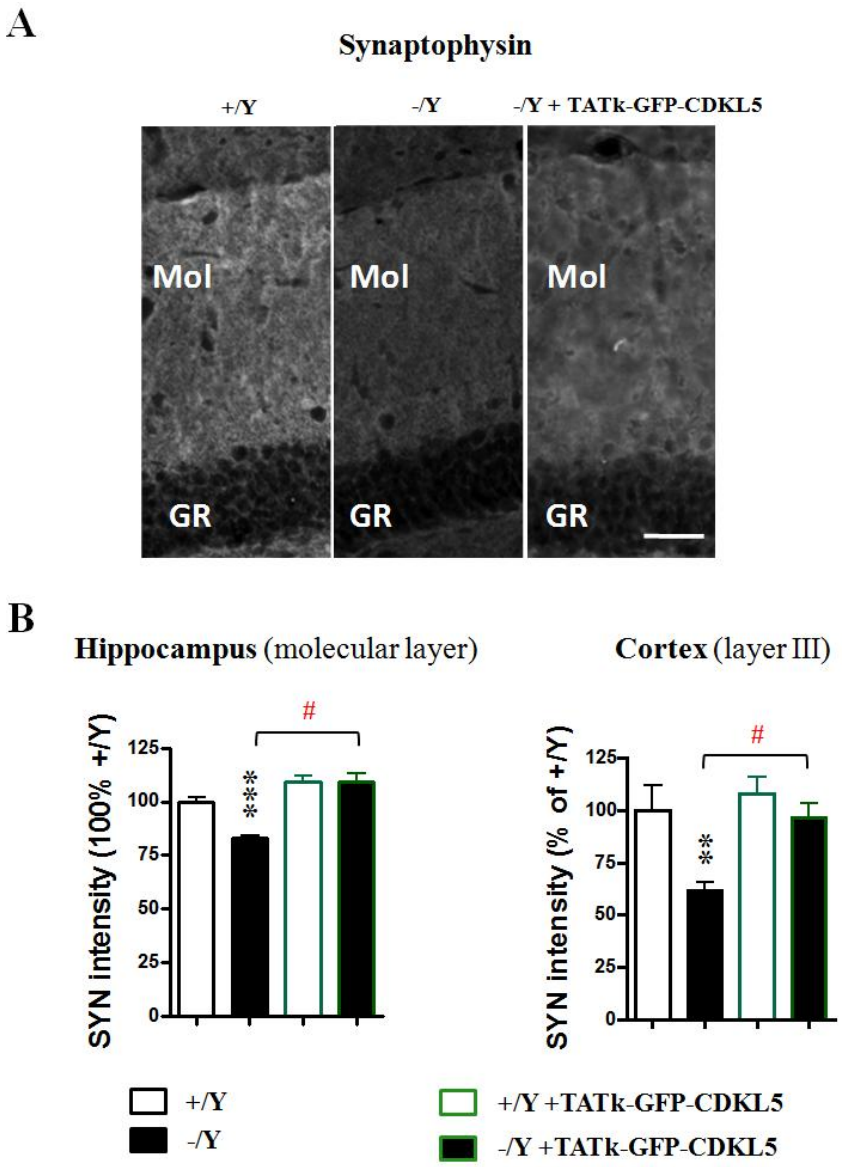

Figure 40. Effects of 5-days treatment with TATκ-GFP-CDKL5$_{115}$ on synaptophysin expression. *(**A**) Representative images of brain sections processed for synaptophysin immunofluorescence from the molecular layer of the dentate gyrus (DG) from a WT male mouse (+/Y) and CDKL5 KO male mice (-/Y) treated with vehicle or TATκ-GFP-CDKL5. Scale bar = 80 µm. Abbreviation: GR, granular layer; Mol, molecular layer. (**B**) Quantification of synaptophysin (SYN) optical density in the molecular layer of the hippocampus (left panel) and layer III of the cortex (right panel) in mice treated as in A. Data are given as fold difference vs. the corresponding zone of the molecular layer or cortex of wild type mice. Values represent mean ± SD. ** p < 0.01; *** p < 0.001 as compared to +/Y; # p < 0.05 as compared to the -/Y samples (Bonferroni's test after ANOVA).*

4.6.2 TATκ-CDKL5 restores spine density and maturation

In Golgi-stained sections, spines of granule cells were counted and spine density was measured on dendritic segments in the inner and outer half of the molecular layer. Untreated CDKL5 KO adult mice showed a lower spine density compared to wild type mice, while treatment with TATκ-GFP-CDKL5$_{115}$ protein fully restored density, erasing the difference between knockout and wild type conditions. Representative images are shown in Fig. 41 and the relative quantification can be observed in the histogram on the right.

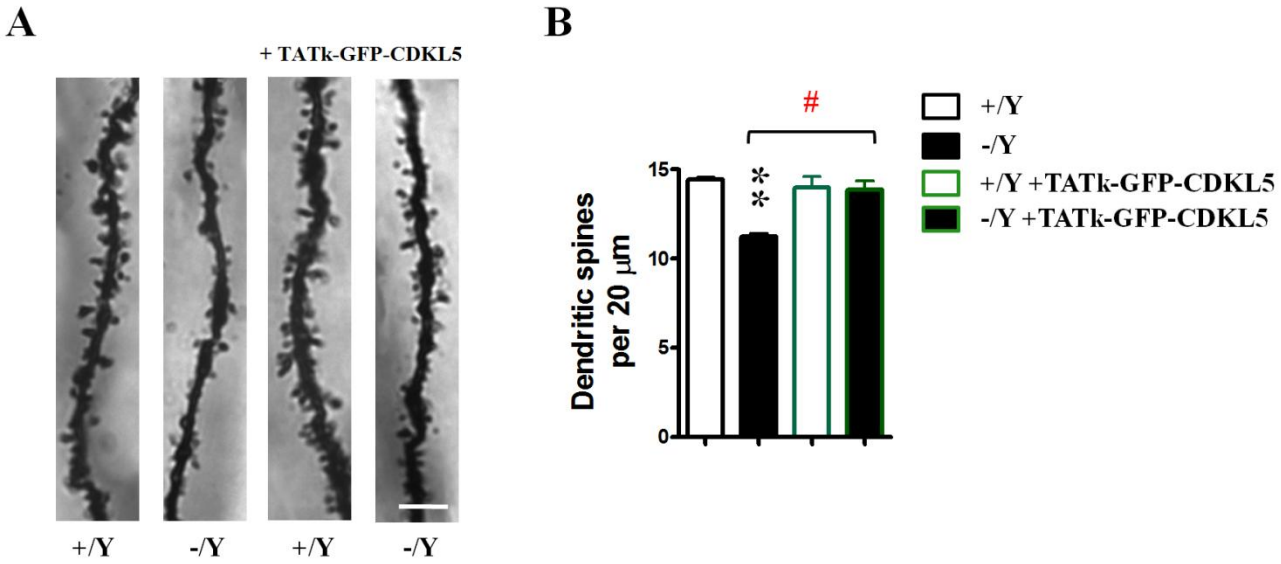

Figure 41. Effects of 5-days treatment with TATκ-GFP-CDKL5$_{115}$ on spine number. *(**A**) Images of Golgi-stained dendritic branches of granule cells of wild-type male mice (+/Y) and CDKL5 KO male mice (-/Y) treated with vehicle or TATκ-GFP-CDKL5 via intraventricular injections given once a day for 5 consecutive days. Scale bar = 5 µm. (**B**) Quantification of number of dendritic spines. Values represent mean ± SE. ** p < 0.05 as compared to +/Y; # p < 0.05 as compared to the -/Y samples (Bonferroni's test after ANOVA).*

To further investigate the effects of treatment with TATκ-GFP-CDKL5 protein on dendritic spines, we examined spine morphology of Golgi-stained granule neurons. Dendritic spines are heterogeneous in size and shape, and can be classified as: filopodia, thin-shaped, stubby-shaped for immature spines, while mushroom and cup shapes indicate mature spines (see Fig. 42-A).

As shown in Fig. 42-C, the percentage of mature spines is lower in CDKL5 KO mice compared to wild type littermates, while the percentage increases to reach that of the wild type

condition in knockout mice treated with TATκ-GFP-CDKL5$_{115}$. Conversely, the percentage of immature spines is higher in knockout mice and diminishes, reaching a similar percentage to the wild type condition after treatment with TATκ-GFP-CDKL5$_{115}$. Images of Golgi-stained dendritic spines from granule cells of wild type male (+/Y) mice and CDKL5 KO (-/Y) mice are shown in Fig. 42-B.

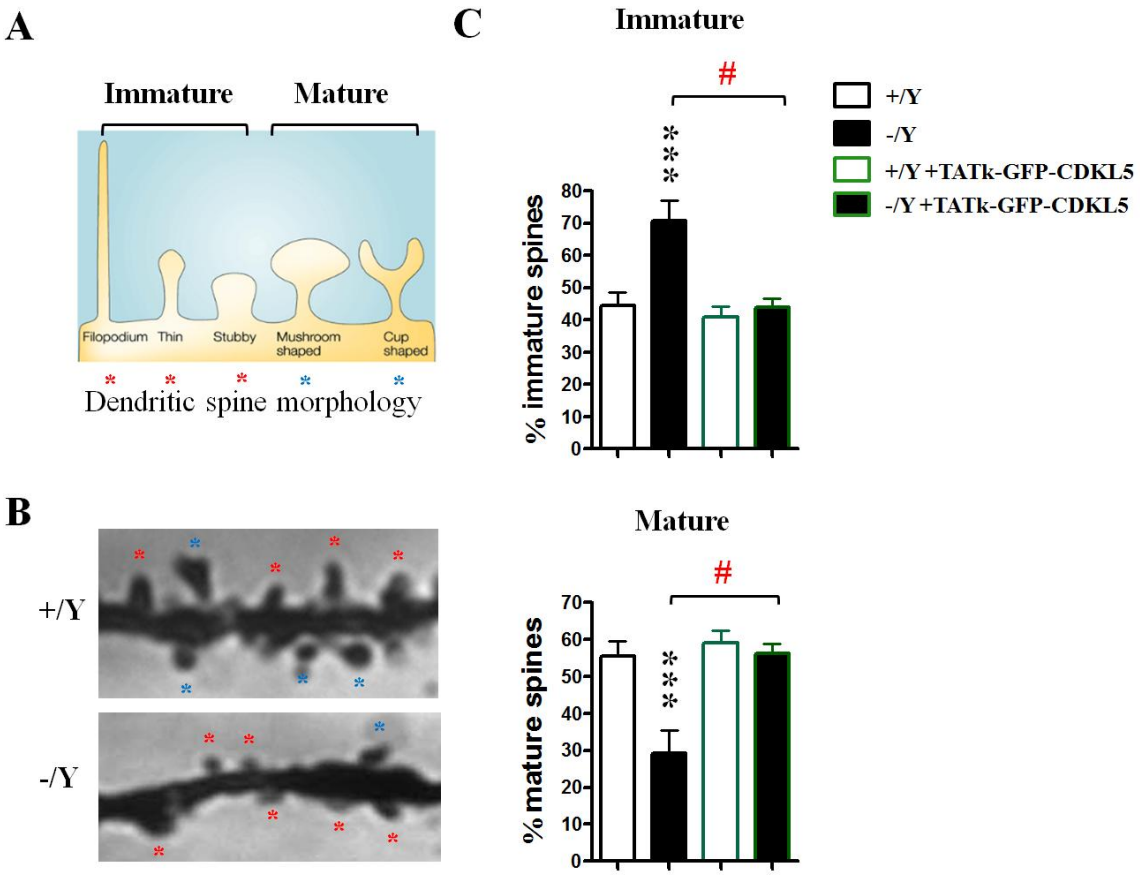

Figure 42. Effects of 5-days treatment with TATκ-GFP-CDKL5$_{115}$ on spine morphology. *(**A**) Schematic depiction of dendritic spines classified by shape as thin, stubby, mushroom- and cup-shaped. Red asterisks indicate immature spines (filopodia + thin + stubby), blue asterisks over the mature spines (mushroom + cup). (Image taken from [Hering and Sheng 2001]) (**B**) Images of Golgi-stained dendritic spines of granule cells of wild-type male mice (+/Y) and CDKL5 KO male mice (-/Y) treated with vehicle or TATκ-GFP-CDKL5 via intraventricular injections given once a day for 5 consecutive days. Scale bar = 5 µm. Mature and immature spine are marked with blue and red asterisks respectively. (**C**) Percentage of immature and mature spines in mice as in A. *** p < 0.001 as compared to +/Y; # p < 0.01 as compared to the -/Y samples (Bonferroni's test after ANOVA).*

Taken together, these data demonstrate that treatment with TATκ-GFP-CDKL5$_{115}$ completely recovers connectivity in CDKL5 −/Y mice, by restoring synaptophysin expression and by correcting dendritic spine number and maturation.

4.7 Intracerebroventricular treatment with TATκ-CDKL5 improves cognitive performance

Following histological studies on the hippocampal region we investigated the effect of TATκ-GFP-CDKL5$_{115}$ on hippocampus-dependent behavior after a short course of treatment (5 days). Mice that had been injected for 5 days were subjected to a preliminary behavioral test, namely the passive avoidance task. This test is a fear-aggravated test used to evaluate learning and memory in rodent models of CNS disorders and requires the subjects to behave contrarily to their innate tendency to prefer dark areas and avoid bright areas (Fig. 43). Memory for the passive avoidance task is disrupted by hippocampal lesions [Deacon et al. 2002], demonstrating the involvement of this brain region in the tasks required for this behavioral test.

After the mice spend an initial day exploring the chambers into which they are placed, they receive a foot shock. Mice with normal learning and memory will avoid entering the chamber where they were previously exposed to the shock. We previously reported that CDKL5 KO mice do not avoid the shock chamber on the second day, indicating a disruption of memory function [Fuchs et al. 2014]. Unfortunately, we observed that after undergoing 5 days of treatment with TATκ-GFP-CDKL5$_{115}$ the hippocampal cognitive functions of knockout mice were not restored, as they showed a significantly shorter latency compared to their wild type counterparts (Fig. 43-C).

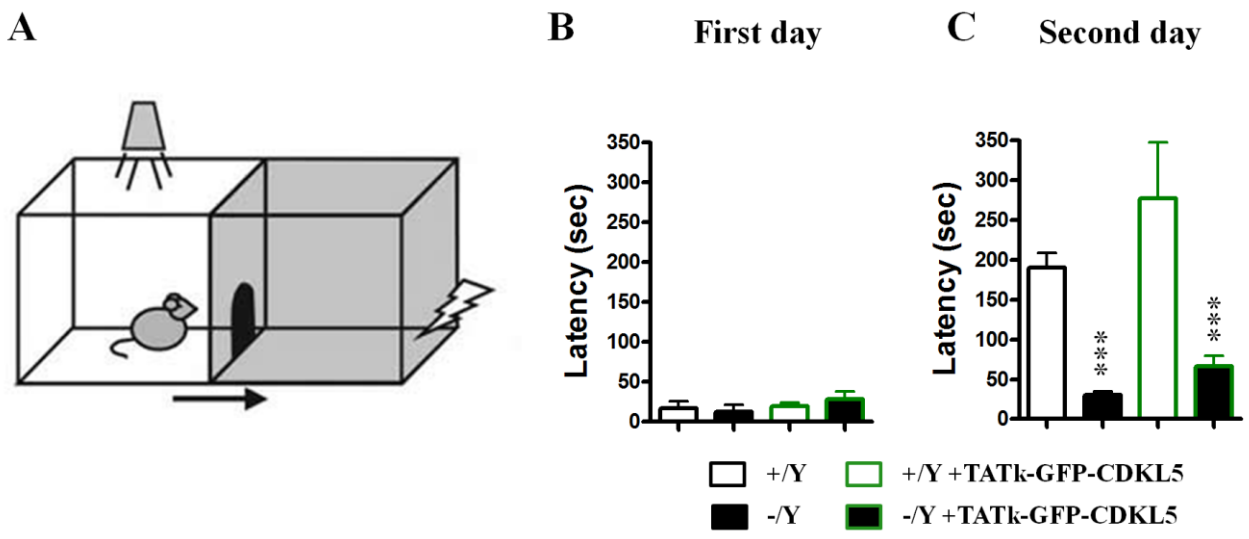

Figure 43. Effects of 5-days treatment with TATκ-GFP-CDKL5$_{115}$ on hippocampus-dependent behavior. *(**A**) Scheme of a passive avoidance apparatus. (**B-C**) Passive avoidance test in WT male mice (+/Y) and CDKL5 KO male mice (-/Y) treated with vehicle or TATκ-GFP-CDKL5. Graphs show the latency time for entering the dark compartment on the first day (**B**) and on the second day (**C**). Values represent mean ± SE. *** $p < 0.001$ as compared to the untreated wild-type condition as tested with Fisher LSD after ANOVA.*

For this reason we prolonged the treatment with TATκ-GFP-CDKL5$_{115}$ to 12 days (see treatment schedule shown in Fig. 44). The treatment period consisted of a single daily injection for 5 consecutive days, followed by a two-day rest period and then 5 additional days of a single injection for a total of 10 injections. Moreover, after ascertaining that treatment did not cause evident side effects in terms of body weight and inflammatory response (see Fig. 45), we also started treating a group of mice with a higher dose of TATκ-GFP-CDKL5, by injecting the 107 kDa isoform of CDKL5. Experimental groups were subject to various behavioral tests starting from the least stressful ones, and the results, which are promising, are presented below.

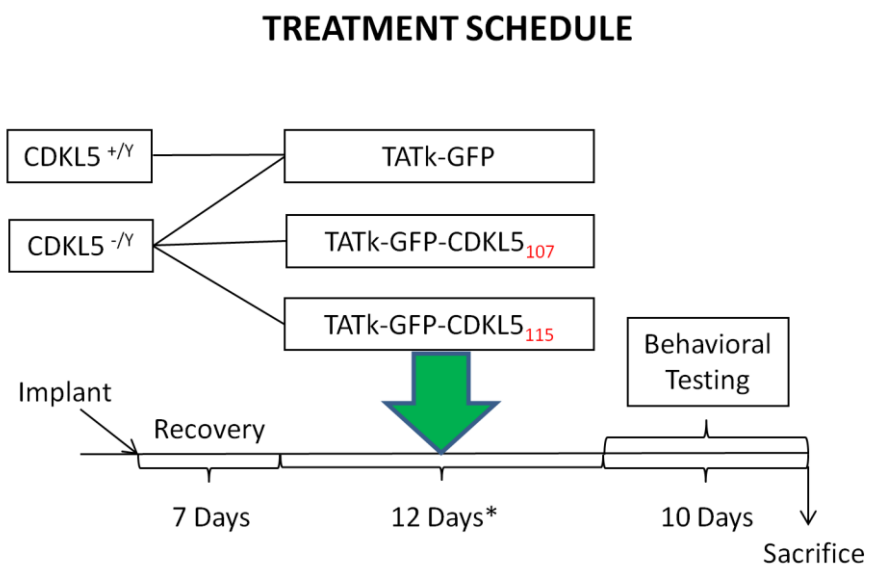

Figure 44. Prolonged ICV treatment schedule. *Male CDKL5 WT (CDKL5$^{+/Y}$) received treatment with TATκ-GFP (n=6) while CDKL5 KO (CDKL5$^{-/Y}$) were treated with TATκ-GFP (n=6), TATκ-GFP-CDKL5$_{115}$ (n=10) or TATκ-GFP-CDKL5$_{107}$ (n=6) as indicated above. Treatment period consisted of a single daily injection for 5 consecutive days, followed by a two day rest period and then 5 additional days of a single injection. There was a total of 10 injections which were done in a 12 day period.*

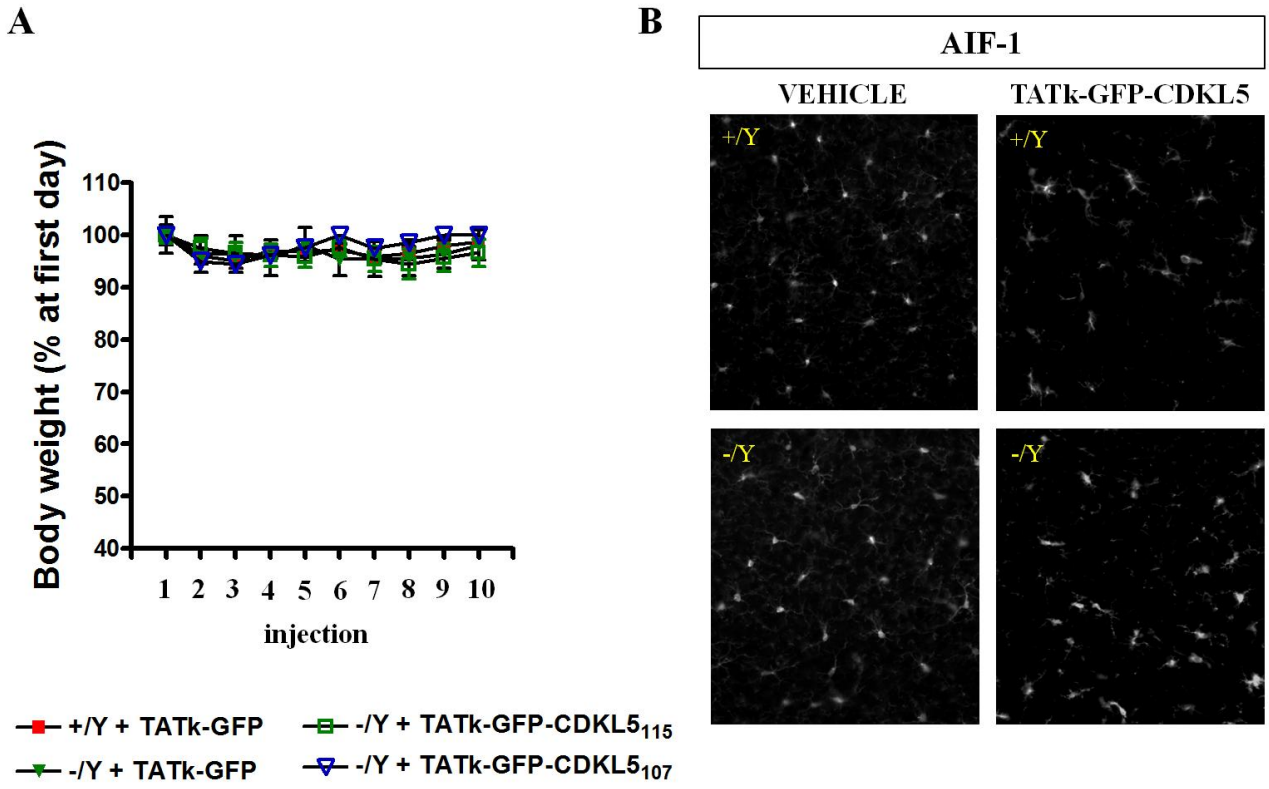

Figure 45. Monitoring of body weight and inflammatory response in mice treated with one daily intraventricular injection of protein for a total of 10 injections. *(**A**) Body weight of CDKL5 KO (-/Y) and wild-type (+/Y) mice treated with TATκ-GFP or CDKL5 KO (-/Y) mice treated with TATκ-GFP-CDKL5$_{115}$ or TATκ-GFP-CDKL5$_{107}$. Mice were allowed to recover for 7 days after cannula implantation and sacrificed 10 days after the last injection. (**B**) Immunohistochemical analysis of AIF-1 in brain slides of wild-type (+/Y) and CDKL5 KO (-/Y) mice treated with TATκ-GFP-CDKL5$_{115}$ or vehicle. Allograft inflammatory factor 1 (AIF-1) is an inflammation-responsive scaffold protein that is mainly expressed in immunocytes. It was reported to be associated with the activation of microglia/macrophages post central nervous system injury [Zhao, Yan, and Chen 2013]. Note that no significant differences were observed in body weight nor in AIF-1 inflammatory activation, indicating no evident side effects in 12-days treated mice.*

4.7.1 TATκ-CDKL5 improves learning and memory ability

As already stated, CDKL5 KO mice exhibit learning and memory deficits when compared to wild type mice. To examine memory and learning ability, both CDKL5 KO and wild type mice were administered 10 daily intraventricular injections of TATκ-GFP-CDKL5$_{115}$, TATκ-GFP-CDKL5$_{107}$ or TATκ-GFP. After a two-day rest period following the conclusion of the injections, all experimental

groups were tested with the Morris Water Maze (MWM). MWM measures the ability to find and recall the position of a platform submerged in water. Mice were trained for 5 consecutive days in the MWM task to locate the hidden escape platform in a circular pool. The latency to find the hidden platform during the trials was used as a measure of learning. After the training period, on the sixth day animals were subjected to a probe trial without a platform in order to test memory.

The results of the MWM test are shown in Fig. 46. The graph shows quantification of the learning phase as determined via the MWM test in wild type (+/Y) mice treated with TATκ-GFP control protein and CDKL5 KO (−/Y) mice treated with TATκ-GFP, TATκ-GFP-CDKL5$_{115}$, or TATκ-GFP-CDKL5$_{107}$. Following treatment with the control protein (TATκ-GFP), no changes were shown in the learning curve compared to the previously reported trend of untreated wild type and CDKL5 KO mice [Fuchs et al. 2014]. TATκ-GFP treated wild type mice learned to find the platform by the third day, but no significant learning was detected in TATκ-GFP treated CDKL5 KO mice, indicating a learning deficit. Importantly, TATκ-GFP-CDKL5$_{115}$ treated CDKL5 KO mice began to recover their learning ability on day 4 with continued improvement on day 5, while TATκ-GFP-CDKL5$_{107}$ treated CDKL5 KO mice began to recover their learning ability on day 3 and reached a performance similar to that of WT on days 4 and 5 (Fig. 46-A).

Concerning the probe test, histograms in Fig. 46 B-D show the memory performance of experimental groups. TATκ-GFP treated CDKL5 KO (-/Y) mice found the platform with a longer latency (B), entered the quadrant with a reduced frequency (C), and spent a reduced amount of time in the quadrant of the platform (D) in comparison with TATκ-GFP treated WT (+/Y) mice. TATκ-GFP-CDKL5$_{115}$ treated CDKL5 -/Y mice showed a positive trend that was not statistically significant while TATκ-GFP-CDKL5$_{107}$ treated CDKL5 -/Y mice showed statistically significant improvement in all parameters (Fig. 46 B-D).

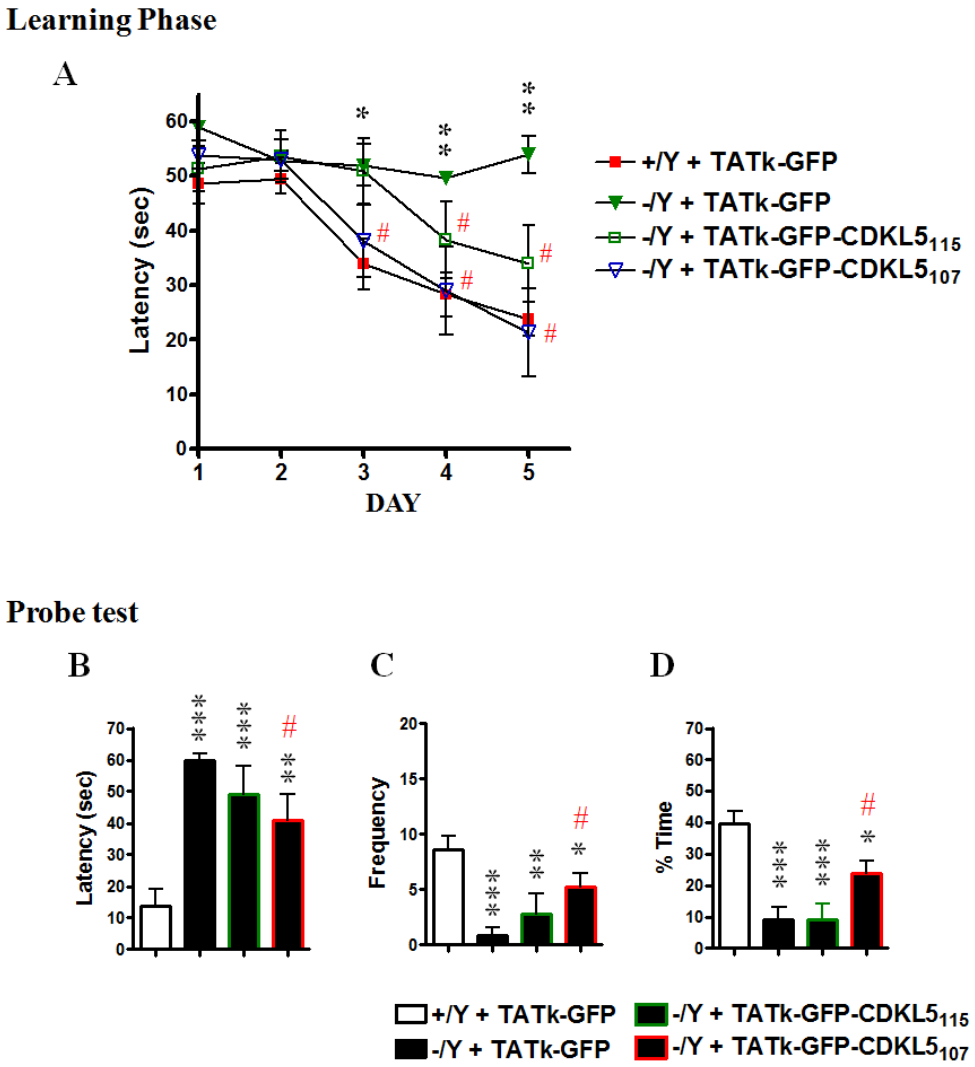

Figure 46. Effect of treatment on hippocampus-dependent behavior assessed with the Morris water maze (MWM). *(**A**) Spatial learning of WT male mice (+/Y) and CDKL5 KO male mice (-/Y) treated with TATκ-GFP (n = 6) or CDKL5 KO male mice (-/Y) treated with TATκ-GFP-CDKL5$_{115}$ (n = 10) or TATκ-GFP-CDKL5$_{107}$ (n = 6) for 10 days. After treatment period and a two day rest period, mice received MWM testing. (**B-D**) Probe test showing that CDKL5 KO male mice (-/Y) found the platform with a longer latency (**B**), entered the quadrant with a reduced frequency (**C**) and spent a reduced amount of time in the quadrant of the platform (**D**) in comparison with WT (+/Y) mice. TATκ-GFP-CDKL5$_{115}$ treated CDKL5 -/Y mice showed a positive trend that was not statistically significant while TATκ-GFP-CDKL5$_{107}$ treated CDKL5 -/Y mice showed statistically significant improvement in all parameters (**B-D**). Values represent mean ± SE. * p < 0.05, ** p < 0.01, *** p < 0.001 as compared to the wild type condition; # p < 0.05 as compared to the TATκ-GFP treated CDKL5 KO condition (Fisher LSD test after ANOVA).*

Memory and learning abilities were further examined in response to TATκ-GFP-CDKL5 protein treatment using the Y-maze spontaneous alternation test. This hippocampus-dependent spatial reference memory task is used for measuring the willingness of mice to explore new environments. TATκ-GFP treated CDKL5 KO (-/Y) mice showed impairment in memory function in this task, as shown by a reduced percentage of correct alternations in comparison with TATκ-GFP treated wild type (+/Y) mice. CDKL5 KO mice treated with TATκ-GFP-CDKL5$_{115}$ showed a slight, although not significant, improvement while CDKL5 KO mice treated with TATκ-GFP-CDKL5$_{107}$ showed a performance that was similar to that of wild types treated with TATκ-GFP (see Fig. 47).

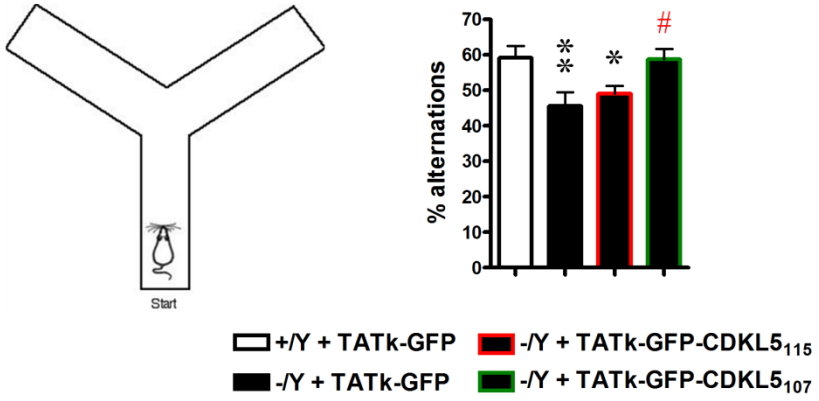

Figure 47. Effect of treatment on hippocampus-dependent spatial reference memory assessed with the Y-maze Spontaneous Alternation test. *WT male mice (+/Y) and CDKL5 KO male mice (-/Y) treated with TATκ-GFP (n = 6) or CDKL5 KO male mice (-/Y) treated with TATκ-GFP-CDKL5$_{115}$ (n = 10) or TATκ-GFP-CDKL5$_{107}$ (n = 6) for 10 days were tested. One alternation is defined as consecutive entries in three different arms. The percentage of spontaneous alternations is defined as: (total alternations/total arm entries-2) x 100. TATκ-GFP treated CDKL5 KO (-/Y) mice were impaired in this task, as shown by a reduced percentage of right alternations in comparison with TATκ-GFP treated wild type (+/Y) mice. CDKL5 KO mice treated with TATκ-GFP-CDKL5$_{115}$ showed slight improvement while CDKL5 KO treated with TATκ-GFP-CDKL5$_{107}$ showed performance similar to WT treated with TATκ-GFP. * $p < 0.05$, ** $p < 0.01$ as compared to the wild type condition; # $p < 0.05$ as compared to the TATκ-GFP treated CDKL5 KO -/Y condition (Fisher LSD test after ANOVA).*

Finally, the passive avoidance task, which was unsatisfactory after a short period of treatment (5 days), was repeated after a more prolonged treatment phase. Accordingly, after 10 days of

treatment, 2 days of rest and 6 days of MWM test, mice from the various groups received passive avoidance testing (Fig. 48). This test was performed after all the other behavioral tests, because it is rather stressful for animals in that it uses an electrical shock as an aversive stimulus. Fig. 48 demonstrates the results from the passive avoidance test. Fig. 48-A indicates that on the first day the latency time to enter the dark chamber was similar for all groups. On day two, namely the testing period (Fig. 48-B), animals were placed in the light chamber once again. Memory of the adverse event received on the first day in the dark chamber was measured by latency time to enter that chamber. TATκ-GFP treated CDKL5 KO (−/Y) mice were severely impaired in performing this task, as demonstrated by a reduced latency to enter the dark compartment in comparison with TATκ-GFP treated wild type (+/Y) mice. It is important to note that TATκ-GFP-CDKL5 treated knockout mice, however, showed a similar latency time to that of wild type mice. This effect was observed with both of the TATκ-GFP-CDKL5 isoforms, and it was statistically significant in comparison to TATκ-GFP treated CDKL5 KO mice.

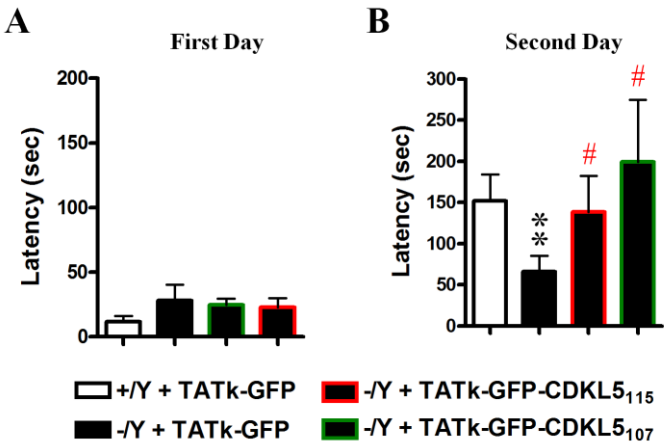

Figure 48. Effect of treatment on hippocampus-dependent memory assessed with the passive avoidance (PA) test. *(**A**-**B**) WT male mice (+/Y) and CDKL5 KO male mice (-/Y) treated with TATκ-GFP (n = 6) or CDKL5 KO male mice (-/Y) treated with TATκ-GFP-CDKL5$_{115}$ (n = 10) or TATκ-GFP-CDKL5$_{107}$ (n = 6) for 10 days were tested. The latency time to enter the dark chamber on the first day (**A**) and on the second day (testing period, **B**). TATκ-GFP treated CDKL5 KO (-/Y) mice were severely impaired in this task, while TATκ-GFP-CDKL5$_{115}$ and TATκ-CDKL5$_{107}$ treated CDKL5 KO mice showed similar latency time as compared to wild type mice (**B**). These differences were statistically significant in comparison to TATκ-GFP treated CDKL5 KO mice. ** p < 0.01 as compared to the wild type condition; # p < 0.05 as compared to the TATκ-GFP treated CDKL5 KO (-/Y) condition (Fisher LSD test after ANOVA).*

Taken together, these data demonstrate that TATκ-CDKL5 treatment partially (at a lower dosage with 115 kDa CDKL5 isoform) or completely (at a higher dosage with 107 kDa CDKL5 isoform) restores hippocampus-dependent learning and memory ability in CDKL5 KO mice.

4.7.2 TATκ-CDKL5 improves motor behavior

In order to examine the effect of TATκ-GFP-CDKL5 protein on motor behavior, mice were tested for limb clasping. To better evaluate the effect of treatment on clasping behavior and to eliminate intra-strain variability, each animal was tested both before and after the 10 days of treatment. Animals were suspended in the air by the tail for 2 minutes and the total time of clasping was measured from a video recording. Results from this test are shown in the histogram in Fig. 49 and representative screenshots taken from videos show clasping behavior of experimental groups in the panels below. While wild type mice never exhibited hind-limb clasping, TATκ-GFP treated CDKL5 KO mice spent more than 30 % of the time in the clasping position. Similar data was observed in untreated CDKL5 KO mice, indicating that surgery and intraventricular injections, which may be stressful, do not alter clasping behavior (data not shown). Importantly, CDKL5 KO mice treated with TATκ-GFP-CDKL5$_{115}$ or TATκ-GFP-CDKL5$_{107}$ show a significant decrease in clasping time.

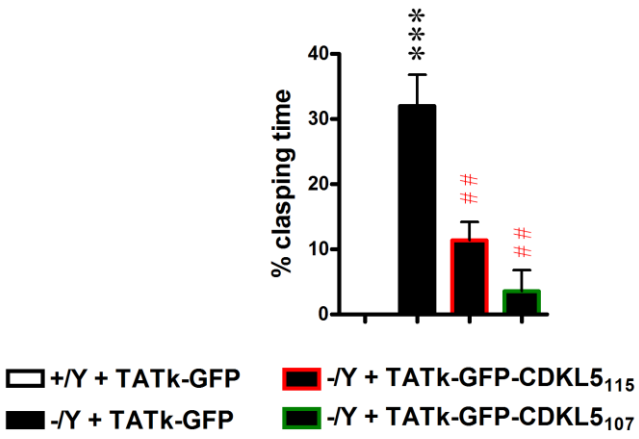

Figure 49. Effect of treatment on motor behavior assessed with the hind-limb clasping test. *All animals were suspended for 2 minutes and total time of hind-limb clasping was measured. The histogram reports time of hind-limb clasping as a percentage of the total time suspended. Treatment with TATκ-GFP-CDKL5$_{115}$ and TATκ-GFP-CDKL5$_{107}$ led to a statistically significant reduction in clasping time as compared to TATκ-GFP treated CDKL5 KO (-/Y). Below the histogram representative images of clasping behavior are shown. Values represent mean ± SE. *** $p < 0.001$ as compared to the wild type condition; ## $p < 0.01$ as compared to the TATκ-GFP treated CDKL5 KO -/Y condition (Fisher LSD test after ANOVA).*

Taken together, these data demonstrate that treatment with TATκ-CDKL5 improved motor control in CDKL5 KO mice.

4.8 TATκ-CDKL5 effects on neuronal maturation and survival are long lasting

A protein replacement therapy needs to be continued during the whole life span of the patient. With the idea of possibly reducing the frequency of injections in view of a future treatment protocol in humans, we evaluated the persistence of positive effects after treatment cessation.

Hence, twelve days after the completion of the treatment period, immediately after the behavioral tests, animals were sacrificed and histological analyses were performed. Granule cell dendritic morphology was analyzed through immunohistochemistry for DCX. Quantification of total dendritic length of newborn neurons in the dentate gyrus demonstrated that CDKL5 KO mice treated with TATκ-GFP-CDKL5$_{107}$ maintained longer dendrites compared to TATκ-GFP treated CDKL5 KO mice (Fig. 50). This finding indicates that treatment with TATκ-GFP-CDKL5$_{107}$ leads to a

morphological change that is durable for at least 12 days from treatment cessation. The treatment dose, however, seems to be important; in fact, treatment with a lower dose of TATκ-GFP-CDKL5 (isoform 115) did not have the same lasting effect on dendritic maturation (Fig. 50-A).

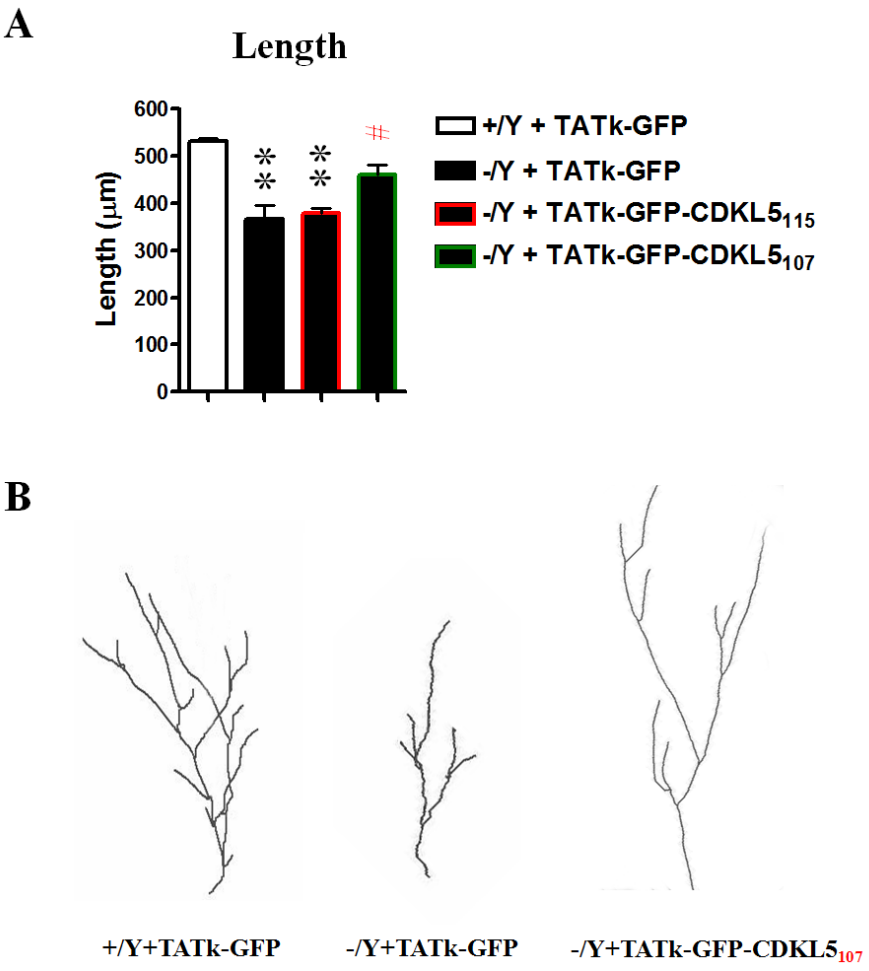

Figure 50. Long-term effect of treatment on dendritic arborization of newborn neurons. *(**A**) Quantification of total dendritic length in the dentate gyrus of WT (+/Y) and CDKL5 KO (-/Y) treated with TATκ-GFP and CDKL5 KO (-/Y) treated with TATκ-GFP-CDKL5$_{115}$ or TATκ-GFP-CDKL5$_{107}$. (**B**) Examples of the reconstructed dendritic tree of newborn granule cells of WT (+/Y) treated with TATκ-GFP, KO (-/Y) treated with TATκ-GFP and KO (-/Y) treated with TATκ-GFP-CDKL5$_{107}$ respectively. Data indicate that treatment with TATκ-GFP-CDKL5$_{107}$ leads to a morphological change that is durable for at least 12 days from time when dosing was discontinued. Values represent mean ± SE. ** $p < 0.01$ as compared to the wild type condition; # $p < 0.01$ as compared to the TATκ-GFP treated CDKL5 KO (-/Y) condition (Bonferroni test after ANOVA).*

Furthermore, quantification of the number of DCX-positive cells in the dentate gyrus (Fig. 51-A), together with the quantification of the total number of cleaved Caspase 3-positive cells in the same region (Fig. 51-B), revealed that treatment with either TATκ-GFP-CDKL5$_{115}$ or TATκ-GFP-CDKL5$_{107}$ can induce long-lasting survival of postmitotic granule neurons.

Figure 51. Long-term effect of treatment on neuronal survival. *(**A**) Quantification of the number of DCX-positive cells in the hippocampus (dentate gyrus) of WT male mice (+/Y), CDKL5 KO male mice (-/Y), and CDKL5 KO male mice treated with TATκ-GFP-CDKL5$_{115}$ or TATκ-GFP-CDKL5$_{107}$. Treatment period consisted of once daily intraventricular injection for 5 days followed by two day rest period then an additional 5 injections. Animals were sacrificed 12 days after the last injection. (**B**) Quantification of the total number of cleaved Caspase 3-positive cells in the hippocampus (dentate gyrus) of the same mice as in A. Mean ± SE * p < 0.05, ** p < 0.01 as compared to +/Y; # p < 0.05; ## p < 0.001 as compared to the -/Y samples (Bonferroni's test after ANOVA).*

These data indicate that the positive effects of treatment with TATκ-GFP-CDKL5, in particular at a high dosage (107 isoform), persist for two weeks after treatment cessation.

4.9 Systemically injected TATκ-CDKL5 reaches the mouse brain

The route of administration of a drug can be a key problem for CNS drug delivery due to the presence of the blood brain barrier, a highly selective permeability barrier that separates the circulating blood from the brain extracellular fluid in the central nervous system. At the base of protein therapy is the design of a non-invasive strategy that allows administration of a therapeutic

protein to CNS. The possibility of the TATκ-CDKL5 systemic administration is, therefore, an essential step for the development of a protein therapy that is suitable for clinical treatment of patients with CDKL5 disorder.

For this reason we assessed whether TATκ-GFP-CDKL5 protein crossed the blood brain barrier. We first evaluated whether TATκ-GFP-CDKL5 protein crossed the blood brain barrier in newborn mice, since they still have an "immature" and "leakier" blood brain barrier. Seven-day old mouse pups were subcutaneous injected with a single dose of culture medium of 293T cells transfected with TATκ-GFP-CDKL5$_{115}$, TATκ-GFP or medium from untrasfected cells (vehicle); the dose corresponded to about 200 ng of the fusion protein. Localization of TATκ-GFP-CDKL5 and TATκ-GFP in the brain was evaluated by immunohistochemistry using an anti-GFP antibody and a TSA amplification kit. Images were taken at the level of the sensory-motor cortex and the cerebellum. Cells were counterstained using 4',6-diamidino-2-phenylindole (DAPI). Representative images demonstrating presence of the TATκ-GFP-CDKL5 protein in the sensory-motor cortex of mice are shown in Fig. 52. Given that the TATκ-GFP-CDKL5 protein was subcutaneous administered, this data demonstrates that TATκ-GFP-CDKL5 protein is effectively transported across an "immature" blood brain barrier and enters into brain cells.

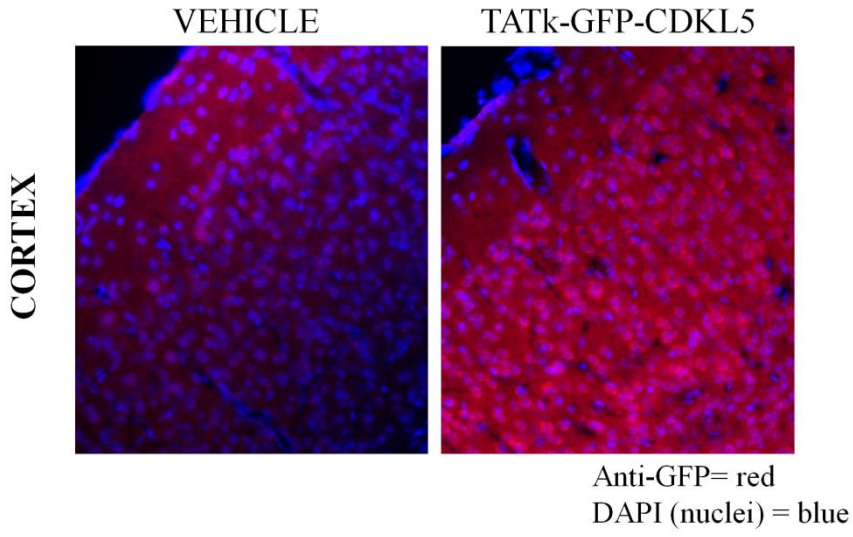

Figure 52. Localization of TATκ-GFP-CDKL5 into the brain after 4 hours from a single subcutaneous injection in 7-days old mouse pups. *Immunohistochemistry was performed using an anti-GFP antibody and a TSA amplification kit. Images were taken at the level of sensory-motor cortex.*

On the basis of these promising results, we evaluated whether TATκ-GFP-CDKL5 protein crosses the blood brain barrier in adult mice that have a completely formed, highly selective permeability barrier. The treatment schedule was planned as one daily tail vein intravenous injection of TATκ-GFP-CDKL5$_{115}$ for 5 consecutive days (Fig. 53; the dose corresponded to about 200 ng of the fusion protein). Mice were sacrificed 1 hour after the last treatment and localization of TATκ-GFP-CDKL5 and TATκ-GFP in the brain was evaluated by immunohistochemistry using an anti-GFP antibody. We found presence of the TATκ-GFP-CDKL5 protein in the hippocampal dentate gyrus of adult mice (Fig. 54), demonstrating that TATκ-GFP-CDKL5 protein is effectively transported across a "mature" blood brain barrier.

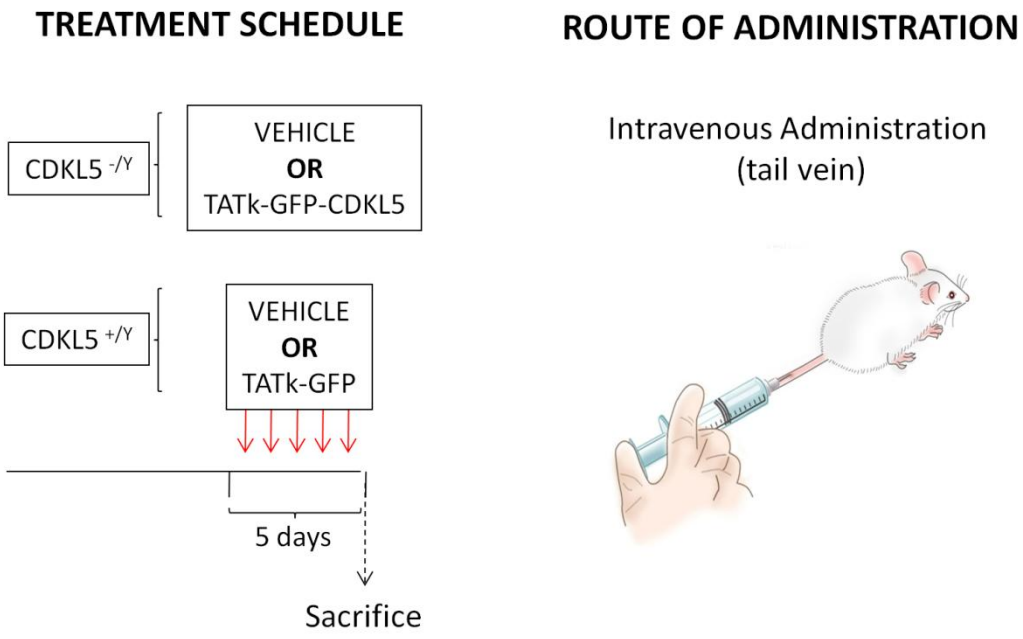

Figure 53. Intravenous treatment schedule. *Mature mice (3-4 months of age) received a single intravenous injection on 5 consecutive days and were sacrificed 1 hour after the last injection. CDKL5 wild type mice (+/Y) received either vehicle or TATκ-GFP (n = 3). CDKL5 KO mice (-/Y) received either vehicle or TATκ-GFP-CDKL5 (n = 3).*

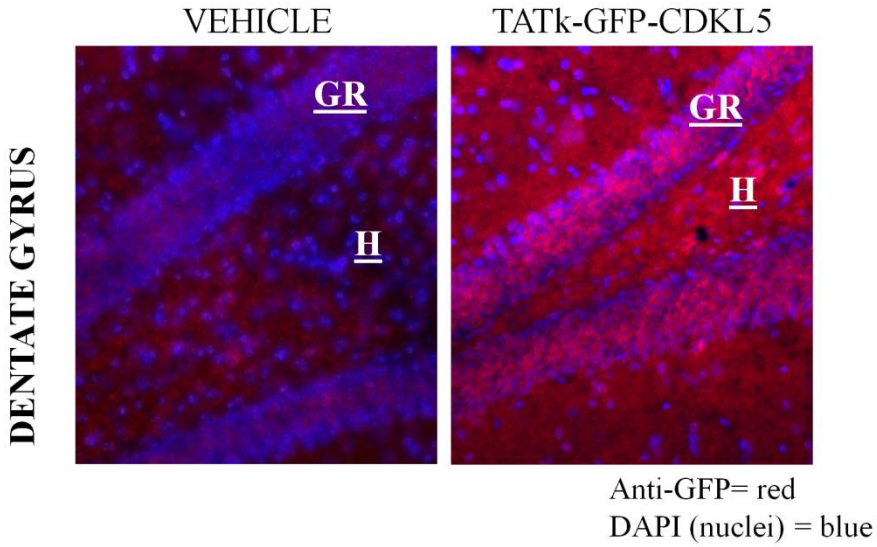

Figure 54. Localization of TATκ-GFP-CDKL5 into the brain after 1 hours from intravenous injection in 3 months old mice. *Immunohistochemistry was performed using an anti-GFP antibody and a TSA amplification kit. Images were taken at the level of hippocampus (dentate gyrus). H = hilus; GR = granular layer.*

4.10 Systemic treatment with TATκ-CDKL5 restores neuronal maturation and survival

In order to evaluate the effects of systemic treatment with TATκ-GFP-CDKL5, adult CDKL5 KO mice were treated with TATκ-GFP-CDKL5 as previously described (Fig. 53, treatment schedule), while wild type counterparts received TATκ-GFP control protein. Control groups treated with vehicle were used for both of the genotypes as a baseline measure.

We first quantified the number of cleaved caspase-3 positive apoptotic cells and DCX-positive newborn neurons in the dentate gyrus of treated animals. Importantly, histograms in Fig. 55 demonstrate that a systemic treatment of 5 days was able to restore neuronal survival in the hippocampal dentate gyrus of CDKL5 KO mice treated with TATκ-GFP-CDKL5.

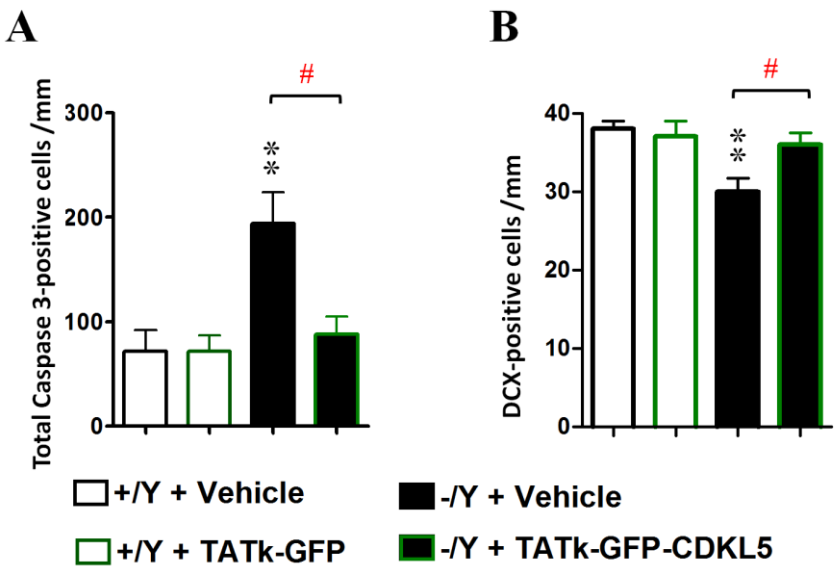

Figure 55. Effect of 5-days intravenous treatment with TATκ-GFP-CDKL5 on neuronal survival. *(**A**) Quantification of apoptotic cells (caspase-3 positive) in WT male mice (+/Y), CDKL5 KO male mice (-/Y), WT male mice treated with TATκ-GFP and CDKL5 KO male mice treated with TATκ-GFP-CDKL5. Values represent mean ± SD. ** p < 0.01 as compared to +/Y; # p < 0.01 as compared to the CDKL5 KO -/Y samples (Bonferroni's test after ANOVA). (**B**) Quantification of DCX positive cells in the hippocampus (dentate gyrus) of WT male mice (+/Y), CDKL5 KO male mice (-/Y), WT male mice treated with TATκ-GFP and CDKL5 KO male mice treated with TATκ-GFP-CDKL5. Values represent mean ± SD. ** p < 0.01 as compared to +/Y; # p < 0.01 as compared to the CDKL5 KO -/Y samples (Bonferroni's test after ANOVA).*

We then evaluated the morphology of DCX-positive newborn hippocampal neurons and noticed a small but significant increase in neuronal maturation of TATκ-GFP-CDKL5 treated CDKL5 KO mice in terms of total dendritic length and number of ramifications (Fig. 56).

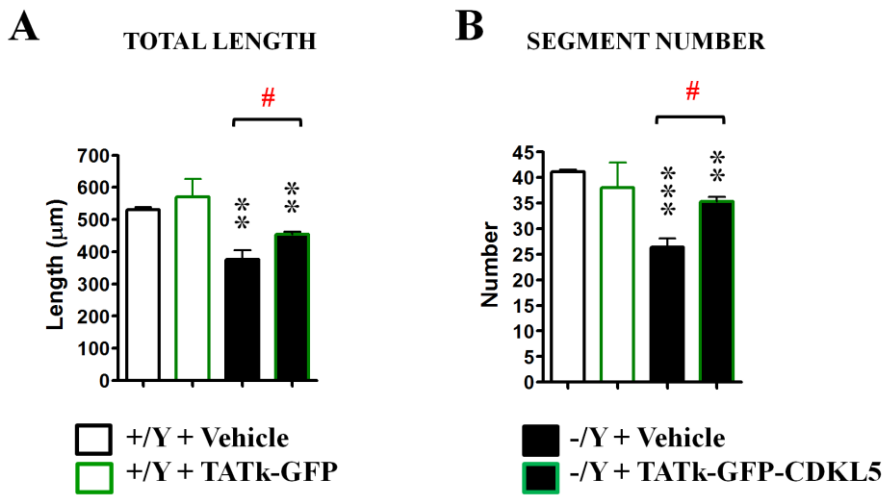

Figure 56. Effect of 5-days intravenous treatment with TATκ-GFP-CDKL5 on neuronal maturation. *(**A**-**B**) Partial (but significant) recovery of dendritic tree length (**A**) and segment number (**B**) of newborn granule cells in CDKL5 KO (-/Y) mice following once daily intravenous injection for 5 consecutive days with TATκ-GFP-CDKL5. WT male mice (+/Y) were treated with TATκ-GFP. Values represent mean ± SE. ** $p < 0.01$; *** $p < 0.001$ as compared to the wild type +/Y samples; # $p < 0.05$ as compared to the CDKL5 KO -/Y samples (Duncan's test after ANOVA).*

Taken together these data indicate that a short systemic treatment with TATκ-GFP-CDKL5$_{115}$ has positive effects on hippocampal neuronal maturation and survival. It is reasonable to hypothesize that a prolonged systemic treatment with TATκ-GFP-CDKL5$_{115}$ may also recover the behavioral defects that were restored after ICV treatment in CDKL5 KO mice.

5 DISCUSSION

No therapies are presently available for the improvement of the neurological phenotypes associated with CDKL5 disorder. Since mutations in the CDKL5 gene lead to a lack of functional CDKL5, delivery of a functional CDKL5 protein to the brain represents the best therapeutic approach. Our study provides novel evidence that an innovative approach, named protein substitution therapy, aimed at compensating for the lack of CDKL5 function by targeting a functional recombinant CDKL5 protein into the brain, is feasible. To deliver an active CDKL5 into the nervous system and within brain cells, we constructed the TATκ-CDKL5 fusion protein using the modified HIV protein transduction domain TAT as a delivering moiety. We demonstrated that TATκ-CDKL5 fusion proteins can be delivered into cells and retain CDKL5 activity after internalization. When injected *in vivo*, TATκ-CDKL5 fusion protein was able to cross the blood brain barrier and diffuse into the brain. Finally, we treated CDKL5 KO mice with TATκ-CDKL5 protein and showed that neurobiological and neurobehavioral defects underwent an improvement, in several cases bringing brain development and behavior up to wild-type levels.

It is worth noting that all the presented results were obtained in adult mice, indicating that neurodevelopmental defects in the CDKL5 KO condition may be corrected even after the early stages of brain development. Such promising results strengthen the idea that a protein substitution therapy with TATκ-CDKL5 fusion protein may be successfully developed for CDKL5 patients.

5.1 Optimization of TATκ-CDKL5 fusion protein production

In the present study we succeeded in producing and purifying a functional TAT-CDKL5 fusion protein. We found that TAT-CDKL5 cannot be produced through *E. coli* expression system, as it is probably massively degraded. Indeed, various authors in the past years reported the difficulty in obtaining a constitutively active full-length CDKL5 through this system (e.g. [Katayama, Sueyoshi, and Kameshita 2015]). Conversely, we found that purification of TAT-CDKL5 in mammalian expression systems is feasible, but it is inefficient due to protein instability and poor solubility. In order to optimize production yields, we modified the TAT construct for secretion in the culture medium of transfected HEK 293T cells and we found that the new TATκ-CDKL5 secretable protein was more stable in this production system, giving higher amounts of full-length protein. Furthermore, we found that with a secretable TATκ-CDKL5, but not with the unmodified TAT-

CDKL5 (data not shown), it is possible to select 293T stable clones expressing the fusion protein. A protein production through stable clone allows a more reproducible protein purification and it lowers costs. In the future, our results may help pharmaceutical companies to set up an efficient large-scale production system that might lead to the development of a TATκ-CDKL5 protein therapy for CDKL5 patients.

5.2 Which TATκ-CDKL5 isoforms for protein substitution therapy?

The first described CDKL5 protein isoform that was shown to be relevant in the brain was the 115 kDa transcript [Fichou et al. 2011]. Nevertheless, another isoform identified by Williamson and colleagues, the 107 kDa isoform with an alternative C-terminus, was reported to be highly expressed in human and mouse brains, resulting, on average, to be 37-fold more highly-expressed than $CDKL5_{115}$ [Williamson et al. 2012]. In the current study we exploited both the CDKL5 isoforms, creating various TATκ-CDKL5 constructs which differ in their purification tags. We found that TATκ-$CDKL5_{107}$ fusion proteins are produced with higher yields compared to TATκ-$CDKL5_{115}$ constructs, consistently with the previous observation that $CDKL5_{107}$ is more stable [Williamson et al. 2012]. Thanks to the modified TATκ sequence, all the TATκ-CDKL5 constructs were able to cross cell membranes indicating that, during the secretion process driven by the Ig κ-chain leader sequence at the N-terminus, the TAT was not inactivated. Conversely, unmodified TAT fusion proteins, when secreted by producer cells, are usually unable to enter the target cells, probably due to the furin-mediated cleavage within the TAT peptide [Flinterman et al. 2009]. The successful uptake of the secreted TATκ-CDKL5 proteins was demonstrated by several target cells, including cell lines (HEK 293T, SH-SY5Y) and primary cultures (NPCs). In order to investigate TATκ-CDKL5 fusion protein activity, we treated a neuroblastoma cell line (SH-SY5Y) with conditioned media containing secreted TATκ-CDKL5, which was previously reported to arrest the cell cycle and start differentiation under CDKL5 overexpression stimulus [Valli et al. 2012]. As expected, increasing levels of CDKL5 in neuroblastoma cells, brought about by treatment with TATκ-CDKL5, caused a reduced proliferation and improved differentiation. We observed a comparable anti-proliferative effect of $CDKL5_{115}$ and $CDKL5_{107}$ fusion proteins on neuroblastoma cells, indicating a similar cellular activity of the two CDKL5 isoforms.

As specified above, TATκ-CDKL5 protein production in mammalian cells is limited. For this reason we first carried out *in vivo* treatment through intracerebroventricular (ICV) infusions in order to lower the total amount of protein required and reduce the physiological washout of administered protein. Since we did not have information on the quantity of CDKL5 protein needed to restore brain

levels in the knockout mice, we established the dosage of TATκ-CDKL5 protein to inject by taking into account the maximum achievable concentration of protein and the maximum bolus volume. Starting with the ICV infusion of TATκ-CDKL5$_{115}$ protein, we observed an important amelioration in the neurological defects of CDKL5 KO mice, but not a full restoration. Thus we decided to treat animals with a higher dose of protein - maintaining the same concentration factor and the bolus volume - taking advantage of the more stable 107 kDa isoform. Importantly, with a higher dose of recombinant CDKL5 protein we observed a greater improvement in brain development and in the behavioral defects that characterize CDKL5 KO mice. These data suggest a dose-dependent effect of the CDKL5 protein therapy. An accurate investigation into dosage and effects, comparing the two CDKL5 isoforms, needs to be carried out in future studies.

5.3 Pharmacological aspects of a protein therapy with TATκ-CDKL5

5.3.1 Toxicology

The longer treatment period consisted in 10 injections administered in 12 days. We did not observe evident side effects of treatment in terms of body weight variations or inflammatory local response. No toxic effects or immunogenicity problems regarding the TAT-PTD have been reported so far. Our results confirmed previous studies, showing that it is possible to deliver TAT-PTD *in vivo* without eliciting an immune reaction. To evaluate the toxicity of CDKL5 overdosing, we tested a group of wild-type mice that had been ICV-treated with TATκ-CDKL5$_{115}$. No behavioral changes or adverse effects were found in these animals, indicating that there are no toxic effects of CDKL5 overdosing in the brain. This could be explained by the fact that CDKL5 is an endogenous protein that undergoes a physiological turnover, thus limiting its local concentration and avoiding overdosing problems. Notably, our results suggest that the therapeutic dose of TATκ-CDKL5 fusion protein has a wide safety window.

5.3.2 Therapeutic systems

We evaluated the stability of TATκ-CDKL5 at different temperatures: storage temperature (-80°C) and physiological temperature (37°C). We found that TATκ-CDKL5 fusion protein is stable and does not degrade or lose activity when it is preserved for a long time at low temperatures. Furthermore, we found that at 37°C a substantial amount of TATκ-CDKL5 protein is stable after 3 days and is still detectable after 7 days. Such information enables the use of reservoir-based

therapeutic systems in future preclinical studies and drug development. This finding may also represent useful information in view of clinical trials that require patient compliance, which is surely higher with a therapeutic system than with lifelong daily injections. Furthermore, therapeutic systems allow for a controlled release, which enables a constant release of protein and, importantly, can be adapted to the patient.

These experiments represent important translational research aimed at developing a safe and targeted treatment for CDKL5 disease. Our testing in animals provides the very first essential pharmacological information in terms of safety, dosage, and measures of efficacy that may guide the design of future human trials.

5.4 Protein therapy with TATκ-CDKL5 restores neuronal survival and dendritic development in CDKL5 KO mice

We have recently found that CDKL5 KO mice exhibit severe defects in the hippocampal region in terms of survival of immature granule cells and maturation of postmitotic neurons [Fuchs et al. 2014]. CDKL5 seems to modulate the intricate balance between precursor proliferation/survival and differentiation during the process of postnatal neurogenesis, thus playing a central role in brain development. As a consequence, inefficient expression of CDKL5 protein in the knockout condition is responsible for the neurological phenotype characterized, above all, by cognitive impairment.

We exploited the new therapeutic tool of protein replacement therapy in order to compensate for the lack of CDKL5 protein in CDKL5 KO mice, with the intent of rescuing the levels of this kinase in the brain that are necessary for proper neuronal development. Accordingly, we found that a protein therapy with TATκ-CDKL5 restored the survival and maturation of neuronal cells of CDKL5 KO mice. In particular, the survival of immature granule neurons of the hippocampal dentate gyrus was fully rescued and granule cell number was restored. In the CDKL5 KO mouse the dendritic arbor of granule cells exhibits a reduced length and number of branches, indicating a severe dendritic hypotrophy. We found that it is possible to restore the dendritic architecture of hippocampal granule neurons of adult CDKL5 KO mice by compensating for CDKL5 hypo-functionality with TATκ-CDKL5. Taken together our results indicate that TATκ-CDKL5 replacement therapy restores two major developmental defects that characterize the brain of CDKL5 KO mice.

5.5 Protein therapy with TATκ-CDKL5 rescues connectivity in CDKL5 KO mice

It was recently reported that in neurons CDKL5 mainly localizes to dendritic spines and is necessary for their correct genesis and maintenance, and for synapse formation [Ricciardi et al. 2012]. Consistently with this observation, CDKL5 KO mice exhibit abnormally long and thin dendritic spines, with a sparse distribution, indicating an immature phenotype [Della Sala et al. 2015; Fuchs et al. 2014]. In parallel, an overall reduction of the inputs to the hippocampal molecular layer has been observed in young CDKL5 KO mice, as indicated by a reduced synaptophysin expression [Fuchs et al. 2014].

Importantly, protein therapy with TATκ-CDKL5 fully restores spine morphology and distribution in adult CDKL5 KO mice. Furthermore, we found a defective expression of synaptophysin in layer III of the neocortex and in the molecular layer of the hippocampus of untreated adult CDKL5 KO mice compared to their wild-type counterparts. The restoration of spine development induced by TATκ-CDKL5 was accompanied by an increase in synaptophysin immunoreactivity throughout the molecular layer and in cortical layer III, suggesting restoration of the input to neurons localized in these areas.

5.6 Protein therapy with TATκ-CDKL5 restores memory performance in CDKL5 KO mice

We previously reported that CDKL5 KO mice show a poorer performance in hippocampus dependent memory and learning tasks compared to wild-type mice [Fuchs et al. 2014]. This is consistent with the reduced number, impaired dendritic and synaptic development of the granule cells and dendritic hypotrophy of hippocampal pyramidal neurons. In the current study we found that when CDKL5 protein brain levels were restored through daily administrations of TATκ-CDKL5 fusion protein, the cognitive performance of CDKL5 KO mice in hippocampus-dependent behavioral tasks was significantly improved. This indicates that the full recovery of hippocampal neurogenesis and synaptic development in treated mice were functionally effective.

In particular, while TATκ-GFP-CDKL5$_{115}$ fusion protein partially rescued the performance of knockout mice, treatment with the recombinant protein in the CDKL5$_{107}$ isoform led knockout mice to levels that were similar to those of wild-type mice. Whether these results are due to the fact that the 107 kDa is the brain-specific CDKL5 isoform or simply indicate a dose-dependent effect still

remains to be clarified.

5.7 Protein therapy with TATκ-CDKL5 restores stereotypic motor performance in CDKL5 KO mice

It has been previously described that, when suspended by their tails, CDKL5 KO mice tend to retract their limbs toward their trunks in a dystonic fashion rather than extending them as observed in wild-type mice [Amendola et al. 2014]. Clasping behavior resembles the hand-wringing stereotype, a prominent motor phenotype in CDKL5 patients, and may be considered a motor function test. The clasping phenotype is observed in mice with lesions in the cerebellum, basal ganglia and neocortex [Lalonde and Strazielle 2011]. The underlying mechanism appears to include cerebello-cortico-reticular and cortico-striato-pallido-reticular pathways, possibly triggered by changes in noradrenaline and serotonin transmission [Lalonde and Strazielle 2011]. Furthermore, it has been reported that mice lacking the postsynaptic scaffold PSD-95, a protein strongly linked to CDKL5 function [Della Sala et al. 2015; Ricciardi et al. 2012; Zhu et al. 2013], develop dyskinesia phenotypes including limb clasping [Zhang et al. 2014]. Treatment with TATκ-CDKL5 fusion protein led to a strong reduction of the clasping trend in knockout mice. This finding suggests that TATκ-CDKL5 protein injected in the third cerebral ventricle diffused in a significant amount to the brain regions involved in the clasping phenotypes, and that increasing local levels of CDKL5 improved neurotransmission in such areas.

5.8 Current perspectives of protein replacement therapies with PTDs

Protein therapy exhibits several advantages over small molecule drugs and is increasingly being developed for the treatment of disorders ranging from single enzyme deficiencies to cancer. Intracellular delivery is crucial for many therapeutic molecules; however, the ability to get large molecules across the plasma membrane poses great challenges. Protein Transduction Domains (PTDs), a group of small peptides capable of promoting transport of molecular cargo across the plasma membrane, have become important tools in promoting the cellular uptake of exogenously delivered proteins. Although the molecular mechanisms of uptake are not firmly established, PTDs have been shown to promote uptake of various molecules, including large proteins over 100 kDa (e.g. TAT-β-galactosidase, 120 kDa. [Schwarze et al. 1999]). PTDs have been widely used to facilitate the entry of proteins, small molecules, DNA and RNA into cells (reviewed in [Copolovici

et al. 2014]). The first PTD was discovered in the late 1980s when a group studying the human immunodeficiency virus (HIV) described the PTD of the trans-activator of transcription protein, TAT [Green, Ishino, and Loewenstein 1989]. An 11-amino acid transduction domain (residues 47–57 of HIV-1 TAT) was developed by Dowdy and co-workers in 1999 [Schwarze et al. 1999] and the following year the minimal PTD of TAT was identified as a 9-amino acid protein sequence [Wender et al. 2000]. TAT protein transduction domain nowadays represents the most characterized and the most widely used PTD.

Protein replacement therapy is commercially available for various lysosomal storage diseases and represents a potentially exciting avenue for other inherited enzyme deficiency disorders that currently lack available treatments. Protein replacement therapies have the benefit of well-understood safety profiles when compared with gene therapies, and also generally show increased specificity compared with small molecule mimetics [Zhang, Yang, and Gray 2009]. Protein replacement therapies are currently in development for various inherited disorders, including mitochondrial disorders [Rapoport et al. 2011], X-linked myotubular myopathy [Lawlor et al. 2013], Fabry disease [Higuchi et al. 2010] and phenylketonuria [Eavri and Lorberboum-Galski 2007]. Furthermore, protein transduction is also used in non-inherited conditions, such as ischemia/reperfusion-induced damage after myocardial infarction, and for other purposes, such as facilitation of intranasal delivery of insulin or facilitation of anticancer therapy (reviewed in [Dinca, Chien, and Chin 2016]).

Importantly, several compounds involving PTDs have been tested in humans with no serious adverse effects [Verdurmen and Brock 2011]. These studies demonstrate that it is possible to safely administer PTD constructs *in vivo* as long as careful consideration is given to potential novel effects of conjugating a PTD to a previously untested cargo [Dinca, Chien, and Chin 2016].

To the best of our knowledge, no PTD-tagged proteins have yet entered human clinical trials. However, it is worth considering that numerous PTDs have entered clinical trials and that the extensive use of PTD-protein therapy in experimental disease models has demonstrated the feasibility and efficacy of using PTD-tagged proteins as therapeutic agents. These considerations strongly suggest the potential impact on developing novel PTD-protein therapies for human disease.

5.9 Protein therapy with TATκ-CDKL5 as an ideal tool to treat CDKL5 patients

To date no cure is available for CDKL5 disorder and the standard of care for patients only targets specific symptoms. For instance there have been outlined treatment regimens for epilepsy, which, unfortunately, often appears to be refractory [Fehr et al. 2013]. In addition, symptomatic

treatments have shown different effects on different patients, probably due to the variety of mutations in the CDKL5 gene, thus hindering the possibility to establish clear guidelines for clinicians.

Very recently, some pharmacological treatments that are able to rescue various aspects of brain development have been discovered. These therapies are targeted to molecules in the CDKL5 KO mouse that have been found to manifest an altered expression or activity at particular stages of life [Della Sala et al. 2015; Fuchs et al. 2015]. Nevertheless, the treatments may not have an effect in all phases of development, and may not act on all the central and peripheral symptoms typical of the knockout condition, because molecule expression and the activation of signaling pathways varies depending on age and localization. This point represents a major issue, since the hyper-activation/inhibition of a signaling cascade may cause significant adverse effects. Furthermore, it remains to be assessed whether the targeted pathways that are exploited in order to treat the CDKL5 mouse model are also altered in CDKL5 patients.

The only common feature that is certainly shared by all CDKL5 patients is the lack of a functional CDKL5 protein, and this deficiency is the uphill cause of all the molecular alterations which could result. Therefore, compensation of CDKL5 protein levels with gene or protein therapy should theoretically restore all the reversible alterations of CDKL5 patients. In particular, protein substitution therapy has the great advantages of a relatively rapid translation to humans and the possibility to control the dosage for a patient-based treatment. It is particularly important to fit a protein therapy to the single patient because different mutations in the large CDKL5 gene cause a certain variability in the expression of CDKL5 fragments, which, in some cases may be partially active. In such cases, for instance, the dose of recombinant CDKL5 administered should be lowered.

To conclude, this study states the practicability of a protein substitution therapy for CDKL5 disorder, showing that the major defects observed in the CDKL5 KO mouse model can be rescued by restoring CDKL5 brain levels through TATκ-CDKL5 fusion protein administration. Hopefully our findings may pave the way for studies in humans.

6 REFERENCES

Amendola, E., Y. Zhan, C. Mattucci, E. Castroflorio, E. Calcagno, C. Fuchs, G. Lonetti, D. Silingardi, A. L. Vyssotski, D. Farley, E. Ciani, T. Pizzorusso, M. Giustetto, and C. T. Gross. 2014. 'Mapping pathological phenotypes in a mouse model of CDKL5 disorder', *PLoS One*, 9: e91613.

Bahi-Buisson, N., and T. Bienvenu. 2012. 'CDKL5-Related Disorders: From Clinical Description to Molecular Genetics', *Mol Syndromol*, 2: 137-52.

Bahi-Buisson, N., N. Villeneuve, E. Caietta, A. Jacquette, H. Maurey, G. Matthijs, H. Van Esch, A. Delahaye, A. Moncla, M. Milh, F. Zufferey, B. Diebold, and T. Bienvenu. 2012. 'Recurrent mutations in the CDKL5 gene: genotype-phenotype relationships', *Am J Med Genet A*, 158A: 1612-9.

Bertani, I., L. Rusconi, F. Bolognese, G. Forlani, B. Conca, L. De Monte, G. Badaracco, N. Landsberger, and C. Kilstrup-Nielsen. 2006. 'Functional consequences of mutations in CDKL5, an X-linked gene involved in infantile spasms and mental retardation', *J Biol Chem*, 281: 32048-56.

Bienvenu, T., and J. Chelly. 2006. 'Molecular genetics of Rett syndrome: when DNA methylation goes unrecognized', *Nat Rev Genet*, 7: 415-26.

Borg, I., K. Freude, S. Kübart, K. Hoffmann, C. Menzel, F. Laccone, H. Firth, M. A. Ferguson-Smith, N. Tommerup, H. H. Ropers, D. Sargan, and V. M. Kalscheuer. 2005. 'Disruption of Netrin G1 by a balanced chromosome translocation in a girl with Rett syndrome', *Eur J Hum Genet*, 13: 921-7.

Carouge, D., L. Host, D. Aunis, J. Zwiller, and P. Anglard. 2010. 'CDKL5 is a brain MeCP2 target gene regulated by DNA methylation', *Neurobiol Dis*, 38: 414-24.

Chen, Q., Y. C. Zhu, J. Yu, S. Miao, J. Zheng, L. Xu, Y. Zhou, D. Li, C. Zhang, J. Tao, and Z. Q. Xiong. 2010. 'CDKL5, a protein associated with rett syndrome, regulates neuronal morphogenesis via Rac1 signaling', *J Neurosci*, 30: 12777-86.

Copolovici, D. M., K. Langel, E. Eriste, and Ü Langel. 2014. 'Cell-penetrating peptides: design, synthesis, and applications', *ACS Nano*, 8: 1972-94.

Deacon, R. M., D. M. Bannerman, B. P. Kirby, A. Croucher, and J. N. Rawlins. 2002. 'Effects of cytotoxic hippocampal lesions in mice on a cognitive test battery', *Behav Brain Res*, 133: 57-68.

Della Sala, G., E. Putignano, G. Chelini, R. Melani, E. Calcagno, G. Michele Ratto, E. Amendola, C. T. Gross, M. Giustetto, and T. Pizzorusso. 2015. 'Dendritic Spine Instability in a Mouse Model of CDKL5 Disorder Is Rescued by Insulin-like Growth Factor 1', *Biol Psychiatry*.

Dinca, A., W. M. Chien, and M. T. Chin. 2016. 'Intracellular Delivery of Proteins with Cell-Penetrating Peptides for Therapeutic Uses in Human Disease', *Int J Mol Sci*, 17.

Eavri, R., and H. Lorberboum-Galski. 2007. 'A novel approach for enzyme replacement therapy. The use of phenylalanine hydroxylase-based fusion proteins for the treatment of phenylketonuria', *J Biol Chem*, 282: 23402-9.

Evans, J. C., H. L. Archer, J. P. Colley, K. Ravn, J. B. Nielsen, A. Kerr, E. Williams, J. Christodoulou, J. Gécz, P. E. Jardine, M. J. Wright, D. T. Pilz, L. Lazarou, D. N. Cooper, J. R. Sampson, R. Butler, S. D. Whatley, and A. J. Clarke. 2005. 'Early onset seizures and Rett-like features associated with mutations in CDKL5', *Eur J Hum Genet*, 13: 1113-20.

Fehr, S., M. Wilson, J. Downs, S. Williams, A. Murgia, S. Sartori, M. Vecchi, G. Ho, R. Polli, S. Psoni, X. Bao, N. de Klerk, H. Leonard, and J. Christodoulou. 2013. 'The CDKL5 disorder is an independent clinical entity associated with early-onset encephalopathy', *Eur J Hum Genet*, 21: 266-73.

Fichou, Y., J. Nectoux, N. Bahi-Buisson, J. Chelly, and T. Bienvenu. 2011. 'An isoform of the severe encephalopathy-related CDKL5 gene, including a novel exon with extremely high sequence conservation, is specifically expressed in brain', *J Hum Genet*, 56: 52-7.

Flinterman, M., F. Farzaneh, N. Habib, F. Malik, J. Gäken, and M. Tavassoli. 2009. 'Delivery of therapeutic proteins as secretable TAT fusion products', *Mol Ther*, 17: 334-42.

Fuchs, C., R. Rimondini, R. Viggiano, S. Trazzi, M. De Franceschi, R. Bartesaghi, and E. Ciani. 2015. 'Inhibition of GSK3β rescues hippocampal development and learning in a mouse model of CDKL5 disorder', *Neurobiol Dis*, 82: 298-310.

Fuchs, C., S. Trazzi, R. Torricella, R. Viggiano, M. De Franceschi, E. Amendola, C. Gross, L. Calzà, R. Bartesaghi, and E. Ciani. 2014. 'Loss of CDKL5 impairs survival and dendritic growth of newborn neurons by altering AKT/GSK-3β signaling', *Neurobiol Dis*, 70: 53-68.

Green, M., M. Ishino, and P. M. Loewenstein. 1989. 'Mutational analysis of HIV-1 Tat minimal domain peptides: identification of trans-dominant mutants that suppress HIV-LTR-driven gene expression', *Cell*, 58: 215-23.

Guerrini, R., and E. Parrini. 2012. 'Epilepsy in Rett syndrome, and CDKL5- and FOXG1-gene-related encephalopathies', *Epilepsia*, 53: 2067-78.

Guidi, S., F. Stagni, P. Bianchi, E. Ciani, E. Ragazzi, S. Trazzi, G. Grossi, C. Mangano, L. Calzà, and R. Bartesaghi. 2013. 'Early pharmacotherapy with fluoxetine rescues dendritic pathology in the Ts65Dn mouse model of down syndrome', *Brain Pathol*, 23: 129-43.

Hagebeuk, E. E., R. A. van den Bossche, and A. W. de Weerd. 2013. 'Respiratory and sleep disorders in female children with atypical Rett syndrome caused by mutations in the CDKL5 gene', *Dev Med Child Neurol*, 55: 480-4.

Hering, H., and M. Sheng. 2001. 'Dendritic spines: structure, dynamics and regulation', *Nat Rev Neurosci*, 2: 880-8.

Higuchi, K., M. Yoshimitsu, X. Fan, X. Guo, V. I. Rasaiah, J. Yen, C. Tei, T. Takenaka, and J. A. Medin. 2010. 'Alpha-galactosidase A-Tat fusion enhances storage reduction in hearts and kidneys of Fabry mice', *Mol Med*, 16: 216-21.

Intusoma, U., F. Hayeeduereh, O. Plong-On, T. Sripo, P. Vasiknanonte, S. Janjindamai, A. Lusawat, S. Thammongkol, A. Visudtibhan, and P. Limprasert. 2011. 'Mutation screening of the CDKL5 gene in cryptogenic infantile intractable epilepsy and review of clinical sensitivity', *Eur J Paediatr Neurol*, 15: 432-8.

Kalscheuer, V. M., J. Tao, A. Donnelly, G. Hollway, E. Schwinger, S. Kübart, C. Menzel, M. Hoeltzenbein, N. Tommerup, H. Eyre, M. Harbord, E. Haan, G. R. Sutherland, H. H. Ropers, and J. Gécz. 2003. 'Disruption of the serine/threonine kinase 9 gene causes severe X-linked infantile spasms and mental retardation', *Am J Hum Genet*, 72: 1401-11.

Kameshita, I., M. Sekiguchi, D. Hamasaki, Y. Sugiyama, N. Hatano, I. Suetake, S. Tajima, and N. Sueyoshi. 2008. 'Cyclin-dependent kinase-like 5 binds and phosphorylates DNA methyltransferase 1', *Biochem Biophys Res Commun*, 377: 1162-7.

Katayama, S., N. Sueyoshi, and I. Kameshita. 2015. 'Critical Determinants of Substrate Recognition by Cyclin-Dependent Kinase-like 5 (CDKL5)', *Biochemistry*, 54: 2975-87.

Katz, D. M., J. E. Berger-Sweeney, J. H. Eubanks, M. J. Justice, J. L. Neul, L. Pozzo-Miller, M. E. Blue, D. Christian, J. N. Crawley, M. Giustetto, J. Guy, C. J. Howell, M. Kron, S. B. Nelson, R. C. Samaco, L. R. Schaevitz, C. St Hillaire-Clarke, J. L. Young, H. Y. Zoghbi, and L. A. Mamounas. 2012. 'Preclinical research in Rett syndrome: setting the foundation for translational success', *Dis Model Mech*, 5: 733-45.

Kawahara, M., T. Hori, Y. Matsubara, K. Okawa, and T. Uchiyama. 2007. 'Cyclin-dependent kinaselike 5 is a novel target of immunotherapy in adult T-cell leukemia', *J Immunother*, 30: 499-505.

Khwaja, O. S., E. Ho, K. V. Barnes, H. M. O'Leary, L. M. Pereira, Y. Finkelstein, C. A. Nelson, V. Vogel-Farley, G. DeGregorio, I. A. Holm, U. Khatwa, K. Kapur, M. E. Alexander, D. M. Finnegan, N. G. Cantwell, A. C. Walco, L. Rappaport, M. Gregas, R. N. Fichorova, M. W. Shannon, M. Sur, and W. E. Kaufmann. 2014. 'Safety, pharmacokinetics, and preliminary assessment of efficacy of mecasermin (recombinant human IGF-1) for the treatment of Rett syndrome', *Proc Natl Acad Sci U S A*, 111: 4596-601.

Kilstrup-Nielsen, C., L. Rusconi, P. La Montanara, D. Ciceri, A. Bergo, F. Bedogni, and N. Landsberger. 2012. 'What we know and would like to know about CDKL5 and its involvement in epileptic encephalopathy', *Neural Plast*, 2012: 728267.

La Montanara, P., L. Rusconi, A. Locarno, L. Forti, I. Barbiero, M. Tramarin, C. Chandola, C. Kilstrup-Nielsen, and N. Landsberger. 2015. 'Synaptic synthesis, dephosphorylation, and degradation: a novel paradigm for an activity-dependent neuronal control of CDKL5', *J Biol Chem*, 290: 4512-27.

Lalonde, R., and C. Strazielle. 2011. 'Brain regions and genes affecting limb-clasping responses', *Brain Res Rev*, 67: 252-9.

Lawlor, M. W., D. Armstrong, M. G. Viola, J. J. Widrick, H. Meng, R. W. Grange, M. K. Childers, C. P. Hsu, M. O'Callaghan, C. R. Pierson, A. Buj-Bello, and A. H. Beggs. 2013. 'Enzyme replacement therapy rescues weakness and improves muscle pathology in mice with X-linked myotubular myopathy', *Hum Mol Genet*, 22: 1525-38.

Leoncini, S., C. De Felice, C. Signorini, G. Zollo, A. Cortelazzo, T. Durand, J. M. Galano, R. Guerranti, M. Rossi, L. Ciccoli, and J. Hayek. 2015. 'Cytokine Dysregulation in MECP2- and CDKL5-Related Rett Syndrome: Relationships with Aberrant Redox Homeostasis, Inflammation, and ω-3 PUFAs', *Oxid Med Cell Longev*, 2015: 421624.

Lewis, J. D., R. R. Meehan, W. J. Henzel, I. Maurer-Fogy, P. Jeppesen, F. Klein, and A. Bird. 1992. 'Purification, sequence, and cellular localization of a novel chromosomal protein that binds to methylated DNA', *Cell*, 69: 905-14.

Lin, C., B. Franco, and M. R. Rosner. 2005. 'CDKL5/Stk9 kinase inactivation is associated with neuronal developmental disorders', *Hum Mol Genet*, 14: 3775-86.

Livide, G., T. Patriarchi, M. Amenduni, S. Amabile, D. Yasui, E. Calcagno, C. Lo Rizzo, G. De Falco, C. Ulivieri, F. Ariani, F. Mari, M. A. Mencarelli, J. W. Hell, A. Renieri, and I. Meloni. 2015. 'GluD1 is a common altered player in neuronal differentiation from both MECP2-mutated and CDKL5-mutated iPS cells', *Eur J Hum Genet*, 23: 195-201.

Mari, F., S. Azimonti, I. Bertani, F. Bolognese, E. Colombo, R. Caselli, E. Scala, I. Longo, S. Grosso, C. Pescucci, F. Ariani, G. Hayek, P. Balestri, A. Bergo, G. Badaracco, M. Zappella, V. Broccoli, A. Renieri, C. Kilstrup-Nielsen, and N. Landsberger. 2005. 'CDKL5 belongs to the same molecular pathway of MeCP2 and it is responsible for the early-onset seizure variant of Rett syndrome', *Hum Mol Genet*, 14: 1935-46.

Masiulis, I., S. Yun, and A. J. Eisch. 2011. 'The interesting interplay between interneurons and adult hippocampal neurogenesis', *Mol Neurobiol*, 44: 287-302.

Melani, F., D. Mei, T. Pisano, S. Savasta, E. Franzoni, A. R. Ferrari, C. Marini, and R. Guerrini. 2011. 'CDKL5 gene-related epileptic encephalopathy: electroclinical findings in the first year of life', *Dev Med Child Neurol*, 53: 354-60.

Montini, E., G. Andolfi, A. Caruso, G. Buchner, S. M. Walpole, M. Mariani, G. Consalez, D. Trump, A. Ballabio, and B. Franco. 1998. 'Identification and characterization of a novel serine-threonine kinase gene from the Xp22 region', *Genomics*, 51: 427-33.

Nagahara, H., A. M. Vocero-Akbani, E. L. Snyder, A. Ho, D. G. Latham, N. A. Lissy, M. Becker-Hapak, S. A. Ezhevsky, and S. F. Dowdy. 1998. 'Transduction of full-length TAT fusion proteins into mammalian cells: TAT-p27Kip1 induces cell migration', *Nat Med*, 4: 1449-52.

Neul, J. L., W. E. Kaufmann, D. G. Glaze, J. Christodoulou, A. J. Clarke, N. Bahi-Buisson, H. Leonard, M. E. Bailey, N. C. Schanen, M. Zappella, A. Renieri, P. Huppke, A. K. Percy, and RettSearch Consortium. 2010. 'Rett syndrome: revised diagnostic criteria and nomenclature', *Ann Neurol*, 68: 944-50.

Overton, T. W. 2014. 'Recombinant protein production in bacterial hosts', *Drug Discov Today*, 19: 590-601.

Pecorelli, A., L. Ciccoli, C. Signorini, S. Leoncini, A. Giardini, M. D'Esposito, S. Filosa, J. Hayek, C. De Felice, and G. Valacchi. 2011. 'Increased levels of 4HNE-protein plasma adducts in Rett syndrome', *Clin Biochem*, 44: 368-71.

Pini, G., S. Bigoni, I. W. Engerström, O. Calabrese, B. Felloni, M. F. Scusa, P. Di Marco, P. Borelli, U. Bonuccelli, P. O. Julu, J. B. Nielsen, B. Morin, S. Hansen, G. Gobbi, P. Visconti, M. Pintaudi, V. Edvige, A. Romanelli, F. Bianchi, M. Casarano, R. Battini, G. Cioni, F. Ariani, A. Renieri, A. Benincasa, R. S. Delamont, M. Zappella, and ESRRA group. 2012. 'Variant of Rett syndrome and CDKL5 gene: clinical and autonomic description of 10 cases', *Neuropediatrics*, 43: 37-43.

Rademacher, N., M. Hambrock, U. Fischer, B. Moser, B. Ceulemans, W. Lieb, R. Boor, I. Stefanova, G. Gillessen-Kaesbach, C. Runge, G. C. Korenke, S. Spranger, F. Laccone, A. Tzschach, and V. M. Kalscheuer. 2011. 'Identification of a novel CDKL5 exon and pathogenic mutations in

patients with severe mental retardation, early-onset seizures and Rett-like features', *Neurogenetics*, 12: 165-7.

Rapoport, M., L. Salman, O. Sabag, M. S. Patel, and H. Lorberboum-Galski. 2011. 'Successful TAT-mediated enzyme replacement therapy in a mouse model of mitochondrial E3 deficiency', *J Mol Med (Berl)*, 89: 161-70.

Ricciardi, S., C. Kilstrup-Nielsen, T. Bienvenu, A. Jacquette, N. Landsberger, and V. Broccoli. 2009. 'CDKL5 influences RNA splicing activity by its association to the nuclear speckle molecular machinery', *Hum Mol Genet*, 18: 4590-602.

Ricciardi, S., F. Ungaro, M. Hambrock, N. Rademacher, G. Stefanelli, D. Brambilla, A. Sessa, C. Magagnotti, A. Bachi, E. Giarda, C. Verpelli, C. Kilstrup-Nielsen, C. Sala, V. M. Kalscheuer, and V. Broccoli. 2012. 'CDKL5 ensures excitatory synapse stability by reinforcing NGL-1-PSD95 interaction in the postsynaptic compartment and is impaired in patient iPSC-derived neurons', *Nat Cell Biol*, 14: 911-23.

Rusconi, L., L. Salvatoni, L. Giudici, I. Bertani, C. Kilstrup-Nielsen, V. Broccoli, and N. Landsberger. 2008. 'CDKL5 expression is modulated during neuronal development and its subcellular distribution is tightly regulated by the C-terminal tail', *J Biol Chem*, 283: 30101-11.

Samaco, R. C., and J. L. Neul. 2011. 'Complexities of Rett syndrome and MeCP2', *J Neurosci*, 31: 7951-9.

Schwarze, S. R., A. Ho, A. Vocero-Akbani, and S. F. Dowdy. 1999. 'In vivo protein transduction: delivery of a biologically active protein into the mouse', *Science*, 285: 1569-72.

Sekiguchi, M., S. Katayama, N. Hatano, Y. Shigeri, N. Sueyoshi, and I. Kameshita. 2013. 'Identification of amphiphysin 1 as an endogenous substrate for CDKL5, a protein kinase associated with X-linked neurodevelopmental disorder', *Arch Biochem Biophys*, 535: 257-67.

Stevens, J. C., R. Chia, W. T. Hendriks, V. Bros-Facer, J. van Minnen, J. E. Martin, G. S. Jackson, L. Greensmith, G. Schiavo, and E. M. Fisher. 2010. 'Modification of superoxide dismutase 1 (SOD1) properties by a GFP tag--implications for research into amyotrophic lateral sclerosis (ALS)', *PLoS One*, 5: e9541.

Sticozzi, C., G. Belmonte, A. Pecorelli, F. Cervellati, S. Leoncini, C. Signorini, L. Ciccoli, C. De Felice, J. Hayek, and G. Valacchi. 2013. 'Scavenger receptor B1 post-translational modifications in Rett syndrome', *FEBS Lett*, 587: 2199-204.

Tao, J., H. Van Esch, M. Hagedorn-Greiwe, K. Hoffmann, B. Moser, M. Raynaud, J. Sperner, J. P. Fryns, E. Schwinger, J. Gécz, H. H. Ropers, and V. M. Kalscheuer. 2004. 'Mutations in the

X-linked cyclin-dependent kinase-like 5 (CDKL5/STK9) gene are associated with severe neurodevelopmental retardation', *Am J Hum Genet*, 75: 1149-54.

Valli, E., S. Trazzi, C. Fuchs, D. Erriquez, R. Bartesaghi, G. Perini, and E. Ciani. 2012. 'CDKL5, a novel MYCN-repressed gene, blocks cell cycle and promotes differentiation of neuronal cells', *Biochim Biophys Acta*, 1819: 1173-85.

Verdurmen, W. P., and R. Brock. 2011. 'Biological responses towards cationic peptides and drug carriers', *Trends Pharmacol Sci*, 32: 116-24.

Wang, I. T., M. Allen, D. Goffin, X. Zhu, A. H. Fairless, E. S. Brodkin, S. J. Siegel, E. D. Marsh, J. A. Blendy, and Z. Zhou. 2012. 'Loss of CDKL5 disrupts kinome profile and event-related potentials leading to autistic-like phenotypes in mice', *Proc Natl Acad Sci U S A*, 109: 21516-21.

Weaving, L. S., J. Christodoulou, S. L. Williamson, K. L. Friend, O. L. McKenzie, H. Archer, J. Evans, A. Clarke, G. J. Pelka, P. P. Tam, C. Watson, H. Lahooti, C. J. Ellaway, B. Bennetts, H. Leonard, and J. Gécz. 2004. 'Mutations of CDKL5 cause a severe neurodevelopmental disorder with infantile spasms and mental retardation', *Am J Hum Genet*, 75: 1079-93.

Weaving, L. S., C. J. Ellaway, J. Gécz, and J. Christodoulou. 2005. 'Rett syndrome: clinical review and genetic update', *J Med Genet*, 42: 1-7.

Wender, P. A., D. J. Mitchell, K. Pattabiraman, E. T. Pelkey, L. Steinman, and J. B. Rothbard. 2000. 'The design, synthesis, and evaluation of molecules that enable or enhance cellular uptake: peptoid molecular transporters', *Proc Natl Acad Sci U S A*, 97: 13003-8.

Williamson, S. L., L. Giudici, C. Kilstrup-Nielsen, W. Gold, G. J. Pelka, P. P. Tam, A. Grimm, D. Prodi, N. Landsberger, and J. Christodoulou. 2012. 'A novel transcript of cyclin-dependent kinase-like 5 (CDKL5) has an alternative C-terminus and is the predominant transcript in brain', *Hum Genet*, 131: 187-200.

Wurm, F. M. 2004. 'Production of recombinant protein therapeutics in cultivated mammalian cells', *Nat Biotechnol*, 22: 1393-8.

Xia, H., Q. Mao, and B. L. Davidson. 2001. 'The HIV Tat protein transduction domain improves the biodistribution of beta-glucuronidase expressed from recombinant viral vectors', *Nat Biotechnol*, 19: 640-4.

Young, J. I., E. P. Hong, J. C. Castle, J. Crespo-Barreto, A. B. Bowman, M. F. Rose, D. Kang, R. Richman, J. M. Johnson, S. Berget, and H. Y. Zoghbi. 2005. 'Regulation of RNA splicing by the methylation-dependent transcriptional repressor methyl-CpG binding protein 2', *Proc Natl Acad Sci U S A*, 102: 17551-8.

Zhang, J., T. Saur, A. N. Duke, S. G. Grant, D. M. Platt, J. K. Rowlett, O. Isacson, and W. D. Yao. 2014. 'Motor impairments, striatal degeneration, and altered dopamine-glutamate interplay in mice lacking PSD-95', *J Neurogenet*, 28: 98-111.

Zhang, J., P. L. Yang, and N. S. Gray. 2009. 'Targeting cancer with small molecule kinase inhibitors', *Nat Rev Cancer*, 9: 28-39.

Zhao, Y. Y., D. J. Yan, and Z. W. Chen. 2013. 'Role of AIF-1 in the regulation of inflammatory activation and diverse disease processes', *Cell Immunol*, 284: 75-83.

Zhu, Y. C., D. Li, L. Wang, B. Lu, J. Zheng, S. L. Zhao, R. Zeng, and Z. Q. Xiong. 2013. 'Palmitoylation-dependent CDKL5-PSD-95 interaction regulates synaptic targeting of CDKL5 and dendritic spine development', *Proc Natl Acad Sci U S A*, 110: 9118-23.